Politecnico di Torino

Master's Degree Thesis in Mechatronics Engineering

Politecnico
di Torino

Master's Degree Thesis

Characterization of communication channel on high voltage energy transport and distribution systems

Supervior
Prof. Claudio Sansoè

Candidate
Marco La Manna, s290604

Company Tutor
Ing. Simone Terrando

Accademic Year 2021/2022

Contents

List of Figures

List of Tables

Acronyms

PLC Power Line Communication

LV Low Voltage

MV Medium Voltage

VNA Vector Network Analyzer

DSO Distribution System Operators

AC Alternating Current

DC Direct Current

EMI Electromagnetic Interference

XLPE Cross Linked Polyethylene

EPR Ethylene Propylene Rubber

HEPR Hard Grade Ethylene Propylene Rubber

PVC Polyvinyl Chloride

PCP Polychloroprene

UNB Ultra Narrowband

NB Narrowband

BB Broadband

ULF Ultra Low Frequency

SLF Super Low Frequency

VLF Very Low Frequency

LF Low Frequency

MF Medium Frequency

HF High Frequency

VHF Very High Frequency

IEEE Electrical and Electronics Engineers

ITU International Telecommunications Union

IEC International Electrotechnical Commission

CENELEC Comité Européen de Normalisation Électrotechnique

FCC Federal Communications Commission

ARIB Association of Radio Industries and Businesses

EPRI Electric Power Research Institute

LDR Low Data Rate

HDR High Data Rate

QAM Quadrature Amplitude Modulation

QPSK Quadrature Phase Shift Keying

BPSK Binary Phase Shift Keying Modulation

FDM Frequency Division Multiplexing

OFDM Orthogonal Frequency Division Multiplexing

FEC Forward Error Correction

GMD Geometric Mean Distance

GMR Geometric Mean Radius

TEM Transverse Electric and Magnetic Mode

TM Transverse Magnetic Mode

TE Transverse Electric Mode

SWR Standing Wave Ratio

S-parameters Scattering Parameters

DUT Device Undre Test

NLT No Load Test

SCT Short Circuit Test

TRT Turn Ratio Tester

TF Transfer Function

MCEP Public Illumination Coupling Module

IL Insertion Losse

RL Return Loss

LB Link Budget

1 Introduction

The company where I performed the stage, AUGIER Energy, is a huge global expert in the distribution and control of Medium-Voltage energy for lengths of up to 50 kilometers. AUGIER is part of Aretè e Cocchi Technologies group that includes OCEM (Bologna, Italy), MultiElectric (Chicago, USA) and Industry Technology (Suzhou, China), the industry pioneer in the energy transport/distribution sector. The goals of the project and an overview of the topic will all be covered in this chapter. The thesis's structure will be explained at the end of the chapter.

1.1 Problem overview

The remote monitoring and control of electrical systems is one of AUGIER's interests. AUGIER offers a communication system that makes use of Power Line Communication (PLC) over Medium-Voltage Networks to achieve that. It enables the establishment of digital communications without the need for extra wires and allow transmition data and electricity over the same media. The system, which is made up of the AUGIER-Master and AUGIER-Slave modules, ensures the monitoring and control of electrical distribution installations over long distances, particularly in situations where maintenance is challenging, like on motorways, highways, junction tunnels, bridges, railway tunnels, parking lots, industrial sites, luna-parks, and military sites.
A single Master can communicate with up to 300 Slave modules, enabling remote control of lighting and any other permanently powered electrical devices like traffic lights, surveillance cameras, emergency equipment, variable signs, and information boards. A Master can also operate remote devices like automation systems or I/O modules (dry contact). These modules are installed following step-down transformers, which are connected to the energy transport network, and are capable of bidirectional communication ($950V$ to $6.6kV$).
The following are this system's key benefits:

- **Plug and Play Installation:** allows to automatically address the communication equipment;
- **Reliable:** it is tolerant to changes in electrical network topologies, even in case of modification due to maintenance the system will keep working without external intervention;
- **Performances:** allows to adapt the communication speed following the measured signal quality and allowing to optimize the communication media use;
- **Secured:** supports an authentication system for the equipments;
- **Compact and easy to install:** it is installed on a standard DIN Rail (6 modules). It uses Combicon connectors for ease of installation and maintenace (safety);

- **Bluetooth:** allowing configuration and maintenace from a PC without physical connection with the AUGIER Master or AUGIER Slave modules;
- **Versatile:** its in/outs allows to respond to a vast majority of installation needs;
- **Communication:** RS485 interface allows communication with industrial automation systems over distances of several Km.

The figure below shows a typical system architecture (**Figure7.1**):

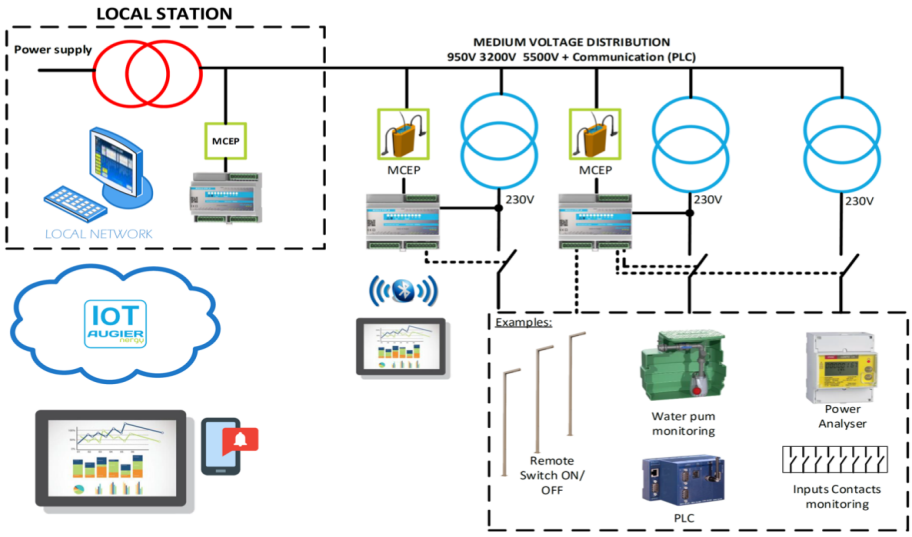

Figure 1.1: Power Line Communication on MV.

1.2 Aim of the Thesis

The following goals are intended to be eviscerate by the thesis:

- The initial step is to define the various components of the distribution system in order to better understand the causes of loss, their magnitude, and strategies to mitigate them. In order to do that, simulation result and measurements were compared. By using fewer or more suitable components along the way, it is possible to optimize the maximum distribution distance in an attempt to lower overall costs.
- The second objective, building on the first one, was to improve the current architecture. That was made possible by thoroughly examining each component and attempting to capitalize on its unique qualities in order to build a leaner and more intelligent system. To accomplish that, we put more of an emphasis on comparing the real and simulated models. The robustness of the simulation and how much the error corresponded exactly to the physical model were evaluated. Changes were made to the real models to discover how predictive the simulated ones were.
  By proceeding in this manner, it is possible to compare the new transmission system with the current one and compare their performances, expenses, and advantages.

1.3 Outline

To begin, a detailed description of the PLC system, outlining advantages and disadvantages over other communication systems, type of modulation, causes of losses and frequency behaviour, will be presented.
The analysis of the transmitted power, the S-parameters, the wave modes inside a coaxial cable and the characteristic parameters of various cable geometries were all provided, particular focus in the subsequent accurate analysis of losses transmission lines. In order to determine how much of an error there was between the ideal model and the real cables, as well as the best geometry and section, the data collected using a Vector Network Analyser and those derived from the formulas as a function of frequency implemented on Matlab, were compared for data exchange and how the attenuation (α_{dB}) and the characteristic impedance (Z_0) changed according to the configuration. Finally a cost-benefit analysis has been done between the various geometries analyzed.
Subsequently, the AUGIER step-down transformes will be analysed. In particular, attention will be paid to two different models of single-phase transformers that work at a different nominal power,trying to study, in as much detail as possible, their behaviour at low and high frequencies, thus presenting the "Augmented model". This was done to understand the amount of attenuation at the working frequency chosen by AUGIER ($133kHz$) for the data exchange with PLC technology, in order to think and propose possible modifications to the existing architectures, thus trying to streamline them.
Subsequently, an existing grid utilised by AUGIER for data exchange via PLC communication, based on the topics taught in the earlier Chapters, has been presented. It consists of a single AUGIER MASTER, placed in Low Voltage and powered at $230V$, which is capable of sending an high frequency ($133kHz$) and Low Voltage ($5V/10mA$) signal on a Medium Voltage ($3.2-5.5-6.6kV$) and low frequency electrical power line ($50-60Hz$), modulating the two waves through a signal coupler (MCEP) placed between the two voltage levels.
A single MASTER can talk to up to 300 SLAVES modules and over long distances (several tenth of km) through the G3-PLC communication standard, since the line being bidirectional and each SLAVE being a repeater. The project allows a total extension of the line of up to $40km$, with a maximum distance of $2km$ between the various modules before the the Insertion Losses become to high and the information is lost. This means that on now days PLC line 20 receivers with related transformers and MCEPs are mounted. The Link Budget has been calculated experimentally for this line. It is a fundamental parameter that accounting of all the power gains and losses that a communication signal experiences during the data exchange. With this data, it was possible to comprehend the limits of the existent configuration suggesting optimal solutions with advantages in terms of cost-benefits, by critically analysing the many core components and the different effects they have on the lines.
Finally, an idea was developed to streamline the existing architecture, eliminating the various signal couplers that the line presents (MCEPs) and letting the signal pass directly through the transformers, once the TFs have been analyzed in Chapter 4, showing the limits of this idea, the necessary changes that should be made for it to work and the proposal of a gimmick that increases its performances at the working frequency ($133kHz$).

2 PLC Communication

2.1 PLC: Advantages and Drawbacks

Due to its appealing potential for residential and/or neighborhood network applications as well as smart grid technologies, Power Line Communication, a wired communication technology, has attracted a lot of interest. It enables digital communications without the need for extra wires and offers the opportunity to transmit data and electricity over the same media. In order to offer different data services, one's home and/or neighborhood wiring effectively contributes to a smart grid. Higher protection against cyberattacks is also guaranteed by PLC because potential hackers cannot easily access the communication system. Using the power grid for digital communications will create a network that is as pervasive as the power grid itself, which is one of the most widespread infrastructures created to provide electricity to customers.
Many telecommunications channels often employ wires to provide a physical connection, although the majority of electronic equipment already have a pair of wires attached to the power lines. Because electricity lines are typically owned by the DSO (Distribution System Operators) and are directly and securely controlled by them, they can be utilized to simultaneously establish digital communications with the huge benefit of incurring no additional expenditures for the communication service provider. As a result, power line communications can be used as a substitute for more established technologies including wireless, coaxial, and optical communications. **[1]**.
The graph below depicts some peculiar characteristics of Fiber, Wi-Fi, and PLC communications (**Figure2.1**):

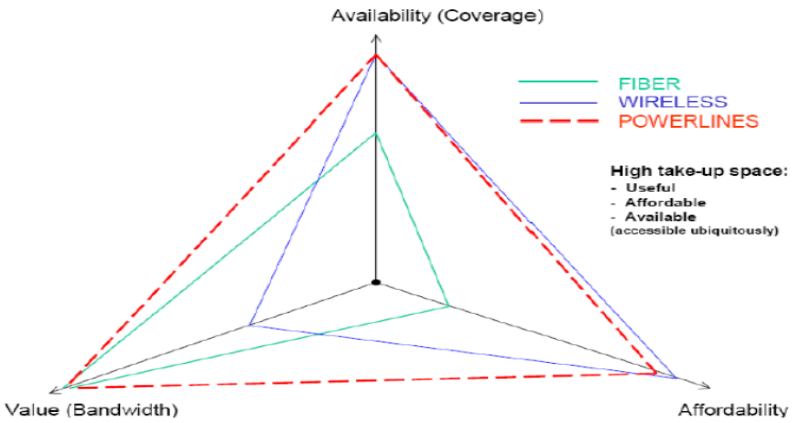

Figure 2.1: Advantages and disadvantages of different communication systems.

Norrowband power line communication over MV networks can be an alternative or a redundant solution. To provide robustness, dependability, and redundancy, they can also be incorporated into hybrid communication systems based on several communication technologies. Despite its benefits, PLC channel is quite harsh and has a number of problems. With respect to frequency, location, environment and the sort of equipment connected to it, a channel's characteristics and properties change.
The range of interest is between $10kHz$ and $500kHz$, and these lower frequency zones are particularly prone to interference.This is primarily due to the fact that the power line channel is still harsh because it was not initially intended to be used for communications. Unpredictable loading characteristics, differential and common-mode characteristic impedance, and various wiring procedures used around the world present further difficulties. As a result, there is a considerable amount of signal attenuation during data transmission **[2]**.
In order to give readers a sense of how many and how wide the variations might be, the following features of various geographical areas are reported below (**Figure2.2**):

- Europe and a large part of the world:
  - Three phase system, $400V$ between phases; loads are typically connected between a phase and neutral $(220-240V)$. Heavy loads are connected between two phases;
  - Operating frequency: $50Hz$;
  - Typically 400 houses are connected to a single distribution step-down transformer in a city environment; these houses can be found in a circle with an average radious of $400m$.
- Eastern Brasil, Perù and Guyana:
  - Three phase system, $400V$ between phases; loads are typically connected between a phase and zero $(220-240V)$. Heavy loads are tipically connected between two or three phases;
  - Operating frequency: $60Hz$;
  - Typically 400 houses are connected to a single distribution step-down transformer in a city environment; these houses can be found in a circlewith an average radious of $400m$.
- USA, Canada,Saudi Arabia and part of the South America:
  - Two phase system, $220V$ between phases; loads are typically connected between a phase and zero $(100-127V)$. Heavy loads are tipically connected between two or three phases;
  - Operating frequency: $60Hz$;
  - Typically about 5 to 20 houses are connected to a single distribution step-down transformer; these houses are located in close proximity to it.
- Japan and Madacascar:
  - Two phase system, $200V$ between phases; loads are typically connected between a phase and zero $(100-127V)$. Heavy loads are tipically connected between two or three phases;
  - Operating frequency: $50Hz$ in the eastern part (Tokyo);
  - Operating frequency: $60Hz$ in the weastern part **[4]**.

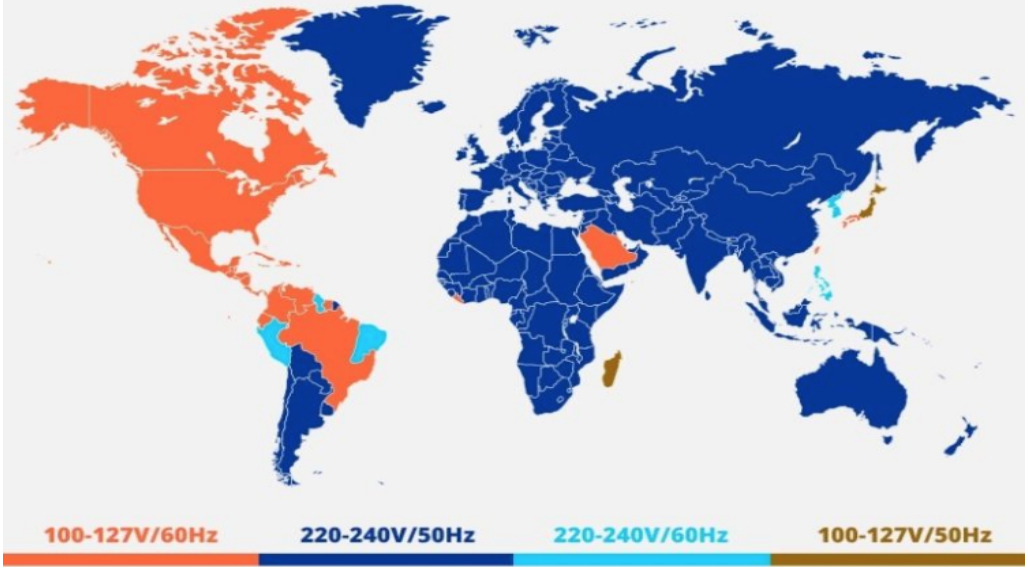

Figure 2.2: Electrical peculiarities of different regions of the world.

2.2 Electrical Power Grid

PLC transmits communication signals using the electrical grid as its transmission medium. According to the country, the power line network was intended transport $50Hz$ or $60Hz$ AC power signals from the production stations to the consumer.
Based on voltage levels, the power line is split into three separate classes:

- High-Voltage level (HV): $110 - 330kV$;
- Medium-Voltage level (MV): $1 - 30kV$;
- Low-Voltage level (LV): $0.1 - 1kV$.

The power line network often operates at low frequencies to reduce the influence of the skin effect. Skin effect is the tendency of an alternating electric current to become distributed within a conductor such that the current density is largest near the surface of the conductor and decreases exponentially with greater depths in the conductor.
The electric current flows mainly at the "skin" of the conductor, between the outer surface and a level called the skin depth.
Skin depth depends on the frequency of the alternating current: as frequency increases, current flow moves to the surface, resulting in less skin depth. Skin effect reduces the effective cross-section of the conductor and thus increases its effective Resistance ($R \propto \frac{1}{\Sigma}$).
Skin effect is caused by opposing eddy currents induced by the changing magnetic field resulting from the alternating current. At $50Hz$ in copper, the skin depth is about $10mm$. At high frequencies the skin depth becomes much smaller (**Figure2.3**).
Power transformers are used to interconnect networks working at different voltage classes. MV and LV classes are of particular relevance since Augier products commonly work in these voltage ranges.
In general, the interconnecting transformers only permit low frequency electrical signals to pass through while blocking high frequency signals as a intrinsic characteristic. **Figure2.4** depicts a typical electrical power grid.

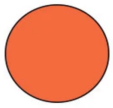

(a) Cross sectional aera of a round conductor avaible for conducting DC current.

(b) Cross sectional aera of the same conductor avaible for conducting low frequency AC.

(c) Cross sectional aera of the same conductor avaible for conducting low frequency AC.

Figure 2.3: Skin effect: skin depth behaviour with respect to the frequency increase.

2.2.1 High-voltage Transmission lines

After being generated, electric power is sent across large distances (up to several hundred kilometers) to several substations through High-Voltage power lines. High-voltage three-phase cables are the most efficient way to transport electrical power throughout lengthy transmission distances.

Overhead transmission lines cables are not insulated primarily due to these reasons:

- **Reduce weight and cost:** the thickness and material of insulation depends on the transmission voltage level: higher the voltage ,thicker shall be the insulation and so higher the weight. Hence, accumulation of ice, water derived from the rain and dirt over the line can add up the load and affect the stability of the line. To avoid this and also to save a lot of money resulting from non-isolation, High Voltage cables are left bare;

- **Reduction in conductivity:** insulating a transmission line can reduce its conductivity (the capacity of the material to carry electric current) and hence its capacity to dissipate heat. Additionally, when the voltage rises, the dielectric strength (which for an insulating material is the maximum electric field it can withstand before experiencing electrical breakdown and turning electrically conductive) drops. In order to have an insulating material capable of being effective with voltage between $110 - 330kV$, this should have an enormous thickness, which would result in an unspeakable increase in weight as well as the impossibility of dissipating the heat produced by the line due to the Joule effect.

Transmission lines don't need any good insulator as long as there is enough space between them and the ground and enough separation between the phases to prevent undesirable interference between cables. Air is a good insulator andthe volume around conductors provide sufficient insulation to the cables.

High voltage lines are nonetheless susceptible to losses, despite the fact that they are less severe than in other configurations. These losses are primarily caused by two types of effects:

- **Joule effect:** the physical effect by which the flow of current through an electrical conductor produces thermal energy. This thermal energy is then evidenced through a rise in the conductor material temperature, for this reason it is possible to call it

also "Joule heating". It is a transformation between "electrical energy" and "thermal energy" due to the resistivity of the conductor material and it is the predominant cause of losses;

- **Corona Losses:** is an electrical discharge caused by the ionization of the surrounding fluid (air) of the conductor that carries the HV. Occurs at locations where the electric field (potential gradient) at the surface of the conductor exceeds a critical value: the dielectric strength of the air. In air at sea level, the pressure is $101kPa$ and the critical value is roughly $30kV/cm$, but since this decreases with pressure, corona discharge is more of a problem at high altitudes.
  Corona discharge usually forms at highly curved regions on electrodes.They cause an high potential gradient where the air breaks down and forms plasma there first. On sharp points in the air, corona can start at potentials of $2-6kV$. It is often seen as a bluish glow in the air adjacent to pointed metal conductors carrying High Voltages and emits a characteristic crackling with a luminous halo. Must be fought decisively because it is the cause of energy losses and a number of disturbances in the form of discharges, whose spectrum exhibits substantial interference up to several MHz, and is thus relevant to PLC communication.

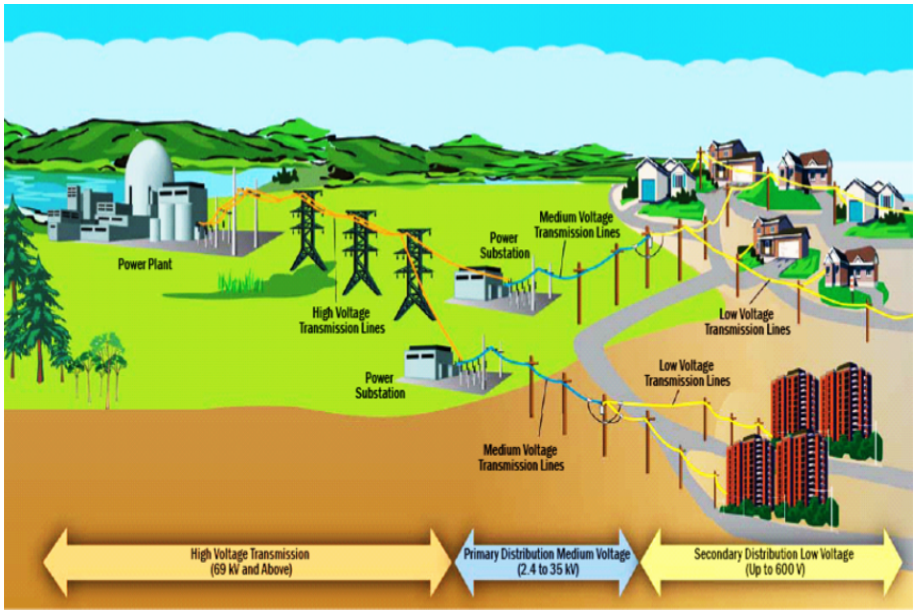

Figure 2.4: Electrical Power Grid.

It is possible to work on the same elements in order to minimize both impacts as well as the skin effect, which is always present even at low frequencies. The best options actually involve making an appropriate choice of conductive material with low resistivity and designs with big sections. Additionally, to reduce the skin effect, ropes with a steel core and a copper or aluminium alloy peripheral region that are sized for the total electric current should be used. This is because steel only serves a mechanical purpose, allowing for longer spans between pylons. About 3% of the overall current is the current that is influencing the steel component. In the case of cross-sections greater than $50mm^2$, the conductors for overhead lines are built of ropes, which are composed of multiple elementary threads wound in a big pitch helix around at the central core. The flexibility of the strings is a major advantage.

Despite the problems analyzed above, High-Voltage lines offer considerably advantages compared to Low-Voltage and Medium-Voltage lines for the power transport. By actually delivering energy at higher voltages, while still transporting the same amount of power, less energy will be lost as heat due to the Joule effect since the value of current results smaller (is proportional to the square of the current) and so the section of the cables in question is smaller. The use of High Voltage cables involves a reduction in total weight and a simplicity of the pylons that support them. Last but not least, it is possible to demostrate that using a three-phase transport method enables the use of cables with a section that is twice as small as a single-phase line while maintaining the same power and line length **[1]**.

2.2.2 Medium-voltage Transmission lines

The High-Voltage and Low-Voltage transmission lines are connected by the Medium-Voltage line. Small towns, rural communities, isolated manufacturing facilities, highways, motorways, junction tunnels, bridges, railroad tunnels, parking lots, industrial sites, amusement parks, and military installations are all served by them. Both overhead and subsurface cables may be used with the Medium-Voltage transmission lines.
In comparison to High-Voltage lines, Medium-Voltage lines employ smaller poles and wire cross sections since they transmit lower currents over distances of 2 to $50km$. These can be insulated or not depending on the mounting method (overhead or subsurface).
The overhead are attached to the pylons, separated and not insulated. Even if they travel close to urban centers, their safety is guaranteed by being at the top, the prevention from undesirable interference effect between cables by the gap between them and the insulation by the air, just like High-Voltage cables.
A typical structure of a Medium-Voltage subsurface cables includes an inner core that is primarily made of copper and aluminum and has a variety of cross sections, including sector-shaped, oval, and circular shapes, a first layer of insulation; an exterior core made of the same materials and the same section as the inner core and two additional cladding layers, as shown in the figure **Figure2.5**.

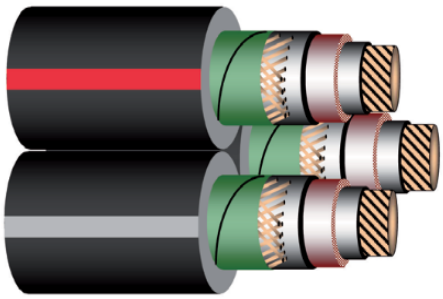

Figure 2.5: Three-wires MV subsurface cable.

Insulation and also shielding is actually necessary for subsurface solutions. It is possible to find an insulating material capable of being effective since the voltage level is between $1 - 30kV$ and also it is possible to dissipate the heat produced by the line due to the Joule effect. The insulation prevents direct contact of the conductive material with the ground, also avoiding the accumulation of dirt, but above all it must guarantee safety at relatively High Voltages. The shield, on the other hand, since this configuration often does not guarantee the spacing between the cables, prevents the interaction with each other and more generally reduces the electromagnetic effects that could come from the outside (Cross-Talk and EMI interfer-

ences). Due to the abundance of tall buildings that define urban areas, subterranean cables are favored in heavily populated places like cities, although, since they need both shielding and insulation, they are a much more expensive solution, difficult to handle and with much greater cable weights.
Normal insulating materials include XLPE (Cross Linked Polyethylene), EPR (Ethylene Propylene Rubber) and PVC (Polyvinyl Chloride). Since AUGIER is mostly focused on the distribution and control of energy across the two configurations, PLC over MV and LV is the configuration of interest **[1]**.

2.2.3 Low-voltage Transmission lines

Consumers receive $100 - 400V$ electrical power from the Low-Voltage network, which is the final segment of the electrical power line network. The LV power lines are connected to Augier's MASTER/SLAVEs by MV to LV transformers at a maximum distance of 20 meters. Typically, Low Voltage cables for industrial applications are not shielded and their phase and neutral are coupled inside of an insulating and protecting coating.
In fact, the protective sheaths guarantee cable insulation, mechanical strength and safety. Industrial applications are more concerned with transferring power than data, so using unshielded cables, even though they are less efficient at preventing interference (albeit minor interference), is not a major issue because the quality of the transferred signal is not the parameter that needs to be optimized. In contrast to MV lines, relatively short poles and wire cross sections are therefore employed since the carried current is much less. The MV version just has materials for insulation that are nearly identical **[1]**.

Figure 2.6: LV unshielded cable for industrial application.

2.3 PLC Standards and Regulations

The PLC can be divided into three different classes:

- Ultra Narrowband (UNB): this type of thecnology works with a very low data rate (about $100bps$) in the field of Ultra Low Frequency ($0.3 - 3kHz$) or at the top of the Super Low Frequency ($30 - 300Hz$).
  Very long distances, even exceeding $150km$, can be reached. The UNB-PLC transmissions are alredy mature, and implemented by at least two decades, but unlikely they adopt proprietary technologies.

- Narrowband (NB): a standard that operate in the frequency bands VLF/LF/MF ($3 - 500kHz$). This range includes the European CENELEC band ($3 - 148.5kHz$), the American FCC band ($10 - 490kHz$), the Japanise ARIB band ($10 - 450kHz$) and the Chinese EPRI band ($3 - 500kHz$). NB-PLC can be further divided between:

  - Low Data Rate (LDR): single-carrier technology with capacity data rate of a few $kbps$;
  - High Data Rate (HDR): multicarrier technology capable of data rates ranging from tens of $kbps$ to $500kbps$.

- Broadband (BB): this technology operates at frequencies of HF/VHF ($1.8-250MHz$) with a data rate range from a few $Mbps$ to several hundred $Mbps$.

Considering the NB, in different regions of the world there are different allocations of the frequency bands. The main organizations that regulate the use of the frequency bands are summarized in **Figure2.7**:

- CENELEC: European Commitee for Electrotechnical Standardization, valid for Western Europe (the countries forming the Europian Union plus Iceland, Norwey, Switzerland and England);
- ARIB: Association of Radio Industries and Businesses;
- EPRI: Electric Power Research Institute;
- FCC Federal Communications Commission **[3]**.

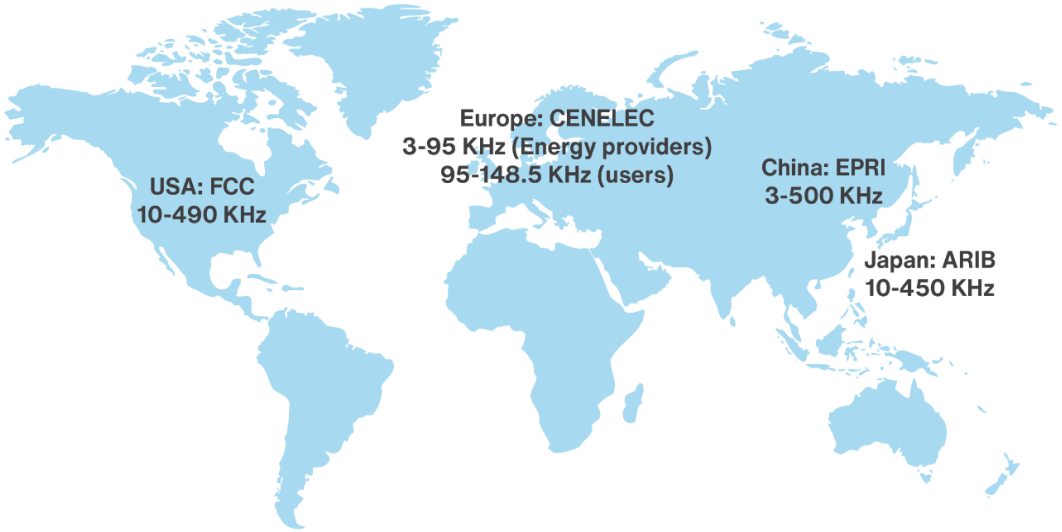

Figure 2.7: Main organizations that regulate the use of the frequency bands around the world.

The regulations related to CENELEC range are described in standard EN 50065-1 entitled "Signalling on Low-Voltage electrical installations in the frequency range $3kHz$ to $148.5kHz$". In part one of the EN-standardization paper, CENELEC range is regulated and it is subdivided into five sub-bands.
Other regulatory standards pertaining to powerline carrier communications include:

- The IEC 870 international standard on telecontrol, teleprotection and associated telecommunications for electrical power systems, as well as the IEC 1107 and 1142 standards pertaining to equipment for electrical energy measurement and load control;
- The CENELEC ENG1107 standard specifies equipment for electrical energy measurement and load control;
- In Japan a frequency band ranging from 10 to $450kHz$ is allowed **[4]**.

The **Tab7.1** shows all the frequencies made avaible from the organisations mentioned before.

REGION	*ORGANIZATION*	*FREQUENCY RANGE [kHz]*
EUROPE	CENELEC A	3-9
	CENELEC B	9-95
	CENELEC C	95-125
	CENELEC D	125-140
		140-148.5
JAPAN	ARIB	10-450
CHINA	EPRI	3-90
		3-500
USA	FCC	100-490

Table 2.1: Summary of all the frequency ranges and their sub-bands made avaible from the different world organisations.

2.4 PLC Modulation

The fundamental principle of the system is the carrier wave concept. In order to send information, the transmitter (AUGIER Master), which is connected to the LV electrical system $(100-240V)$, modulates a low-frequency electrical wave $(50-60Hz)$ with higher frequency $(\sim kHz)$ and lower voltage data signals $(5V)$. Signals at different frequencies are allowed on the same cables and transferred to the Power Line via a step-up transformer and a signal coupler (MCEP), capable of adapting the LV modulated signal to the MV line.
After traveling a distance of several kilometers, a step-down transformer performs the opposite function, and the receiver separates the signal from the electrical one using the proper filters (AUGIER SLAVE). One MASTER and multiple SLAVEs are typically on the same line and able to communicate back and forth to exchange information.
Figure (**Figure2.8**) illustrates an example of modulation for a PLC system. To maximize the number of channels and maintain excellent noise immunity, the modulation strategy needs special consideration **[3]**.

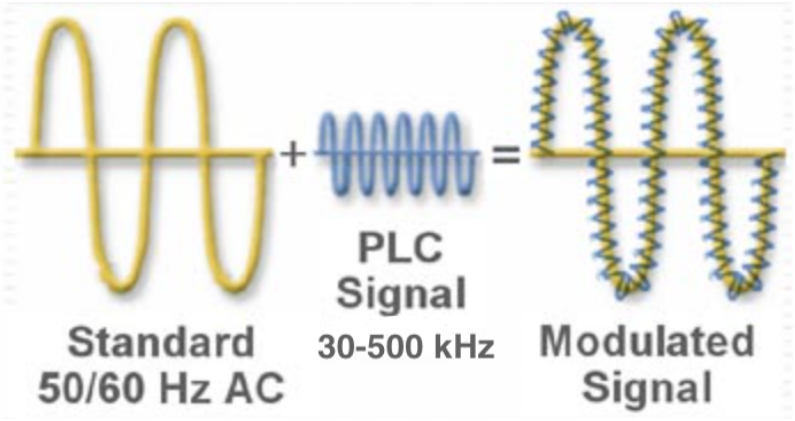

Figure 2.8: The basic principle of Power Line Communication.

2.4.1 Orthogonal Frequency Division Multiplexing (OFDM)

Background noise, impulsive noise, and narrowband interferences, which are frequently seen in both LV and MV distribution networks, can have a substantial impact on the PLC channel. According to the location, the type of connected equipment, frequency and environment, the PLC channel's parameters and characteristics can vary greatly; in fact, the power line is quite hostile. International standards have adopted the OFDM (Orthogonal Frequency Division Multiplexing) modulation techniques based on multiple carrier frequencies as a way to get around these limitations and improve the robustness of PLC.
On the basis of multi-carrier OFDM, the International Telecommunications Union (ITU) and the Institute of Electrical and Electronics Engineers (IEEE) have developed some guidelines for NB-PLC up to $500kHz$. While the G3-PLC protocol (ITU-T G.9903) is one of the narrow-band OFDM approaches that the ITU specifies, IEEE P1901.2 (IEEE 1901.2-2013) advised using a related OFDM technique at the physical layer **[6]**.
OFDM is a method of digital data modulation, whereby a single stream of data is divided into several parallel sub-streams for transmission via multiple channels. It uses the principle of Frequency Division Multiplexing (FDM), where the available bandwidth is divided into a set of sub-streams having separate frequency bands.
The main concept in OFDM is orthogonality of the sub-carriers. The orthogonality allows simultaneous transmission on a lot of sub-carriers in a tight frequency space without interference from each other. In case of FDM, guard bands are inserted so that interference between the signals, resulting resulting in channel cross-talk, does not occur.
However, since orthogonal signals are used in OFDM, no interference occurs between the signals even if their sidebands overlap. So, guard bands can be removed, thus saving bandwidth as shown in the figure below (**Figure2.9**).

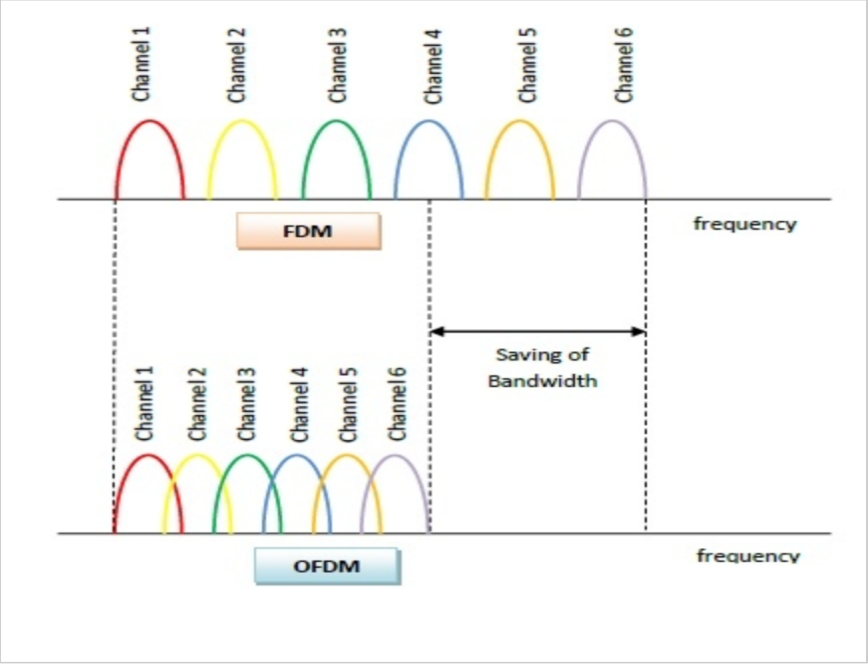

Figure 2.9: FDM and OFDM working principles and the saving in bandwidth obtained by OFDM.

Each subcarrier is modulated with a conventional digital modulation scheme (such as QPSK, 16QAM) at low symbol rate. In the frequency domain, each transmitted subcarrier results in a sinc function spectrum with side lobes that produce overlapping spectra between subcarriers. as shown in **Figure2.10**. This results in subcarrier interference except at orthogonally spaced frequencies. At orthogonal frequencies, the individual peaks of subcarriers all line up with the nulls of the other subcarriers. This overlap of spectral energy does not interfere with the system's ability to recover the original signal. The receiver multiplies the incoming signal by the known set of sinusoids to recover the original set of bits sent.

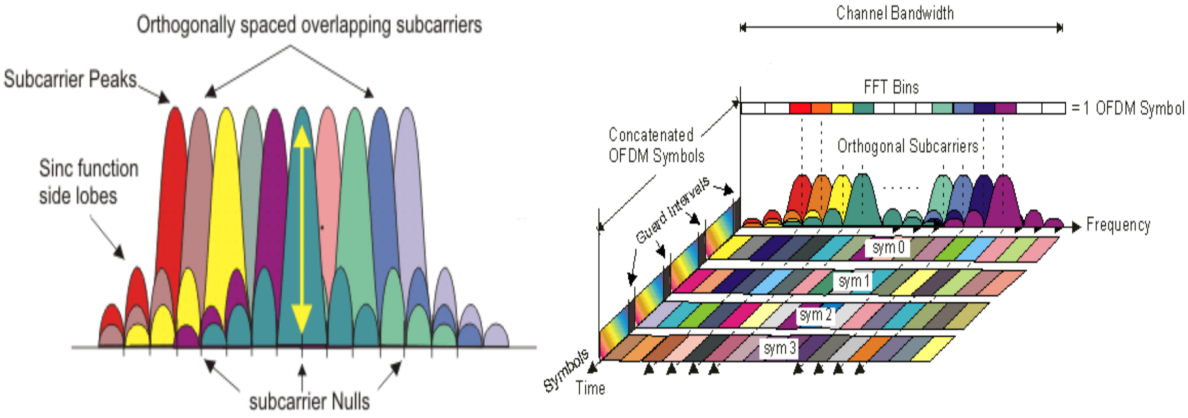

Figure 2.10: OFDM frequency spectra and time representation.

An OFDM signal offers an advantage in a channel that is affected by a deep frequency fading. From **Figure2.11**, it can be seen that when using an OFDM modulation, only two small portions of the sub-carriers would be affected by the fading; the remaining portion of the lobes is unaffected. With this type of modulation, it is possible to maintain the signal largely intact losing just a small subset of the (1/N) bits. With proper coding, this can be recovered, which would not be possible with other types of modulation.

2.4.2 G3-PLC

G3-PLC is a proven Powerline Communication technology offering lowest total cost of ownership and independency on telecom operators. It facilitates high-speed, highly-reliable, long-range communication over the existing powerlines. The features and capabilities of G3-PLC have been developed to address the difficult challenges of powerline communications. While earlier approaches were a step in the right direction, they fall short of meeting the technical and reliability requirements necessary in the hostile environment of PLC. G3-PLC meets these requirements because of its unique features such as a mesh routing protocol to determine the best path between remote network nodes, a "robust" mode to improve communication under noisy channel conditions and channel estimation to select the optimal modulation scheme between neighbouring nodes. The unique features of G3-PLC meet these requirements:

- OFDM-based PHY (BPSK, QPSK, 8PSK) makes efficient use of the spectrum;
- compliant with world regulatory bodies such as CENELEC, ARIB, and FCC ($30 - 500kHz$);

- standards based — pre-standard in IEEE, ITU, IEC/CENELEC and IEC/SAE;
- two layers of Forward Error Correction (FEC) for robust data communication in harsh channels;
- adaptive tone mapping for optimal bandwidth utilization;
- channel estimation to select the optimal modulation scheme between neighbouring nodes;
- "robust" mode to improve communication under noisy channel conditions;
- IEEE 802.15.4-based MAC layer well suited to low data rates;
- AES-128 cryptographic engine for optimum data security;
- mesh routing protocol to determine the best path between remote network nodes.

Usually PLC can reach point-to-point ransmission distances up to $1,7km$ point-to-point communication, depending on network characteristics and the electrical grid topology, can be achieved in actual field conditions.
The Data Rate is up to $281kbps$ in FCC and up to $45kbps$ in CENELEC-A (typical UDP throughput in FCC is $83kbps$ and in CENELEC-A $17kbps$).

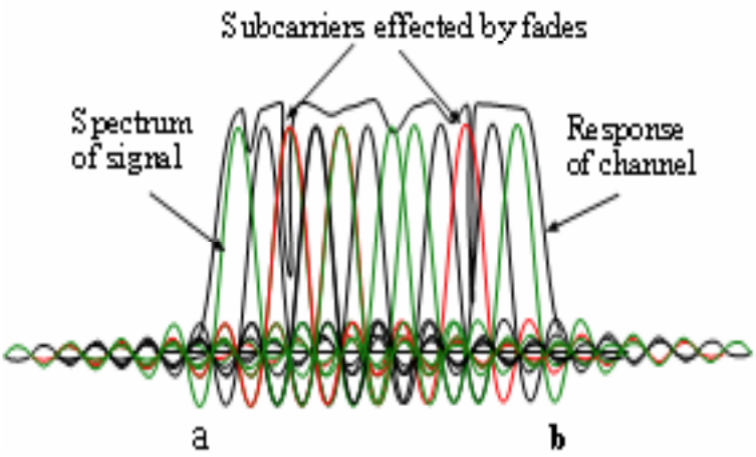

Figure 2.11: Channel affected by fading ad its effect on the lobes of the modulated signal.

2.5 Noise Characteristics of a PLC Circuit

A PLC line is a very tough system, as is already explained. Unlike at high frequencies required for data transmission, power line cables are made to transmit High Voltage at low frequencies. Additionally, the network of power lines has erratically connected and disconnected electric equipment. As a result, there are substantial noise, fluctuating network impedance, and high attenuation. Impedance mismatch is also caused by the diverse nature of wiring techniques, loads connected to the PLC network with mismatched impedance to the feed lines, and branches connected to the network.
In contrast to other communication channels, the powerline channel also experiences noise that is dependent on the electrical devices connected to the line and that can change extremely rapidly. Four main categories can be used to separate them.

2.5.1 Noise Synchronous to the (50 or 60Hz) power system frequency

All types of switching devices, specific power supplies, and silicon-controlled rectifiers (SCRs), which are nearly typically found in light dimmers in the form of triacs and are synced with the main frequency, are the main generators of this sort of noise.
These switches emit noise at high harmonics of the power system frequency because they switch an integer number of times each cycle (the pulses have a brief duration of a few microseconds).
This noise's spectrum is made up of a number of harmonics of its fundamental $100Hz$ components. Additionally, photocopies produce loud noise impulses twice as fast as the power system. They can be classified as a Superimposed Transient disturbances with a damped oscillations. In order to decrease the effect of this kind of noise it is possible to install x/x filters at the imput of the receivers with spectral nulls at the power system frequency.

2.5.2 Noise with a smooth spectrum

Appliances like universal motors, electrical drills, and other devices that don't operate synchronously with the powerline frequency are the main producers of this type of noise. The motor's internal brushes, which generate current switching at intervals that depend on motor speed, are the real source of noise.
This kind of noise can be modeled as a white noise over the small CENELEC A-band and in general as Superimposed Disturbances with Persistent and Coherent oscillations. In order to decrease the effect of this kind of noise a Forword Error Correction (FEC) codes combined with interleaving (to provide time diversity) should be implemented.

2.5.3 Single event impulse noise

The main cause of this type of noise is various switching occurrences. Depending on the size of the capacitor, a device's on/off switching that uses a capacitor for power factor correction can result in significant transient voltages. This kind of noise can be classified as a Superimposed Disturbances with a Transient impulses.
In order to decrease the effect of this kind of noise a Forword Error Correction (FEC) codes combined with interleaving (to provide time diversity) should be implemented.

2.5.4 Periodic noise, not synchronous to the power system frequency

Special lines in this form of noise can be seen at frequencies unrelated to the power system frequency. This type of noise was most frequently produced by fluorescent lighting and television receivers. They are extremely harmful for a PLC line, but it is likely that they are not present in the configuration being studied because AUGIER often runs in urban areas and in a closed loop, which prevents interference from civil dwellings.
They can be classified as Superimposed Disturbances with Persistent and Coherent oscillations. In order to avoid the this kind of noise, the television line frequency and its harmonics should be avoided when modulating the signal onto the channel and some kind of frequency diversity (frequency hopping) combined with FEC should be implemented to cope with unknown frequencies of computer monitors **[4]**.

2.6 PLC Transmitter/Receiver Differential signalling

Differential signaling employs two complementary voltage signals in order to transmit one information signal and is largely used when are present common mode interferences. The differential channel requires a pair of conductors: one carrying the signal and the other its inverted copy. The pair of conductors can be wires in a twisted-pair or ribbon cable or traces on a printed circuit board.The transmitter split the sending information signal while the receiver extracts information by detecting the potential difference across the inverted and non-inverted signals. When the signal on one line is logical high, it is logical low on the other line, and vice versa as shown in **Figure2.12**.
The two voltage signals are "balanced," meaning that they have equal amplitude and opposite polarity relative to a common-mode voltage. The return currents associated with these voltages are also balanced and thus cancel each other out; for this reason, it is possible to say that differential signals have (ideally) zero current flowing through the ground connection.With differential signaling, the transmitter and receiver don't necessarily share a common ground reference. However, the use of differential signaling does not mean that differences in ground potential between transmitter and receiver have no effect on the operation of the circuit as shown in the **Figure2.13**.

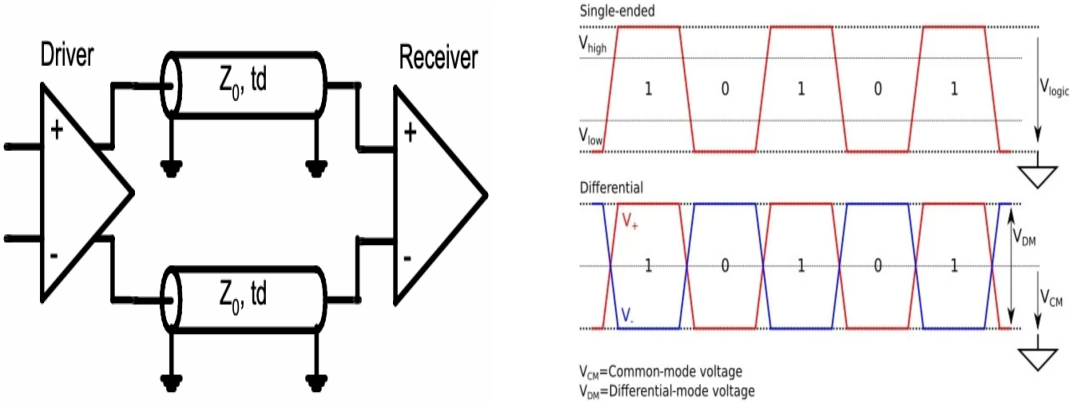

(a) Differential signalling transmission lines.

(b) Single-ended vs Differential-ended: Generic timing diagram.

Figure 2.12: Differential signaling.

If multiple signals are transmitted, two conductors are needed for every signal, and it is often beneficial to include a ground connection, even when all the signals are differential. Thus, for example, transmitting 16 signals would require 33 conductors (compared to 17 for single-ended transmission). This demonstrates an obvious disadvantage of differential signaling.However, there are important benefits of differential signaling that can more than compensate for the increased conductor count.

2.6.1 No Return Current

Since we have (ideally) no return current, the ground reference becomes less important. The ground potential can even be different at the sender and receiver or moving around within a certain acceptable range.

2.6.2 Resistance to Incoming Electromagnetic Interference and "Cross-Talk"

Both inverted and non-inverted signals are equally affected equally by EMI (Electromagnetic Interference) or Cross-talk (interference created by neighboring signals) that couples to the differential conductors from the outside. This is called Common-Mode interference and has the same magnitude (due to the differential conductors being tightly coupled) and polarity for both differential pair conductors. The receiver circuitry will be significantly immune to common-mode interference: as it constructs the received signal by subtracting the voltages present on the differential pair conductors, the aforementioned interference will be mathematically cancelled at the receiver side. For this reason differential pairs have an higher noise immunity (and can use lower voltage levels) than single-ended (i.e., ground-referenced) systems.

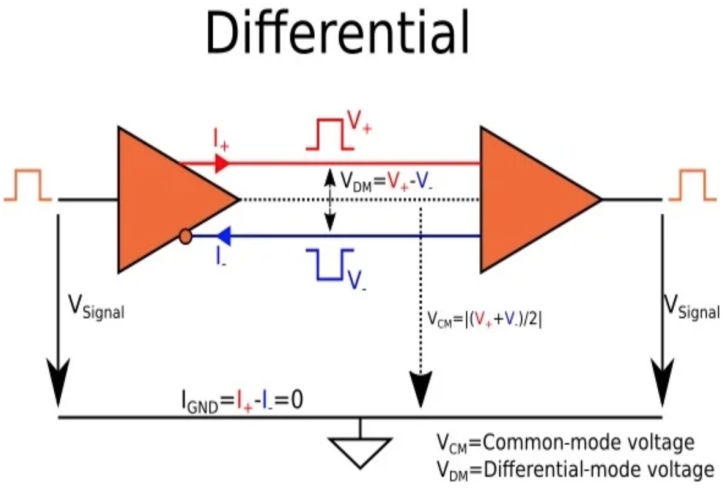

Figure 2.13: Differential signalling topology.

2.6.3 Reduction of Outgoing EMI and Cross-Talk

Significant levels of EMI can be produced during abrupt transitions, such as the rising and falling edges of digital signals. However, the two signals in a differential pair will produce electromagnetic fields that are (ideally) equal in magnitude but opposite in polarity. Both single-ended and differential signals produce EMI. This assures that the emissions from the two wires will mostly cancel each other out, together with methods that preserve close closeness between the two conductors.

2.6.4 Lower-Voltage Operation

Single-ended signals must maintain a relatively high voltage to ensure adequate signal-to-noise ratio (SNR). Common single-ended interface voltages are $3.3V$ and $5V$.
Because of their improved resistance to noise, differential signals can use lower voltages and still maintain adequate SNR. Also, the SNR of differential signaling is automatically increased by a factor of two relative to an equivalent single-ended implementation, because the dynamic range at the differential receiver is twice as high as the dynamic range of each signal within

the differential pair, as shown in **Figure2.14**. They are also less sensitive to the attenuation of the signal in the transmission medium because the receiver design typically allows sufficient gain to reproduce the original signal.

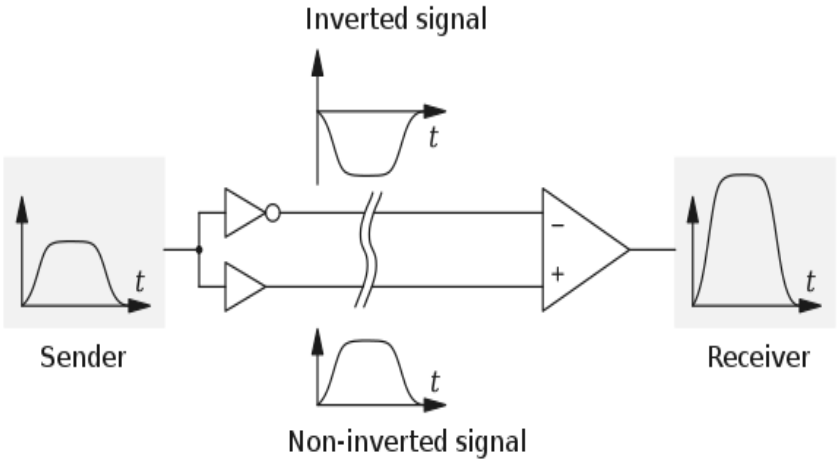

Figure 2.14: A signal transmitted differentially. Notice the increased amplitude at the receiving end.

2.6.5 High or Low State and Precise Timing

In differential signals, determining the logic state is straightforward. If the non-inverted signal's voltage is higher than the inverted signal's voltage, you have logic high. If the non-inverted voltage is lower than the inverted voltage, you have logic low.
The transition between the two states is the point at which the non-inverted and inverted signals intersect and it is called the crossover point. It is important to match the lengths of wires or traces carrying differential signals in order to obtain the best timing precision.
The crossover point must correspond exactly to the logic transition, for this reason is important to match the lengths of wires or traces carrying differential signals, to obtain the correct digital 1 or 0. When the two conductors in the pair are not of equal length, the difference in propagation delay will cause the crossover point to shift, deleting some digital transition with the lost of some bits as a consequence.

2.7 PLC Transmitter/Receiver Impedance Variation

When building PLC systems, impedance characterisation is crucial because it establishes where the transmitter operates and where the receiver takes the signal. PLC network access impedance varies with time, frequency, location, and whether the transmitter and receiver are turned on or off. It is a complex-valued number and the impedance magnitudes ($|Z|$) and phase (ϑ) of a PLC network access can be used to express the total complex impedance. Some impedance matching techniques are based on impedance magnitudes ($|Z|$), which simplify the circuit construction (the phases are not considered).

It is typical to assume that the internal impedance of PLC communication devices is 50Ω; nevertheless, this value is highly dependent on the operating frequency.
The absolute value of a transmitter/receiver impedance measured as a function of frequency and as determined by the least squared fit, is expressed with an experimental relation **[8]**:

$$|Z| = 0.005 * f^{0.63}[\Omega] \tag{2.1}$$

Impedance matching issues can be divided into three groups based on the source/load impedance types. The real-to-real impedance matching problem (also known as the Insertion Loss problem) is the first, and it takes into account the impedance matching between a resistive source and resistive load. Second, the difficulty of matching a resistive source to a complex load is known as the real-to-complex impedance matching problem. The third problem is the complex-to-complex impedance matching problem, in which the impedances of the source and load are both complex-valued. The **Tab7.2** shows astandard overview of the access impedance measurements for narrowband and broadband PLC **[8]**.
Knowing that the transmission frequency chosen by AUGIER falls within the CENELEC-C range and is specifically $133kHz$, it is possible to derive an impedance value of $|Z| = 8.45\Omega$ from the relation above (**7.1**), which falls into the range for urban application ($1\Omega<|Z|<17\Omega$) indicated in **Tab7.2**.

FREQUENCY BANDS	***FREQUENCIES***	**$\|Z\|$ or R/X**
Narrowband	5-20kHz	$0\Omega<R<4\Omega$ $1\Omega<X<12\Omega$
	10-170kHz	$3\Omega<\|Z\|<17\Omega$ for rural; $1\Omega<\|Z\|<17\Omega$ for urban; $1\Omega<\|Z\|<21\Omega$ for industrial;
	0-500kHz	$1\Omega<\|Z\|<90\Omega$
BroadBand	20kHz-30MHz	$0.3\Omega<\|Z\|<800\Omega$ $0\Omega<R<598\Omega$, $-800\Omega<X<686\Omega$
	1–100 MHz	$0\Omega<R<250\Omega$, $-175\Omega<X<150\Omega$

Table 2.2: The overview of the access impedance measurements for narrowband and broadband PLC.

It was decided to use $|Z| = 10\Omega$ as a suitable approximation for the transmitter/receiver's imput impedance (AUGIER MASTER/SLAVEs) at the target frequency of $133kHz$.
The impedance mismatch between the MASTER/SLAVEs and the transmission line and, conseuqntly, the value of the associated reflections that will be used to calculate the maximum power transfer, are all evaluated using this parameter, making it crucial for the future work. Real-to-real impedance matching between a resistive transmitter/receiver and a resistive power line characteristic impedance must be achieved in order to reduce signal reflections. To enhance signal power transfer, real-to-complex impedance matching is performed between a resistive transmitter/receiver and a complex PLC network access impedance.
In order to establish a complex-to-complex impedance matching between a complex generator and a complex load, decreasing the Insertion Losses, the maximization power transfer matching is run at $Rg = Rl$ and $Xg = -Xl$.

3 Transmission Lines

In an isotropic and homogeneous medium, the electric and magnetic field components are mutually transverse (perpendicular to each other) to the direction of propagation (direction of energy transfer), assumed to be the z-direction as shown in the figure below (**Figure3.1**).

- **Isotropic:** no dependency of the medium properties with field direction (the refractive index n is equal evrywhere);
- **Homogeneous:** no dependency of medium properties with point position (the refractive index n does not depend on the position).

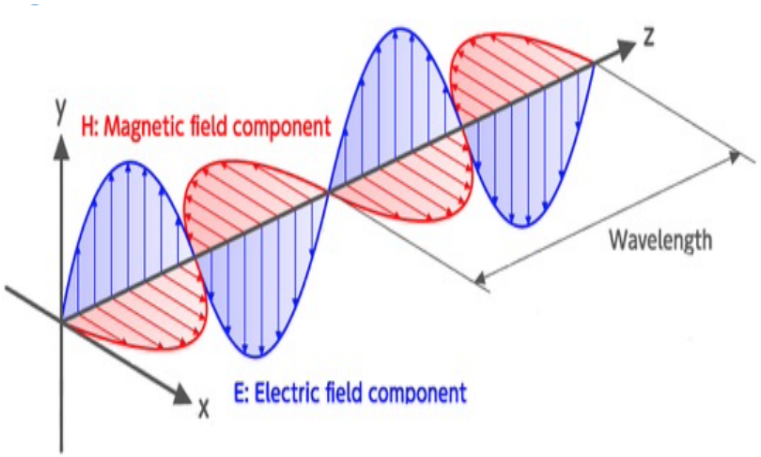

Figure 3.1: Electromagnetic Field propagation.

A PLC signal passes through cables of various geometries to which there is a metal conductor and generally an insulator. The Electric and the Magnetic Field propagates in the conductor which can be described as a transmission line, surrounded by a medium that is neither isotropic nor homogeneous, but always along the z-direction.

3.1 Distributed Circuit Model of a Transmission Line

Consider a conductor with negligible transverse dimensions ($a \ll \lambda, b \ll \lambda$), where λ is the wavelength of the signal under interest and length L is the only relevant dimension, as shown in the figure **Figure3.2**.

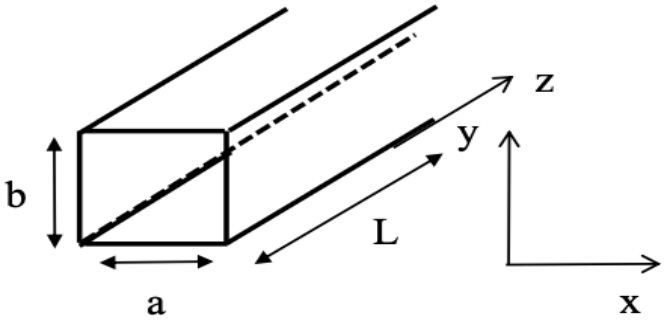

Figure 3.2: Conductor with negligible transverse dimensions with respect to the transverse one.

It is possible to distinguish three main situations:

- $l = \frac{L}{\lambda} \ll 1$, Quasi static regime $\Rightarrow$ Lumped parameter circuit;
- $l = \frac{L}{\lambda} \simeq 1$, Resonance regime $\Rightarrow$ Distributed parameter circuit;
- $l = \frac{L}{\lambda} \gg 1$, "Optical" regime $\Rightarrow$ (Classical) Optical components.

The Distributed parameter Circuit is the model under interest and the one used to describe transmission lines since the length of the circuit (L) is comparable with the period (T) of the propagating wave. In fact, it is not possible to neglect the propagation time t to travel the length L with respect to the period T or the "change of the wave in space" L with respect to λ.

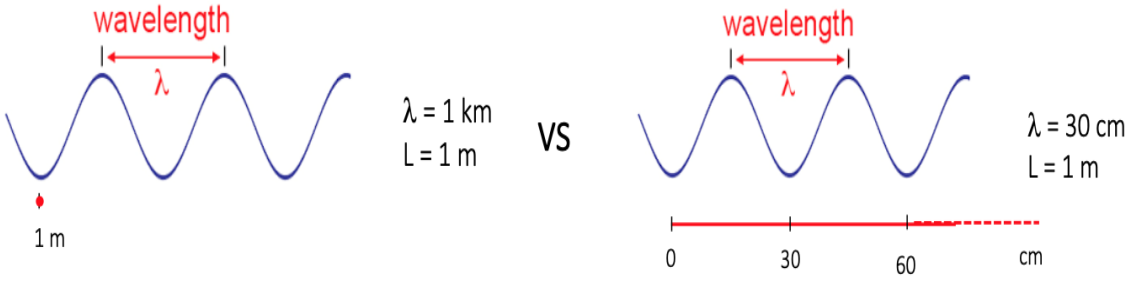

Figure 3.3: Wavelength vs length of the line.

3.2 Lines with losses

Transmission lines can be modeled with L' (inductance per unit length $\left[\frac{H}{m}\right]$), C' (capacitance per unit length $\left[\frac{F}{m}\right]$) parameters, which describe their lossless operation, and in addition, the parameters R' (resistance per unit length $\left[\frac{\Omega}{m}\right]$), G' (conductance per unit length $\left[\frac{S}{m}\right]$) which describe the losses **[9]**. A transmission line can be considered as a cascade of infinitesimal segments Δz, each consisting of a resistance in series with an inductance and a conductive

element in parallel to a capacitive one as shown in the figure below (**Figure3.4**):

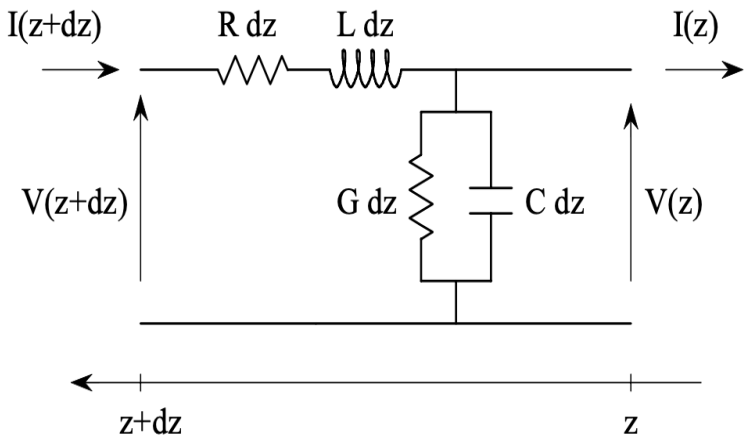

Figure 3.4: Distributed parameter model of a transmission line.

Applying Kirchhoff's voltage and current laws, it is possible to obtain:

$$\begin{aligned} V(z) &= V(z+dz) + (Rdz + j\omega Ldz)V(z+dz) \\ I(z) &= I(z+dz) + (Gdz + j\omega Cdz)V(z+dz) \end{aligned} \tag{3.1}$$

From the equation above (**3.1**), after some manipulations it is possible to get the following differential equations also called Telegrapher's equations, which show how the voltage and current along a line can change due to its non-idealities:

$$\begin{aligned} \tfrac{dV(z)}{dz} &= V'(z) = -(R + j\omega L)V(z) \\ \tfrac{dI(z)}{dz} &= I'(z) = -(G + j\omega C)I(z) \end{aligned} \tag{3.2}$$

It is easily verified that the most general solution of this coupled system is expressible as a sum of a forward/incident (V_+, I_+; travels/hifts toward positive z values) and a backward/reflected (V_-, I_-; travels/shifts toward negative z values) moving wave:

$$\begin{aligned} V(z) &= V_+e^{-jkz} + V_-e^{jkz} = V_+e^{-(\alpha+j\beta)z} + V_-e^{(\alpha+j\beta)z} \\ I(z) &= I_+e^{-jkz} + I_-e^{jkz} = I_+e^{-(\alpha+j\beta)z} + I_-e^{(\alpha+j\beta)z} \end{aligned} \tag{3.3}$$

Where:

- k is the complex wavenumber $k = \beta - j\alpha \ \epsilon \ \mathbb{C}$;
- β is the propagation constant $\left[\frac{rad}{m}\right]$;
- α is the attenuation constant $\left[\frac{Np}{m}\right]$;

The attenuation constant (α) can be further divided into two different contributions, each of which due to a characteristic parameter of the line: the resistance and conductance per unit

length, R' and G'. These two attenuation coefficients due to conductor and dielectric losses are then expressible in terms of characteristic impedance Z_0 by the following equations:

$$\alpha_c = \frac{R'}{2Z_0}, \qquad \alpha_d = \frac{1}{2}G'Z_0 \tag{3.4}$$

Finally α can be obtained as the sum of the two contributions:

$$\alpha = \alpha_c + \alpha_d \tag{3.5}$$

The attenuation in $\frac{dB}{m}$ will be $\alpha_{dB} = 8.686\alpha$. This expression tend to somewhat underestimate the actual losses, but it is generally a good approximation. Usually the α_c term grows in frequency like $\sqrt{f}$ and the α_d, like f.
Propagation means time shift which, in the phasor domain, results in a phase change given by the propagation constant along the z direction ($\mp\beta z$). It is possible then to define a series impedance Z' and a shunt admittance Y' per unit length by combining R' with L' and G' with C':

$$\begin{aligned} Z' &= R' + j\omega L' \\ Y' &= G' + j\omega C' \end{aligned} \tag{3.6}$$

Finally the characteristic complex impedance of the line is given by the equation below:

$$Z_{0,complex} = \sqrt{\frac{Z'}{Y'}} = \sqrt{\frac{R' + j\omega L'}{G' + j\omega C'}}\ \epsilon\ \mathbb{C} \tag{3.7}$$

If there are no losses ($R' = G' = 0$), the characteristic impedance of the line will be purely real. However, even in the presence of losses ($R' \neq 0, G' \neq 0$) it can be demonstrated that the complex impedance of the network turns out to be real.

$$Z_0 = \sqrt{\frac{L'}{C'}}\ \epsilon\ \mathbb{R} \tag{3.8}$$

Note however that, in this case, even if the characteristic impedance of the line is purely real, due to the presence of the losses (α), the wave will attenuate in its propagation.
What happen in reality is that the characteristic impedance of a line, although it is a characteristic parameter, does change with frequency. At high frequencies the loss components are effectively zero and Z_0 depends only on L' and C', but at low frequencies, R' and G' cannot be ignored and contribute significantly to the line impedance. There is a "corner frequency" where one regime takes over from the other. So, the Z_0 behaviour can be summarized as follow:

- **Low frequency curve:** $Z_{0,LF} = \sqrt{\frac{R'}{j\omega C'}}$
- **Transition curve:** $Z_{0,complex} = \sqrt{\frac{R'+j\omega L'}{G'+j\omega C'}}$
- **High frequency curve:** $Z_{0,HF} = \sqrt{\frac{L'}{C'}}$

3.3 Typical Transmission Lines Geometries

The geometries of the transmission lines vary depending on the type of application. The primary focus of AUGIER's work is Medium/Low Voltage and the thesis's main objective is

to investigate the data exchange ($\sim kHz$) between the two. It is important to understand the properties of the lines in question because they carry information via real cables, which are subjected to losses and were not initially intended to carry data but rather electrical power, resulting in relative High Voltages at low frequencies ($50 - 60Hz$). Given that AUGIER has selected $133kHz$ (belonging to the CENELEC-C band) as the working frequency for data exchange, special attention will be devoted to the behaviour of the various cables at this frequency and its surroundings. Following the study of the various geometries, the characteristics of the cables with respect to the frequency will be simulated on Matlab and compared to the characteristics of real cables actually involved on a PLC line.

3.3.1 Two-Wire Cables

In a two-wire transmission line, both of the two parallel cylindrical conductors having a radius a, are coated by a dielectric material (ε), such as EPR (Ethylene Propylene Rubber) and are separated from one another by a distance d. The phase is typically carried by the red cable and the neutral is typically carried by the black one. The two cables are joined together by an outer protective sheath made of PCP (Polychloroprene), which also serves as a guarantee of mechanical strength. This is shown in the **Figure3.5**. They are typically used in industrial LV applications such as transformers, because they are not shielded, which implies a considerably more susceptibility to cable interferences than shielded ones.

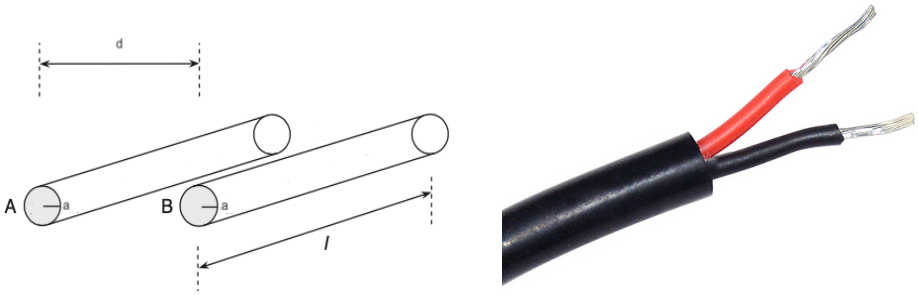

(a) **(b)**

Figure 3.5: Cross section area of a two-wire cables and a real one.

In fact, cables are usually subject to the following interferances:

- **"Cross-Talk" Interference:** is transmitted capacitively or by electromagnetic induction, when DC, AC or pulsating signals are transmitted in the different pairs of cable. Electromagnetic interference can be minimal. Capacitive noise, on the other hand, should be eliminated or reduced;
- **Outside Interference (Electromagnetic Interference EMI):** the influence of magnetic and electrostatic fields cannot be neglected. The type of shielding and the material used must be suitable for the type of interference.

Industrial applications are more concerned with transferring power than data, so using unshielded cables, even though they are less efficient at preventing interference (albeit minor interference), is not a major issue because the quality of the transferred signal is not the parameter that needs to be optimized. These cables also enable the creation of extremely thin sections, have far lower stiffnesses which result in better handling and easier assembly and are significantly less expensive due to their lack of an outer shield, so less material.

PLC communication involves the transmission of data via a line that is already in place and was intended for power transport rather than communication, for the reasons already stated. In reality, even while two-wire cables are highly effective from a cost-benefit standpoint from an industrial perspective, for a PLC line this translates into an increase in terms of losses, noises and interferences. Fortunately, Low Voltage cables on a transmission line are far shorter in length than Medium Voltage cables. Therefore, although more subject to problems, these issues only affect a limited portion of the line, not seriously affecting the PLC signal's quality. Because of this, it will be crucial to understand when to optimise the engaged sections in order to lower the characteristic impedance Z_0 (and subsequently the reflections) and losses α_{dB}, and when this won't be necessary because the cost-benefit ratio won't be much benefited.
Given that data is carried differentially on the phase and neutral wires and that both cables influence each other's behaviour because they are not shielded, the total characteristic parameters can be determined as if the line were a single line:

$$Z_0 = \frac{\eta}{\pi} acosh\left(\frac{d}{2a}\right), \quad L' = \frac{\mu}{\pi} acosh\left(\frac{d}{2a}\right), \quad C' = \frac{\pi\varepsilon}{acosh\left(\frac{d}{2a}\right)} \tag{3.9}$$

$$R' = \frac{1}{a}\sqrt{\frac{\mu f}{\pi\sigma}}, \quad G' \simeq \omega C' tan\delta \tag{3.10}$$

Where:

- μ is the permeability of the material ($\mu = \mu_0\mu_r$);
- μ_0 is the vacuum permeability, equal to $\mu_0 = 4\pi \times 10^{-7}\left[\frac{H}{m}\right]$;
- μ_r is the relative magnetic permeability of the material (dimensionless), that usually is approximate $\simeq 1$ for non magnetic media;
- ε is the dielectric permittivity of the material ($\varepsilon = \varepsilon_0\varepsilon_r$);
- ε_0 is the vacuum dielectric permittivity, equal to $\varepsilon_0 = 8.85 \times 10^{-12}\left[\frac{F}{m}\right]$;
- ε_r is the relative permittivity of the material (dimensionless);
- η is the characteristic impedance of the dielectric medium between the conductors ($\eta = \sqrt{\frac{\mu}{\varepsilon}}[\Omega]$);
- ω is the natural frequency linked to frequency ($f[Hz]$) $\Rightarrow$ $\omega = 2\pi f\left[\frac{rad}{s}\right]$;
- tan δ is the loss tangent (dimensionless);
- σ is the electrical conductivity $\left[\frac{S}{m}\right]$.

These formulas will then be implemented on Matlab as a function of frequency to plot the values in a range that will go from $9kHz$ to $5MHz$ and finally compared with real values acquired from the measurements.

3.3.2 Coaxial Cable

The coaxial cable, depicted in (**Figure3.6**), is the most widely used transmission line. It consists of two concentric conductors of inner and outer radii of a and b, with the space between them filled with a dielectric ε, such as XLPE (Cross Linked Polyethylene), EPR (Ethylene Propylene Rubber) and PVC (Polyvinyl Chloride). In highly populated locations, they are

employed for subterranean Medium Voltage power transmission applications. Although it is a less common technology for this range of Voltage ($\sim kV$) since it requires shielding and insulation that is very expensive expecially for long distances, as well as higher costs assembly because they must be installed underground and therefore include work with all of that involves, it is necessary when overhead assembly is not an alternative.
It is possible to find an insulating material capable of being effective for this voltage level and also it is possible to dissipate the heat produced by the line due to the Joule effect. The insulation prevents direct contact of the conductive material with the ground, also avoiding the accumulation of dirt, but above all it must guarantee safety at relatively High Voltages. The shield, on the other hand, since this configuration often does not guarantee the spacing between the cables, prevents the interaction with each other and more generally reduces the electromagnetic effects that could come from the outside (Cross-Talk and EMI interferences).
The characteristic impedance of the cable (Z_0) and hence the inductance (L'), capacitance (C'), resistance (R') and conductance (G') per unith length, are given by the following equations:

$$Z_0 = \frac{\eta}{2\pi} ln\left(\frac{b}{a}\right), \qquad L' = \frac{\mu}{2\pi} ln\left(\frac{b}{a}\right), \qquad C' = \frac{2\pi\varepsilon}{ln\left(\frac{b}{a}\right)} \tag{3.11}$$

$$R' = \frac{a+b}{2ab}\sqrt{\frac{\mu f}{\pi\sigma}}, \qquad G' \simeq \omega C' tan\delta \tag{3.12}$$

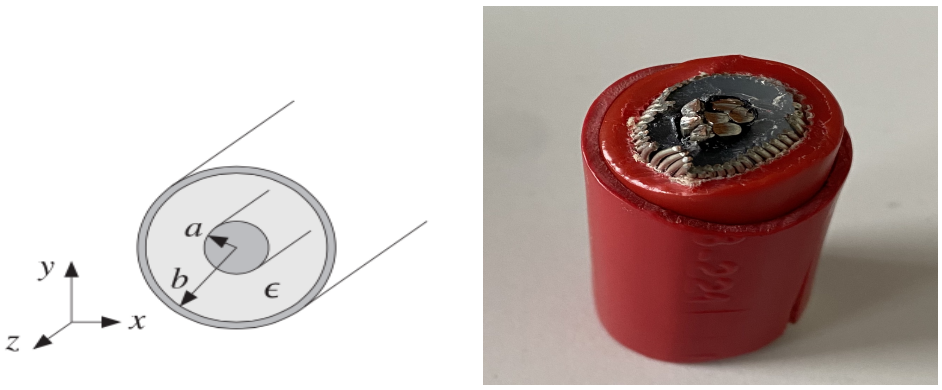

(a) **(b)**

Figure 3.6: Cross section area of a coaxial cable a real one.

Three parallel coaxial cables, each holding one phase, are used in a three-phase power transmission system. Since the signal is differential, two different configurations can be used for data exchange:

- **Phase-Ground configuration:** the same cable's phase and ground carry the signal and the inverted signal;
- **Phase-Phase configuration:** the signal travels on one phase while the inverse one on another.

Also for this geometry, comparisons will be made between experimental data collected from measurements and results from the above formulas as a function of frequency. To determine which design is preferable for data transmission in terms of characteristic impedance (Z_0) and line losses (α_{dB}), the Phase-Ground and Phase-Phase configurations will also be compared.

3.3.3 Three-Wire Coaxial Cable

Another type of transmission line for subsurface three phase Medium Voltage power is a three-wire coaxial cable. A three-wire cable has different advantages over three single-wire coaxial cables when it comes to transporting power over a three-phase line, including:

- there is less stiffness than a single-wire cable, much less when three of these are joined together;
- a three-wire cable weighs less per unit length $\left[\frac{kg}{km}\right]$ than three single-wire cables with the same section;
- a three-wire cable occupies less physical space than three single coaxial cables arranged independently and in parallel because the three single cables are shielded and mounted together inside an outer protective sheath. This makes transport, assembly, and handling considerably simpler;
- three-wire cables are much less expensive overall per unit length $\left[\frac{eur}{km}\right]$ than three single-wire coaxial cables with the same section.

As will be seen later, with the same section, compared to the transmission of data over a three-phase line made up of three single coaxial cables, this geometry has significant advantages in terms of characteristic impedance (Z_0) and losses (α_{dB}) along the line.
Usually, the three wires inside the outer protective sheath have a symmetric configuration as shown in the figure (**Figure3.7**).
For this type of configuration, in order to point out (Z_0), (L'), (C'), (R') and (G') values, it is important to define two different parameters:

- The GMD (Geometric Mean Distance) value, which depends on the distance between phases, can be calculated as:

$$GMD = \sqrt[3]{D_{ab} * D_{bc} * D_{ac}} \tag{3.13}$$

- The GMR (Geometric Mean Radius) value, which depends on the distance between phases and on the radius of the conductor, can be calculated as:

$$GMR = \sqrt[n^2]{r * D_{ab} * D_{bc} * D_{ac}} = \sqrt[9]{r * D_{ab} * D_{bc} * D_{ac}} \tag{3.14}$$

And then, it is possible to obtain:

$$Z_0 = \frac{\eta}{2\pi} ln\left(\frac{GMD}{GMR}\right), \quad L' = \frac{\mu}{2\pi} ln\left(\frac{GMD}{GMR}\right), \quad C' = \frac{2\pi\varepsilon}{ln\left(\frac{GMD}{GMR}\right)} \tag{3.15}$$

$$R' = \frac{GMR + GMD}{2GMR * GMD}\sqrt{\frac{\mu f}{\pi\sigma}}, \quad G' \simeq \omega C' tan\delta \tag{3.16}$$

The Geometric Mean Distance and Geometric Mean Radius were introduced, in relation to the previous geometries, somewhat underestimate the above parameters from those obtained through experimental data.
However, the results are satisfactory because the error does not go above 10%. Since there is no function that approximates the previous relations with respect to the frequency for the three-wire cables, it was not possible to simulate them on Matlab. However, the point values at $133kHz$ obtained from the formulas were compared to those measured.
Also for this geometry, to determine which design is preferable for data transmission in terms of characteristic impedance (Z_0) and line losses (α_{dB}), the Phase-Ground and Phase-Phase configurations will also be compared.

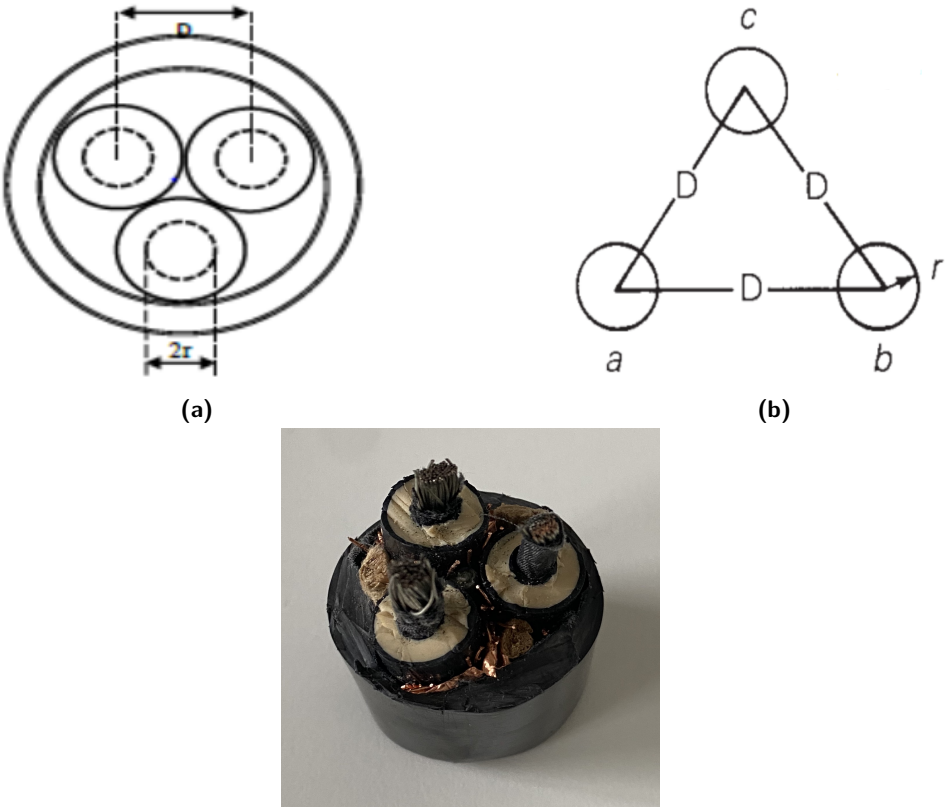

(a) **(b)**

(c)

Figure 3.7: Cross section area of a three-wire coaxial cable, its symmetry and a real one.

3.4 Wave Impedance and Reflection Response

It is possible to define the wave impedance ($Z(z)$) and reflection response ($\Gamma(z)$) at location z in function of the characteristic impedance (Z_0):

$$Z(z) = \frac{V(z)}{I(z)} = Z_0 \frac{V_+(z)+V_-(z)}{V_+(z)-V_-(z)}, \quad \Gamma(z) = \frac{V_-(z)}{V_+(z)} \tag{3.17}$$

It follows from (**3.17**) that $Z(z)$ and $\Gamma(z)$ are related by:

$$Z(z) = Z_0 \frac{1+\Gamma(z)}{1-\Gamma(z)}, \quad \Gamma(z) = \frac{Z(z)-Z(0)}{Z(z)+Z(0)} \tag{3.18}$$

For a forward-moving wave, the conditions $\Gamma(z) = 0$ and $Z(z) = Z0$ are equivalent. The propagation equations of $Z(z)$ and $\Gamma(z)$ between two points z_1,z_2 along the line separated by distance $l = z_2 - z_1$ are given by:

$$\Gamma_1 = \Gamma_2 e^{-2j\beta l} \tag{3.19}$$

It is possible to obtain the relationships between Z_1, Z_2 and Γ_1, Γ_2:

$$Z(1) = Z_0 \frac{1+\Gamma(1)}{1-\Gamma(1)}, \quad Z(2) = Z_0 \frac{1+\Gamma(2)}{1-\Gamma(2)} \tag{3.20}$$

Figure3.8 depicts these various quantities. It is possible to note that the behaviour of the line remains unchanged if the line is cut at the point z_2 and the entire right portion of the

line is replaced by an impedance equal to Z_2. Tis is so because in both cases, all the points z_1 to the left of z_2 see the same voltage-current relationship at z_2, that is $V_2 = Z_2 I_2$ **[9]**.

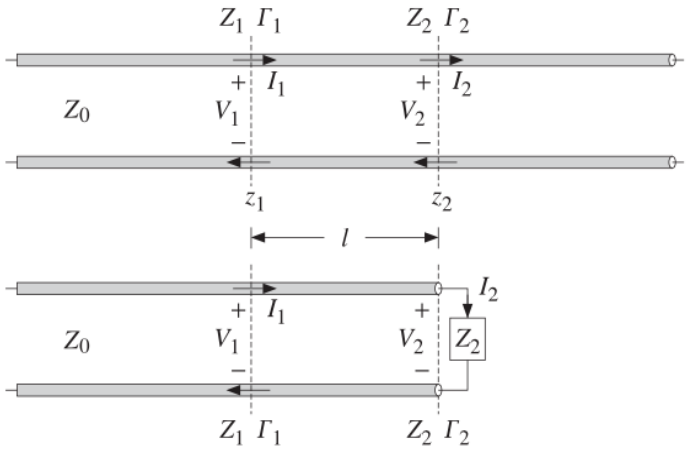

Figure 3.8: Length segment on infinite line and equivalent terminated line.

As in the case of dielectric slabs, the half- and quarter-wavelength separations are of special interest. For a half-wave distance, $\beta l = \frac{2\pi}{2} = \pi$, which translates to $l = \frac{\lambda}{2}$, where $\lambda = \frac{2\pi}{\beta}$ is the wavelength along the line. For a quarter-wave, $\beta l = \frac{2\pi}{4} = \frac{\pi}{2}$ or $l = \frac{\lambda}{4}$. So it is possible to obtain:

$$\begin{aligned} l = \tfrac{\lambda}{2} \quad &\Rightarrow \quad Z_1 = Z_1, \quad \Gamma_1 = \Gamma_2 \\ l = \tfrac{\lambda}{4} \quad &\Rightarrow \quad Z_1 = \tfrac{Z_0^2}{Z_2}, \quad \Gamma_1 = -\Gamma_2 \end{aligned} \tag{3.21}$$

3.5 Two-Port Equivalent Circuit

Since the communication is differential, two-port equivalent has been presented. In fact, any length-l segment of a transmission line may be represented as a two-port equivalent circuit and it is possible to write it in impedance-matrix form:

$$\begin{bmatrix} V1 \\ V2 \end{bmatrix} \begin{bmatrix} Z_{11} & Z_{12} \\ Z_{21} & Z_{22} \end{bmatrix} \begin{bmatrix} I_1 \\ -I_2 \end{bmatrix} \tag{3.22}$$

The negative sign $-I_2$ conforms to the usual convention of having the currents coming into the two-port from either side. This impedance matrix can also be realized in a T-section configuration as shown in **Figure3.9**.
Using (**3.22**) and some trigonometry, the impedances Z_a,Z_b and Z_c have been founded:

$$\begin{aligned} Z_a &= Z_{11} - Z_{12} = jZ_0 tan\tfrac{\beta l}{2} \\ Z_b &= Z_{22} - Z_{12} = jZ_0 tan\tfrac{\beta l}{2} \\ Z_c &= Z_{12} = -jZ_0 \tfrac{1}{sin(\beta l)} \end{aligned} \tag{3.23}$$

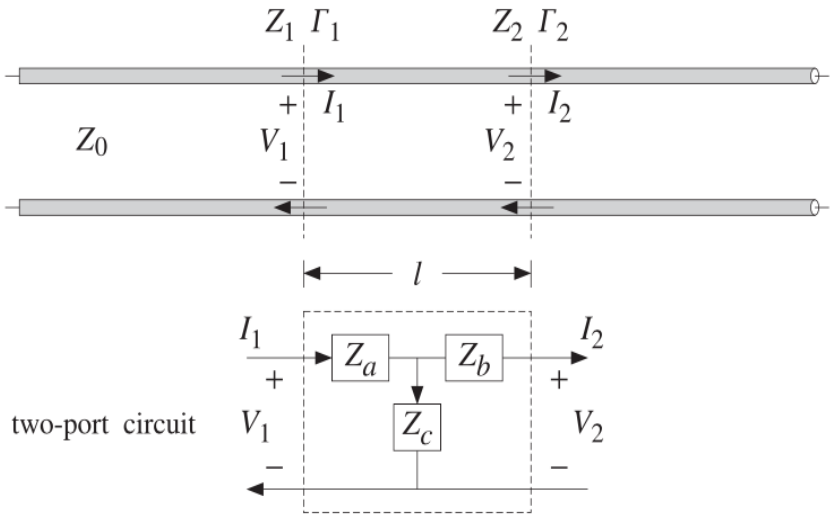

Figure 3.9: Length-l segment of a transmission line and its equivalent T-section.

3.6 Power Transfer from Generator to Load

The total power delivered on a line with losses by the generator (P_{tot}) is dissipated partially in its internal resistance (P_G), partially in the line (P_{line}) and partially in the load (P_L). The power delivered (P_d) to the load is:

$$P_d = P_L + P_{line} \tag{3.24}$$

And thus, it is possible to obtain:

$$P_{tot} = P_G + P_d = P_G + P_{line} + P_L \tag{3.25}$$

Taking **Figure3.10** as a reference:

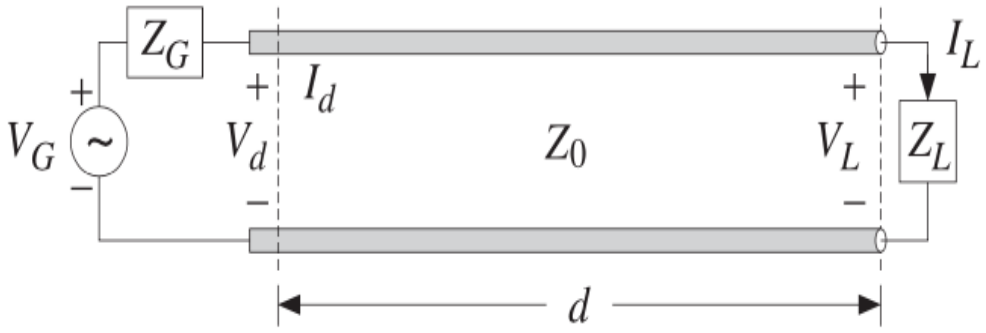

Figure 3.10: Terminated line circuit.

The total real power delivered by the generator can be obtained with the following equation:

$$P_{tot} = \frac{1}{2}\Re\left(V_G I_d^*\right) \tag{3.26}$$

Where I_d^* is the complex conjugate value of the total corrent delivered by the transmitter and the factor $\frac{1}{2}$ is used for peak voltage values (if rms, it must not be present).
Once generated, part of the power is dissipated on the internal resistance of the transmitter:

$$P_G = \frac{1}{2}\Re\left(Z_G I_d I_d^*\right) = \frac{1}{2}\Re(Z_G)\left|I_d^2\right| \tag{3.27}$$

Since the line is lossy the wavenumber is complex $k = \beta - j\alpha \ \epsilon \ \mathbb{C}$, the power at the line's output will be reduced due to both attenuation (α) and reflection (Γ) contributions.
Knowing that:

$$V_{d\pm} = V_L e^{\pm\alpha d} e^{\pm j\beta d} \tag{3.28}$$

The effective power delivered at the input of the line P_d, the one at the output P_L and the one lost along the line P_{line} are:

$$P_d = \tfrac{1}{2Z_0}(|V_{d+}|^2 - |V_{d-}|^2) = \tfrac{1}{2Z_0}(|V_{L+}|^2 e^{2\alpha d} - |V_{L-}|^2 e^{-2\alpha d})$$

$$P_L = \tfrac{1}{2Z_0}(|V_{L+}|^2 - |V_{L-}|^2) \tag{3.29}$$

$$P_{line} = P_d - P_L = \tfrac{1}{2Z_0}(|V_{L+}|^2 (e^{2\alpha d} - 1) + |V_{L-}|^2 (1 - e^{-2\alpha d}))$$

The above expressions can be rewritten in therms of reflection coefficients:

$$P_d = P^+(e^{2\alpha d} - |\Gamma_L|^2 e^{-2\alpha d}) = P^+ e^{2\alpha d}(1 - |\Gamma_d|^2)$$

$$P_L = P^+ - P^- = P^+(1 - |\Gamma_L|^2) \tag{3.30}$$

$$P_{line} = P_d - P_L = P^+(e^{2\alpha d} - 1) + |\Gamma_L|^2 (1 - e^{-2\alpha d})$$

Where P^+ is the active power linked to the direct wave only, in other words the active power incident on a generic transverse section given by:

$$P^+ = \frac{|V_{L+}|^2}{2Z_0} \tag{3.31}$$

$|\Gamma_L|^2$ is the reflectivity ($R = |\Gamma_L|^2$), Z_0 is the characteristic impedance of the line and:

$$|\Gamma_d| = |\Gamma_L| e^{-2\alpha d} \tag{3.32}$$

It is possible to notice that $P_d > P_L$ for all Γ_L since part of the power is dissipated along the transmission line. The total attenuation or loss of the line $\frac{P_d}{P_L}$ (the inverse $\frac{P_L}{P_d}$ is the total gain, which is less than one), takes into account both the contributes given by the loss and by the reflection coefficients. In dB can be expressed as:

$$L = 10log_{10}\left(\tfrac{P_d}{P_L}\right) = 10log_{10}\left(\tfrac{e^{2\alpha d} - |\Gamma_L|^2 e^{-2\alpha d}}{1 - |\Gamma_L|^2}\right) \tag{3.33}$$

If the load is matched to the line $Z_L = Z_0$, so $\Gamma_L = 0$, the loss is referred to as matched-line loss and is due only to the transmission losses along the line:

$$L_M = 10log_{10}(e^{2\alpha d}) = 8.686\alpha d \tag{3.34}$$

Denoting the matched-line loss in absolute units by $a = 10^{\frac{L_M}{10}} = e^{2\alpha d}$, it is possible to write **3.33** in the equivalent form:

$$L = 10log_{10}\left(\tfrac{a^2 - |\Gamma_L|^2}{a(1 - |\Gamma_L|^2)}\right) \tag{3.35}$$

The additional loss due to the mismatch load is the difference:

$$L_R = L - L_M = 10log_{10}\left(\tfrac{1 - |\Gamma_L|^2 e^{-4\alpha d}}{1 - |\Gamma_L|^2}\right) = 10log_{10}\left(\tfrac{1 - |\Gamma_d|^2}{1 - |\Gamma_L|^2}\right) \tag{3.36}$$

3.7 The Modes of Wave Propagation Along a Transmission Line

A waveguide is a structure used to guide waves. At PLC frequencies a conductor such as copper or stranded tinned anealed copper is used to guide waves. They can have different geometries such as rectangular and cylindrical. The propagation in waveguides is in terms of special field distributions called "modes", used as a basis. A modes is the field distributions that propagate maintaining their shape (except for a scaling due tothe presence of attenuation). The guided modes are the field distribution confined in the core.

3.7.1 Transverse Electric and Magnetic (TEM) Mode

TEM, also referred to as transmission line mode, is the principal mode of wave propagation and exists only in transmission lines made of two conductors. This mode becomes dominant in wave propagation where the cross-sectional area of the transmission line is small compared to the signal wavelength (λ). That means the electric and magnetic fields are transverse to the direction of propagation (z) in this mode. The z-axis components of electric and magnetic fields are equal to zero ($H_z = E_z = 0$). Transmission lines support TEM mode with two conductors and have uniquely defined voltage, current and characteristic impedance (Z_0). When the frequency (f) is very small, quasi-TEM modes are used to approximate the TEM modes **[9]**.

3.7.2 Transverse Magnetic (TM) and Transverse Electric (TE) modes

In this mode, the magnetic field is purely transverse to the direction of wave propagation (z) and the electric field does not follow suit. The electric field has both transverse and longitudinal components ($H_z = 0, E_z \neq 0$). In this other, instead, the electric field is transverse to the direction of wave propagation and the magnetic field is not. The magnetic field has both transverse and longitudinal components ($H_z \neq 0, E_z = 0$).

3.7.3 Hybrid Wave Mode

In this mode, the wave propagates in z direction. None of the fields are purely transverse to the direction of propagation. Both the magnetic and electric fields have longitudinal components. When the longitudinal electric field is dominant, the hybrid wave mode is called EH mode. When the longitudinal magnetic field is dominant, the hybrid wave mode is called HE mode. This mode is usually observed in waveguides with inhomogeneous dielectric and in optical fibers. The table below (**Tab3.1**) describes the conductors that support various modes of wave propagation.

MODE WAVE PROPAGATION	*TYPE OF TRANSMISSION LINES*
TEM	Coaxial line, two-wire line, parallel-plate line, stripline, micro-stripline, multi-conductor lines, and coplanar waveguides
TE or TM	Metal or optical fiber waveguides, cavity-resonators
Hybrid Wave Mode	Optical fibers, open conductor guides

Table 3.1: Description of the conductors that support various modes of wave propagation.

3.7.4 Higher Modes

The TEM propagation mode is the dominant one in transmission lines with two conductors and has no cut-off frequency. Its propagation in function of frequency is only influenced by the transmission line's attenuation. TE and TM modes are commonly found in enclosed guiding structures, are generally called waveguide modes and they are dispersive.
TE and TM modes are limited by a cut-off frequency below which there is no wave propagation through it. This cut-off frequency causes limited bandwidth in these modes. As transmission lines generally operate below this cut-off frequency, they support only TEM mode. However, TE and TM modes with higher cutoff frequencies also exist in coaxial lines, with the lowest being a TE_{11} mode with cutoff wavelength (λ_c) and frequency (f_c):

$$\lambda_c = 1.873\frac{\pi}{2}(a+b), \qquad f_c = \frac{c}{\lambda_c} = \frac{c_0}{n\lambda_c} \tag{3.37}$$

Where:

- a is the radius of the inner conductor;
- b is the radius of the outer conductor;
- c_0 is the light velocity in the free space $c_0 = 2.99 \cdot 10^8 \left[\frac{m}{s}\right]$;
- c is the characteristic velocity in the medium;
- n is the refractive index.

This is usually approximated by $\lambda_c = \pi(a+b)$. Thus, the operation of the TEM mode is restricted to frequencies that are less than f_c **[9]**.
For the studied Medium Voltage cables used in the PLC transmission, the cut-off frequency for the TE_{11} mode is at:

- LUMIREP-E single coaxial cable with a section of ($25mm^2$), $a = 2.820mm$ and $b = 6.275mm \Rightarrow \lambda_c = 25.750[mm]$, $f_c = 11.177[GHz]$;
- SENOREP-3G three wires cable, Phase-Ground configuration with a section of ($10mm^2$), $a = 1.780mm$ and $b = 8.050mm \Rightarrow \lambda_c = 28.920[mm]$, $f_c = 10.338[GHz]$.

3.8 Scattering Parameters (S-parameters)

In order to be able to get the description of the transmission line as a T-section, to compare results about characteristic parameters of the cables obtained through equations developed on Matlab in function of the frequency and results collected through measurements, S-parameters have been presented and data has been acquired through a Vector Network Analyser (VNA). It has been choosed an Keysight/Agilent VNA, Model E5071C with 2-ports, working on a range of frequencies from $9KHz$ to $8,5GHz$ in 1601 points (**Figure3.11**).
It is uncommon to find a machine that can detect VLF/LF/MF ranges because a VNA is often employed to operate with very high frequency ranges for telecommunications applications. The range of frequencies set on the VNA is between $9kHz$ and $5MHz$, in order to maintain some margin from the two extremes. This is because the working frequency for the data exchange chosen by AUGIER is $133kHz$, which belongs to the CENELEC-C band, but in general it was tried to study the frequency behaviour of the measured objects in the entire Narrowband standard ($30 - 500kHz$). It is important to understand that the characteristic impedance of the VNA is 50Ω, whereas the receiver and transmitter's are 10Ω, as was

indicated in Chapter 1. Given that the measurements made are absolute and independent of the impedance being utilised as the load, this is not a significant issue for the cables. As will be explained in the following chapter, this will be more important while studying transformers.

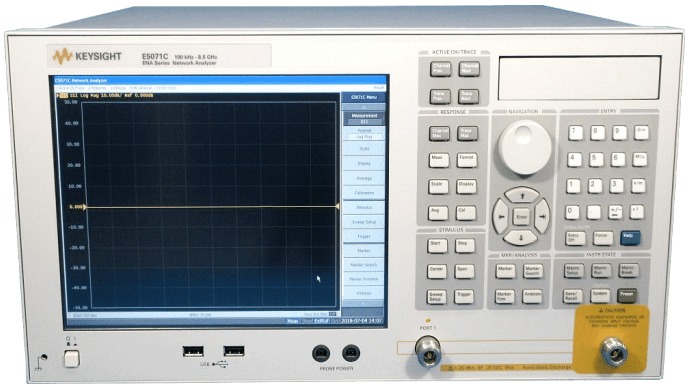

Figure 3.11: Keysight/Agilent E5071C VNA with 2-ports.

Since the data exchange takes place through a differential communication, the cables studied can be considered as a linear quadripole as shown in **Figure3.12**.
It is possible to define an incident power wave a and a reflected one b as a function of the voltage along the line with a characteristic impedance Z_0:

$$a_i = \frac{V_+}{2\sqrt{Z_0}}, \quad b_i = \frac{V_-}{2\sqrt{Z_0}} \tag{3.38}$$

The relationships between the power waves will be linear relationships and it is possible to express the reflected power waves as a function of the incident ones:

$$\begin{cases} b_1 = S_{11}a_1 + S_{12}a_2 \\ b_2 = S_{21}a_1 + S_{22}a_2 \end{cases} \tag{3.39}$$

This system of equations can be interpreted as a definition of the four scattering parameters S_{ij}. Knowledge of the scattering parameters completely defines the behaviour of the quadripole and have been found through the VNA **[9]**.
From the descriptive equations of scattering parameters immediately descend the definitions for the individual parameters:

$$\begin{aligned} S_{11} &= \left(\frac{b_1}{a_1}\right)_{a_2=0} \quad S_{21} = \left(\frac{b_2}{a_1}\right)_{a_2=0} \\ S_{12} &= \left(\frac{b_1}{a_2}\right)_{a_1=0} \quad S_{22} = \left(\frac{b_2}{a_2}\right)_{a_1=0} \end{aligned} \tag{3.40}$$

Where:

- S_{11} is the reflection coefficient at the input with matched output;
- S_{21} is the direct transmission coefficient with matched output;
- S_{12} is the inverse transmission coefficient with matched input;
- S_{22} is the reflection coefficient at the output with adapted input.

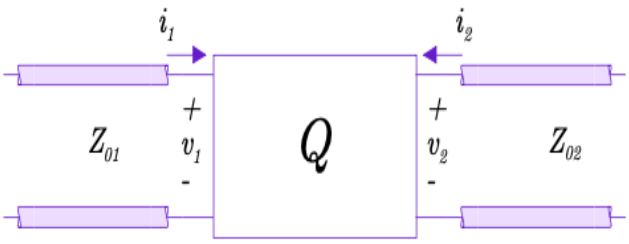

Figure 3.12: Linear quadripole.

Since all the analyzed components were found to be passive and reciprocal, the scattering matrix turns out to be symmetric and dependent on only two independent parameters (S_{11} and S_{21}):

$$\begin{bmatrix} S_{11} & S_{21} \\ S_{21} & S_{11} \end{bmatrix} \tag{3.41}$$

3.9 Smith Chart

The relation between the wave impedance $Z(z)$ and the corresponding reflection response $\Gamma(z)$ along a transmission line Z_0 can be studied as:

$$\Gamma(z) = \frac{Z(z)-Z_0}{Z(z)+Z_0} \quad \Rightarrow \quad Z(z) = Z_0 \frac{1+\Gamma(z)}{1-\Gamma(z)} \tag{3.42}$$

It represents a mapping between a complex $z-plane$ and the complex reflection coefficient $\Gamma-plane$ realising the divided Gamma $\Gamma(z)$ bilinear transformation geometrically.
It allows for complex calculations in a geometric way of a load in terms of its reflection coefficient, that when it was introduced in 1939, were very difficult to do by hand, and help one design matching circuits, where matching means moving towards the center of the chart. A VNA features the Smith chart, which is particularly accurate and effective in studying the nature of the component under investigation, among the visualisation options for measuring a component (**Figure3.13**).

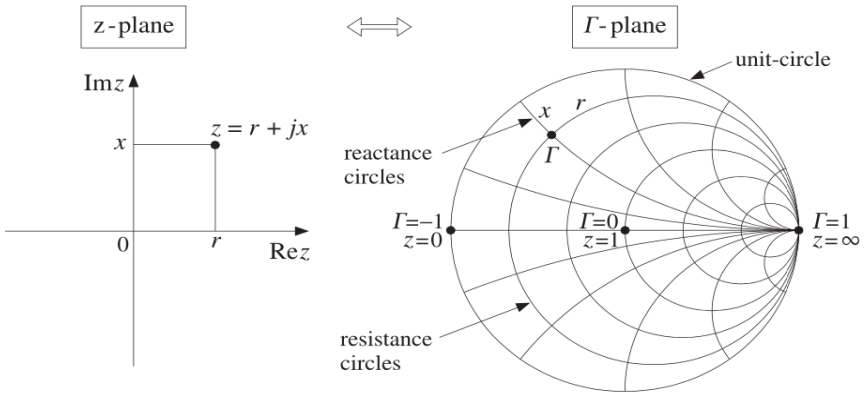

Figure 3.13: Mapping between $z-plane$ and $\Gamma-plane$.

Smith carts are a powerful tool used to visualize an impedance in the complex plane composed of resistive and reactive part ($z = R + jX[\Omega]$) and reflection coefficient (Γ). Taken as a reference the center of the circle, this is defined with a unit radius and significant points can be displayed on it:

- **constant resistance circunferences (R):** circumferences with constant resistance values arising from the right side of the unit circle and contained in it, having larger diameter and therefore lower resistance values ($R \to 0$) near the left limit and smaller diameter and therefore greater resistance values ($R \to \infty$) near the right one;
- **constant reactance grids (X):** curvilinear grids with constant reactance values arising from the right side of the unit circle and contained in it, having less curved section and therefore lower reactance values ($X \to 0$) near the left limit and more curved sections and therefore greater reactance values ($X \to \infty$) near the right one. Those that extend downward or upward have the same constant reactance value, but they behave in the opposite way: positive values are assumed at the top and negative values are assumed at the bottom.

The component exhibits a fully resistive behavior at the diameter of the unit circle, where, as was already noted above, its value decreases as it move away from the extreme right. The internal impedance of a VNA is typically 50Ω and is purely resistive. This serves as a guide for the measurements, hence it is designated as the circle's center. So it follows that a component under study (the line) will match the load and have a value that is precisely in the middle of the circumference when it has a value of 50Ω. The points at the circumference's two extremes are also quite significant; in fact, the point on the extreme left stands for Short ($R \simeq 0$) point instead the one on the extreme right stands for Open ($R = \infty$).

The mirror regions of upper and lower reactance are used to identify the nature of these:

- **upward reactance (X):** inductive behaviour;
- **downword reactance ($-X$):** capacitive behaviour.

A component under study will move further away from the center the more its nature differs from the reference, which is always regarded as the value of the internal impedance of the VNA (50Ω), located at the center of the unit circle. The line will be perfectly matched and placed precisely in the middle of the unit circle if, as previously mentioned, the component and load have the identical impedance value. A component will be entirely resistive if it is located along the circumference, entirely inductive if it is located on the upper profile of the circumference, entirely capacitive if it is located on the lower profile and finally if inside the circumference it will have a resistive nature with a reactive part which will depend on the position (upper or lower) of where it will be.
The Smith chart makes it easy to always determine a component's nature by distinguishing both the resistive and the reactive components of its impedance ($z = R + jX[\Omega]$). Additionally, because the reactive part varies with frequency, the behaviour of the component can be fully investigate within the chosen frequency range by setting it on the VNA.
Since it is defined on a circle with a unit radius, once the nature of a component has been determined, its distance from the circumference's center (occupied by 50Ω) will yield the value of the reflection coefficient (S_{11}), which results from the mismatch between the two impedances between the line (the studied impedance) and the load (of the VNA). So when a line is perfectly matched with the load, the position of its impedance will be perfectly in the center of the circle and its reflection coefficient will be zero since the distance from the center will be zero.

Finally, Smith charts can be used to understand when self-resonance phenomena occur in a given component and at what frequency this happens. Crossings between the capacitive and inductive parts (or vice versa), passing via a resistive portion, indicate the presence of a self-resonance for the component under study, starting at a specific frequency.

3.10 Studied cables

The most common cables in France for the transportation of Medium/Low Voltage were examined, starting from the transmission line theory covered in the earlier chapters. It was decided to study this kind of cables because AUGIER, a French company, has built PLC technology primarily in France. Furthermore, as it is mainly operated in densely populated areas or in airports, the study was done on Medium Voltage subterranean cables, therefore shielded and insulated, as the overhead configuration cannot be mounted. These was done prevalently to try to modify with some advantages the existing architectures.

3.10.1 Low Voltage Cables

Elandcables' H07RN-F cables are mostly utilised for Low Voltage applications. These cables are used into the industrial field and for this reason unshielded. They have different working sections and an outer sheath holds two or more insulated cables inside, depending on whether the application is single-phase or three-phase (usually in the three-phase application three are used for the phases, one for the neutral and one for the ground).
It was done only the analysis of single-phase cables because the study's main focus was on single-phase-single-phase transformers, whose Low Voltage outputs are used to power the various transmitters and on signal couplers (MCEP) that the line uses to couple the signal used for high-frequency ($133kHz$) data exchange with the low-frequency ($50Hz$) one used for energy transport.
Both applications do not require too much power and therefore do not require a three-phase connection, so the study of single-phase cables alone was more than enough.

Figure 3.14: H07RN-F three-phase cable. Note the presence of the phases, the neutral and the ground cables.

3.10.1.1 H07RN-F $1.5mm^2$ monophase cable

The first section examined and one of the most used, was that of the single-phase H07RN-F $1.5mm^2$. From the datasheet, it possible to understand that the conductor is made by copper, the inner and outer insulation is made by EPR (Ethylene Propylene Rubber) and that the Resistance of the conductor per unit length at $20°$ is $R' = 13.3\frac{\Omega}{Km}$.
This cable exhibits the behaviour of a two-wire transmission line. The formulas **3.11**, **3.12** as a function of frequency ($9kHz - 5MHz$) have been implemented to obtain the parameters

L', C', R', G', α_{dB} and Z_0 and compared with the data acquired with the VNA in the form of S-parameters and converted with a specific Matlab functions to obtain the concerned parameters, as shown in the figure **Figure3.15**. Comparing measured and calculated data, we notice oscillations in measured ones at the extremes of the band. Those in low frequencies indicate that the line used to calculate the line parameters must be shorted, those in high frequencies are due to resonance phenomena that the cable has around $5Mhz$.
The green line was obtained through a moving-average filter that is a common method used for smoothing noisy data. It was used the filter function to compute averages along a vector of data obtained from the collected points. The characteristic impedance Z_0 and the other results at $133kHz$ evaluated by comparing the values attained through the simulations and through the Matlab formulas are reported in the **Tab3.2**. As can be seen from the values obtained, the results calculated through the formulas are understimated compared to those measured, especially as regards inductance, capacitance, resistance, conductance and losses per unit length, instead turned out to have an error of only 2.21% the characteristic impedance.

	Measured	**Calculated**
Inductance per unit-length (L') $[\frac{\mu H}{m}]$	1.181	0.562
Capacitance per unit-length (C') $[\frac{nF}{m}]$	0.111	0.059
Resistance per unit-length (R') $[\frac{\Omega}{m}]$	0.567	0.150
Conductance per unit-length (G') $[\frac{\mu S}{m}]$	1.282	0.099
Attenuation per unit-length (α_{dB}) $[\frac{dB}{m}]$	0.022	0.006
Characteristic impedance (Z_0) $[\Omega]$	99.444	97.286

Table 3.2: The characteristic impedance Z_0 and the other results L', C', R', G', α_{dB} at $133kHz$ measured and calculated.

This is clearly caused by the formulas' approximation of the component's actual behaviour, which converts two physical wires into a single component not taking into account the actual interaction of the two wires.
Also the Resistance per unit length at $20°$ reported on the datasheet is quite far from the values obtained, both measured and calculated. This is certainly due to the fact that its value refears to the working frequency in the transport of energy of $50Hz$ and not at $133kHz$.
In fact, as can be seen from formula **3.10** and also from the graphs, its behaviour decreases as the $\sqrt{f}$ decreases, perfectly in line with the fact that at very low frequencies this makes on much lower values than those obtained in the frequency range under test $(9kHz - 5MHz)$.It has an high manageability,is very light and also is very cheap. In fact, the price per meter is $1.5mm^2$ $(0.610\frac{eur}{m})$, one of the cheapest on the market despite all the advantages that this section takes with it.
As will be seen later, once it is understood that as the section increases there is a general improvement trend of the various parameters, the study of Low Voltage cables has focused only on $1.5mm^2$ and $6mm^2$. In fact, it would need huge cables with exaggerated costs before it is possible to see acceptable benefits since, as the section increases, prices rise too much in comparison to the benefits that the data exchange truly gets from it.
At that point, mounting shielded cables with smaller sections would be more practical and capable of lowering interference losses and enhancing data exchange, but this would go beyond the true goal of the power transfer and the benefits that the PLC offers over alternatives communication systems. Acting on Medium Voltage cables and in particular on their sections, studying what are the best geometry and method of placing the signal on the power line is certainly a more efficient and effective method of improving data exchange.

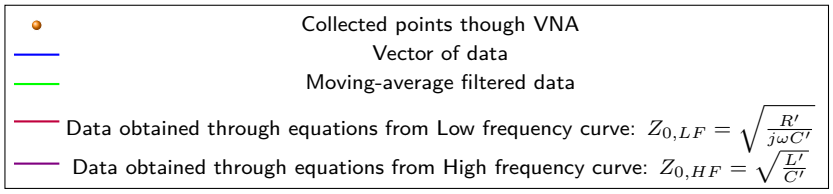

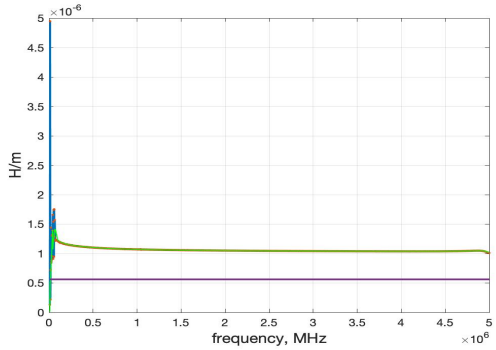

(a) Inductance per unit length $[\frac{H}{m}]$.

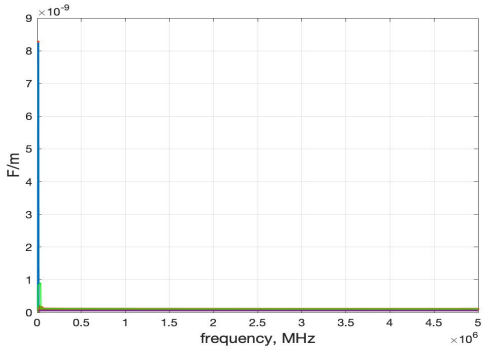

(b) Capacitance per unit length $[\frac{F}{m}]$.

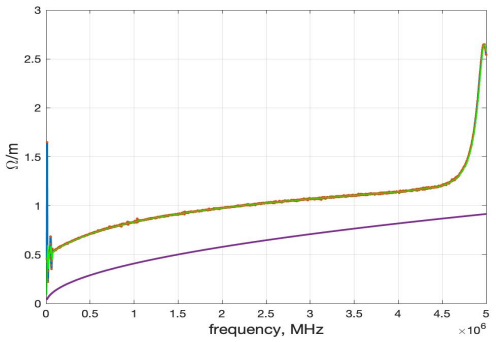

(c) Resistance per unit length $[\frac{\Omega}{m}]$.

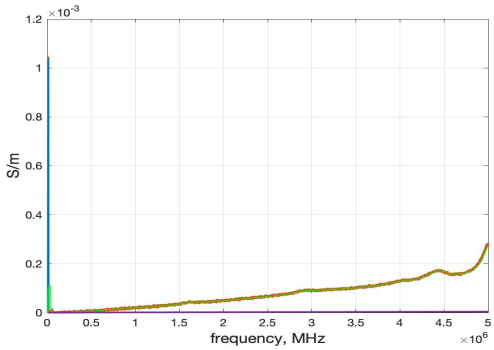

(d) Conductance per unit length $[\frac{S}{m}]$.

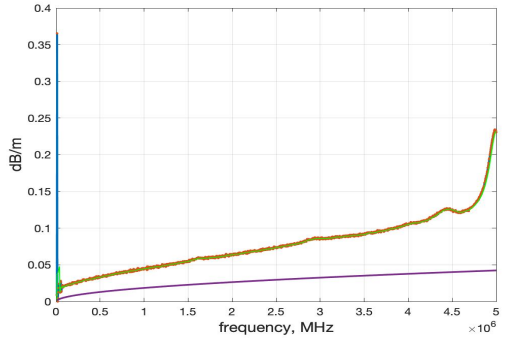

(e) Attenuation per unit length $[\frac{dB}{m}]$.

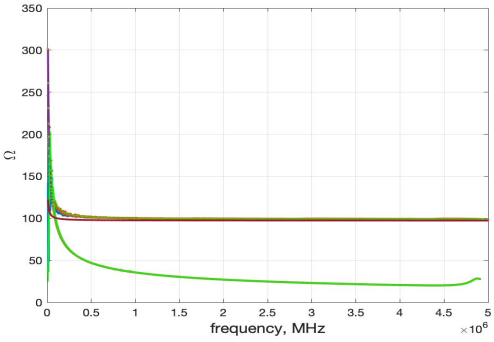

(f) Impedance $[\Omega]$.

Figure 3.15: Parameters in function of frequency for a H07RN-F $1.5mm^2$ LV monophase cable.

3.10.1.2 H07RN-F $6mm^2$ monophase cable

The second section examined and also one of the most used, was that of the single-phase H07RN-F $6mm^2$. Since it is almost the same cable with the same conductors and insulation materials but with only a different sections, it is possible to treat it as a two-wires transmission line. From the datasheet, it possible obtain the Resistance of the conductor per unit length at $20°$ is $R' = 3.3\frac{\Omega}{Km}$. The obtained parameters L', C', R', G', α_{dB} and Z_0 were compared with the data acquired with the VNA in the form of S-parameters, to obtain the concerned ones, are shown in **Figure3.16**. From the simulation it is possible to notice that in low and expecially in high frequencies the cable shows some oscillations, more than the previous section. Those in low frequencies always indicate that the line used to calculate the line parameters must be shorted, those in high frequencies are due to a massive resonance phenomena that the cable has around $5Mhz$.
From the simulation it is possible to see how the error between the graphs obtained through the formulas as a function of frequency and those obtained through measurements, is greater. This is presumably due to the fact that the conductors' sections are larger than those in H07RN-F $1.5mm^2$ and, for this reason, it is more difficult to approximate the behaviour of the two cables as a single one.
The characteristic impedance Z_0 and the other results at $133kHz$ are shown in the **Tab3.3**. Even though the cables' measurements show more problems caused by effects of resonace, it generally exhibits better behaviour in terms of both the characteristic impedance Z_0 and the other parameters that depend on frequency. It can also be seen from the simulation of the formulas as a function of frequency, which are not affected by parasitic phenomena.

	Measured	**Calculated**
Inductance per unit-length (L') $[\frac{\mu H}{m}]$	1.120	0.456
Capacitance per unit-length (C') $[\frac{nF}{m}]$	0.134	0.073
Resistance per unit-length (R') $[\frac{\Omega}{m}]$	0.464	0.118
Conductance per unit-length (G') $[\frac{\mu S}{m}]$	0.591	0.123
Attenuation per unit-length (α_{dB}) $[\frac{dB}{m}]$	0.021	0.006
Characteristic impedance (Z_0) $[\Omega]$	88.538	78.947

Table 3.3: The characteristic impedance Z_0 and the other results L', C', R', G', α_{dB} at $133kHz$ measured and calculated.

This is due to the fact that, for the same power transported and length of the line, larger sections of the conductors always show a better behaviour, as the Resistance of the material to the passage of current is reduced ($R \propto \frac{1}{\Sigma}$).
In fact, as reported on the datasheet, the R' at $20°$ is lower than that of the H07RN-F $1.5mm^2$ always measured at $20°$ ($R'_{H07RN-F,6mm^2} = 3.3\frac{\Omega}{Km}, R'_{H07RN-F,1.5mm^2} = 13.3\frac{\Omega}{Km}$).
The obtained data, although they show the behaviour of the Resistance per unit-length in a range of frequencies different from the working one referred to in the datasheet ($50Hz$), confirm this trend, which in general can be applied to all the searched variables as this beneficial effect it reflects on all other parameters. It always manageable, light and also is cheap but, obviously more than the $1.5mm^2$ one. The price per meter is $1.776\frac{eur}{m}$ and it is possible to note that is more than two times expensive than the one analyzed before, parameter to be taken into consideration in the choice of making any changes. In fact, it would need huge sections with exaggerated costs before it is possible to see acceptable benefits since, as the section increases, prices rise too much in comparison to the benefits that the data exchange truly gets from it.

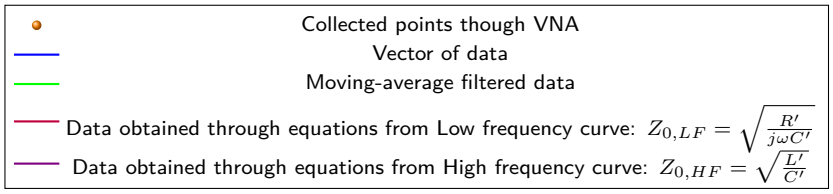

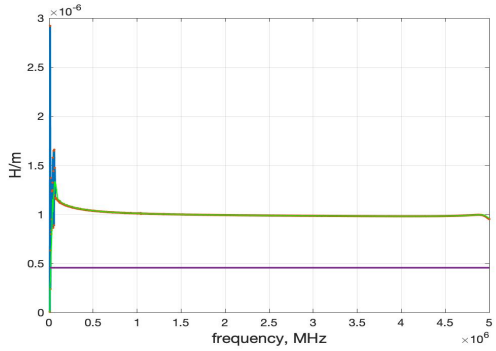

(a) Inductance per unit length $[\frac{H}{m}]$.

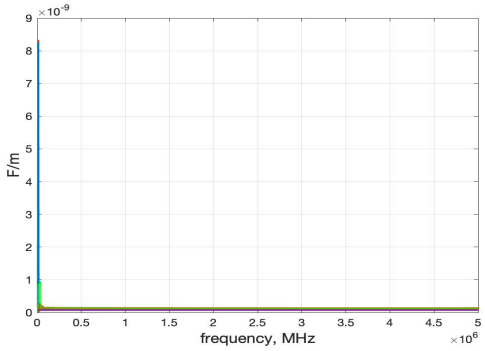

(b) Capacitance per unit length $[\frac{F}{m}]$.

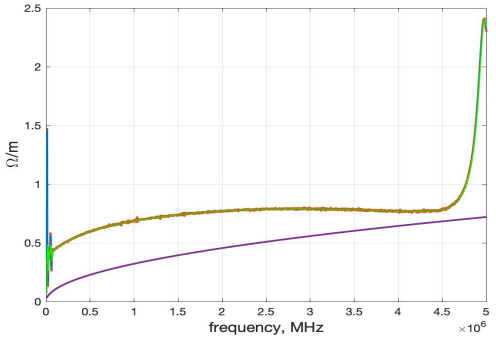

(c) Resistance per unit length $[\frac{\Omega}{m}]$.

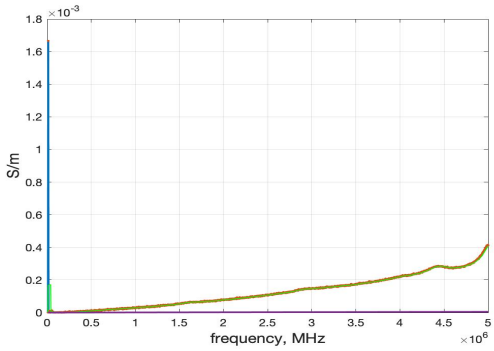

(d) Conductance per unit length $[\frac{S}{m}]$.

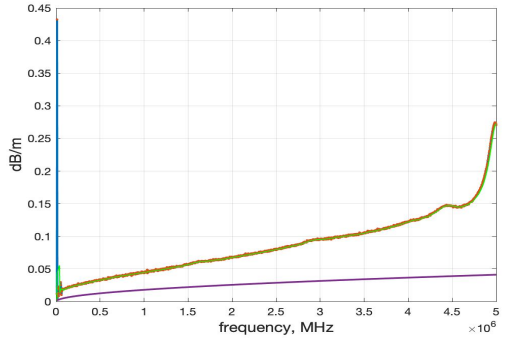

(e) Attenuation per unit length $[\frac{dB}{m}]$.

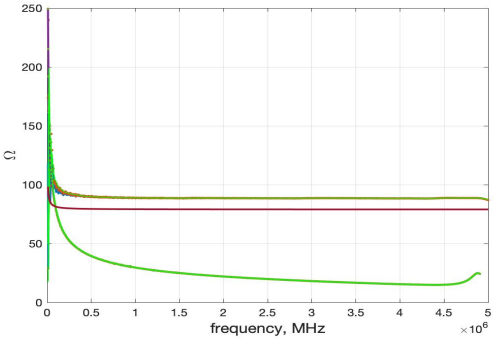

(f) Impedance $[\Omega]$.

Figure 3.16: Parameters in function of frequency for a H07RN-F $6mm^2$ LV monophase cable.

3.10.1.3 Cost-Benefit analysis

Although larger sections have some benefits in terms of data exchange compared to smaller ones, these are much less manageable, heavier and more expensive. In fact, if they are compared the prices per meter of the H07RN-F $1.5mm^2$ $(0.610\frac{eur}{m})$ and of the H07RN-F $6mm^2$ $(1.776\frac{eur}{m})$, it is possible to find that one is more than two times expensive than the other. If all the H07RN-F $1.5mm^2$ were replaced to H07RN-F $6mm^2$ in order to improve data exchange, take use of the Low Voltage waves' total range of around twenty meters, the ultimate cost would be tripled:

- **H07RN-F $6mm^2$ for twenty meters:** $Cost_{20m} = 35.538[eur]$
- **H07RN-F $1.5mm^2$ for twenty meters:** $Cost_{20m} = 12.212[eur]$

Remembering that the characteristic impedance of the transmitter and receiver is $Z_0 = 10\Omega$ a benefit of 3.226% in terms of losses per meter (α_{dB}) and 12.31% in terms of characteristic impedance (Z_0), and consequently of lesser reflections due to mismatch of the line with respect to the generator and the load, demonstrates insufficient to accept a tripling of costs. Once it is understood that as the section increases there is a general improvement trend of the various parameters, the study of Low Voltage cables has focused only on $1.5mm^2$ and $6mm^2$. In fact, it would need huge sections with exaggerated costs before it is possible to see acceptable benefits since, as the section increases, prices rise too much in comparison to the benefits that the data exchange truly gets from it. At that point, mounting shielded cables with smaller sections would be more practical and capable of lowering interference losses and enhancing data exchange, but this would go beyond the true goal of the power transfer and the benefits that the PLC offers over alternatives communication systems.
Acting on Medium Voltage cables and in particular on their sections, studying what are the best geometry and method of placing the signal on the power line is certainly a more efficient and effective method of improving data exchange.

3.10.2 Medium Voltage Cables

PRYSMIAN GROUP manufactures the majority of the Medium Voltage cables used in France for subterranean power transfer. They have various working sections, shapes and materials that are employed with several conductors, insulators, and shields (**Figure3.17**).

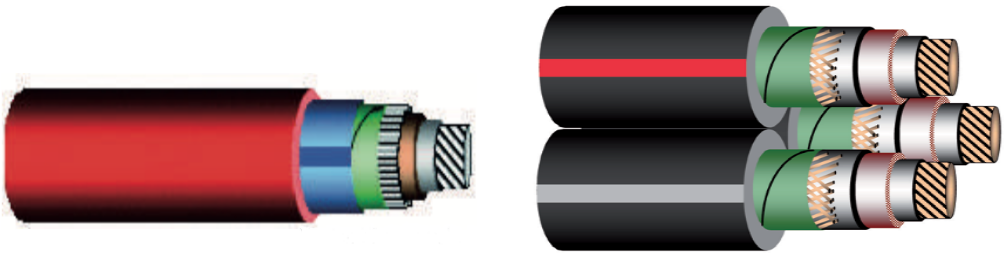

(a) Single wire coaxial cable. **(b)** Three-wire coaxial cable.

Figure 3.17: Different geometries for the MV power transport.

The High-Voltage and Low-Voltage transmission lines are connected by the Medium-Voltage line. MV lines use the three-phase transport method that enables the use of cables with a section that is half as small as a single-phase line while maintaining the same power and line length.

Three parallel coaxial cables, each holding one phase or a three-wire coaxial cable are used in a three-phase power transmission system.
Since the signal is differential, two different configurations can be used for data exchange:

- **Phase-Ground configuration:** the same cable's phase and ground carry the signal and the inverted signal;
- **Phase-Phase configuration:** the signal travels on one phase while the inverse one on another.

For both the geometries, experimental data collected from measurements and results from equations as a function of frequency on Matlab will be compare to determine which is the optimal transmission method in terms of characteristic impedance (Z_0) and line losses (α_{dB}) between the Phase-Ground and Phase-Phase configurations and between the two geometries.

3.10.2.1 LUMIREP-E Phase-Ground configuration

The first cable examined was the LUMIREP-E coaxial cable with a section of ($25mm^2$). It consists of two concentric conductors of inner and outer radii of a ($2.820mm$) and b ($6.275mm$) made by stranded tinned anealed copper, with the space between them filled with a dielectric ε such as XLPE (Cross Linked Polyethylene), an insulation sheat always made by XLPE and an outer sheat made by PVC (Polyvinyl Chloride).
From the datasheet is possible to obtain the Resistance per unith length $R' = 0.000837\frac{\Omega}{m} = 0.837\frac{\Omega}{km}$ as an average between its maximum value at $20°$ and its maximum value at $90°$, the Capacitance per unith length between the phase and the neutral $C' = 0.20\frac{nF}{m} = 200\frac{nF}{Km}$ and the Inductance per unith length $L' = 0.140\frac{\mu H}{m} = 140\frac{\mu H}{Km}$.
These values, as was also true for Low Voltage cables, refer to a working frequency of $50Hz$, far below the range of frequencies studied ($9kHz - 5MHz$).The obtained parameters L', C', R', G', α_{dB} and Z_0 obtained are shown in **Figure3.18**.
The cable is significantly less susceptible to resonance effects and to various high interference phenomena than an unshielded low voltage cable, as can be displayed by the simulations obtained using collecting data.
It always exhibits some oscillations at low frequencies, but this is dependent on the fact that the line used to determine the line parameters must be shorted.
Although the results obtained through the formulas as a function of the frequency on Matlab exhibit a trend much closer to those obtained through measurements and indeed for certain parameters the curves overlap or agree, the error between these is still high.This confirms the fact that the formulas underestimate the real behavior of the cables involved.
The characteristic impedance Z_0 and the other results at $133kHz$ are shown in the **Tab3.4**:

	Measured	**Calculated**
Inductance per unit-length (L') $[\frac{\mu H}{m}]$	0.964	0.240
Capacitance per unit-length (C') $[\frac{nF}{m}]$	0.207	0.102
Resistance per unit-length (R') $[\frac{\Omega}{m}]$	0.441	0.162
Conductance per unit-length (G') $[\frac{\mu S}{m}]$	4.143	0.0856
Attenuation per unit-length (α_{dB}) $[\frac{dB}{m}]$	0.027	0.013
Characteristic impedance (Z_0) $[\Omega]$	59.084	48.568

Table 3.4: The characteristic impedance Z_0 and the other results L', C', R', G', α_{dB} at $133kHz$ measured and calculated.

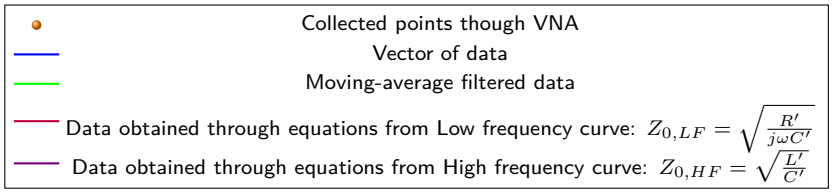

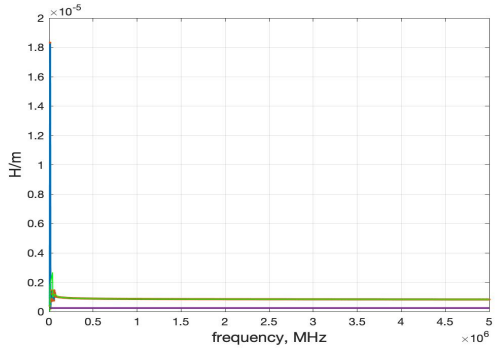

(a) Inductance per unit length $[\frac{H}{m}]$.

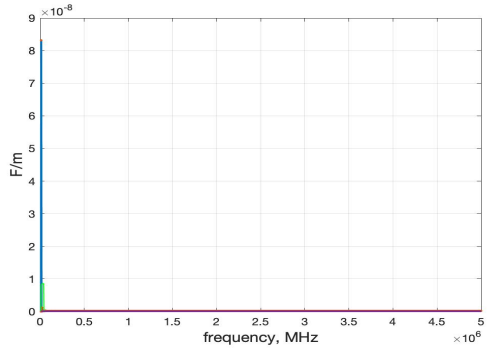

(b) Capacitance per unit length $[\frac{F}{m}]$.

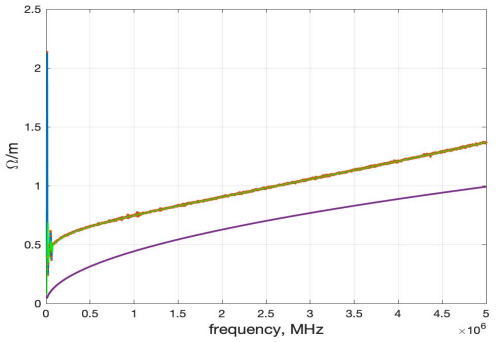

(c) Resistance per unit length $[\frac{\Omega}{m}]$.

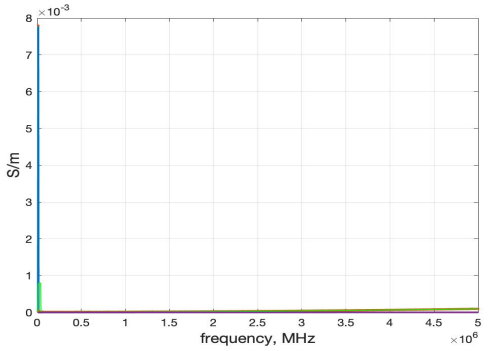

(d) Conductance per unit length $[\frac{S}{m}]$.

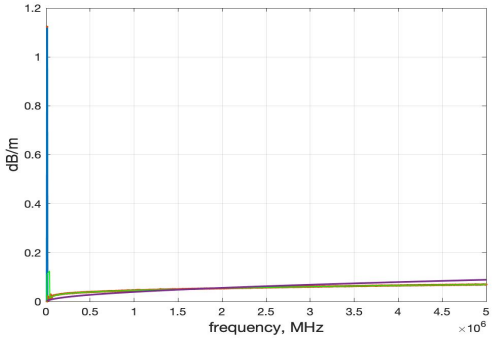

(e) Attenuation per unit length $[\frac{dB}{m}]$.

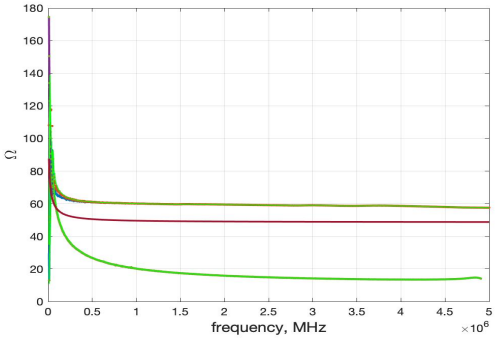

(f) Impedance $[\Omega]$.

Figure 3.18: Parameters in function of frequency for a LUMIREP-E coaxial cable in a Phase-Ground configuration.

From the results obtained through the measurements, it is possible to notice a lowering of the characteristic impedance of the line ($Z_0 = 59.084\Omega$) with respect to LV cables and therefore a clear improvement in terms of matching between the line itself and the transmitter/receivers, thus reducing the power lost due to reflections. However, it is clear from the analysis of the loss coefficient (α_{dB}) that this is still excessively high for a line that is several kilometers long. For instance, the attenuation is $27.9dB$ with a transmitter and a receiver positioned $1km$ apart. This implies the necessity to look at alternative data exchange techniques that are more attenuation-efficient.

3.10.2.2 LUMIREP-E Phase-Phase configuration

To perform the simulations below, two LUMIREP-E coaxial cable with a section of ($25mm^2$), previously studied, were taken and placed in parallel to simulate the injection of the signal on two different phases in a three-phase system. Contrary to earlier simulations when it was always possible to compare measurements' results with formulas in function of frequency on Matlab, for the Phase-Phase configuration equations **3.11**, **3.12** used for a two-wire transmission line, were not developed.
This is due to the fact that, as was already said, a two-wire transmission line approximates the behaviour of two distinct unshielded cables, joined together in an outer protective sheath, which exhibit considerable electromagnetic interference and cross-talk. Instead, two coaxial cables in parallel were each carrying a portion of the differential signal and able to minimises crosstalk and electromagnetic interference were examined in this instance.
The obtained parameters L', C', R', G', α_{dB} and Z_0 acquired with the VNA in the form of S-parameters and adapted on Matlab, are shown in **Figure3.19**. It is possible to note that also in this case at low frequencies, there are some oscillations dependent on the fact that the line used to determine the line parameters must be shorted. Small resonance phenomena are present in the transmission near $5MHz$, although they are not significant.
It is interesting to notice how the attenuation coefficient (α_{dB}) has significantly decreased. Positioning a transmitter and a receiver $1km$ apart, the attenuation is $6.2dB$, very small compared to the Phase-Ground configuration. Instead, it is possible to notice how the characteristic impedance (Z_0) of the line has worsened considerably, reaching a value of 140Ω.
The characteristic impedance Z_0 and the other results at $133kHz$ are shown in the **Tab3.5**:

	Measured
Inductance per unit-length (L') $[\frac{\mu H}{m}]$	1.3222
Capacitance per unit-length (C') $[\frac{nF}{m}]$	0.057
Resistance per unit-length (R') $[\frac{\Omega}{m}]$	0.484
Conductance per unit-length (G') $[\frac{\mu S}{m}]$	10.851
Attenuation per unit-length (α_{dB}) $[\frac{dB}{m}]$	0.0062
Characteristic impedance (Z_0) $[\Omega]$	140.002

Table 3.5: The characteristic impedance Z_0 and the other results L', C', R', G', α_{dB} at $133kHz$ measured.

This creates an higher mismatch between the characteristic impedance of the transmitter, of the line and of the receiver, increasing the losses for reflections. Despite this worsening, Phase-Phase configuration is preferable to the Phase-Ground one because it is always possible to add an impedance coupler between the line and the MASTER/SLAVE to reduce the reflection losses, whereas the attenuation coefficient is an intrinsic parameter unmodifiable.

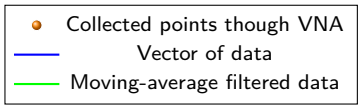

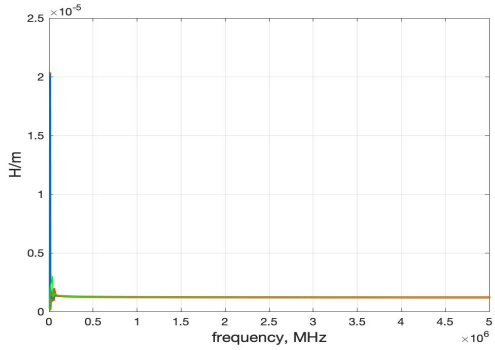

(a) Inductance per unit length $[\frac{H}{m}]$.

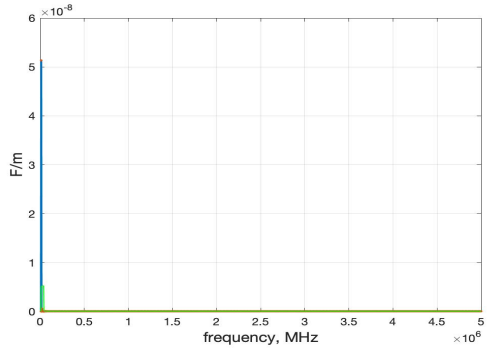

(b) Capacitance per unit length $[\frac{F}{m}]$.

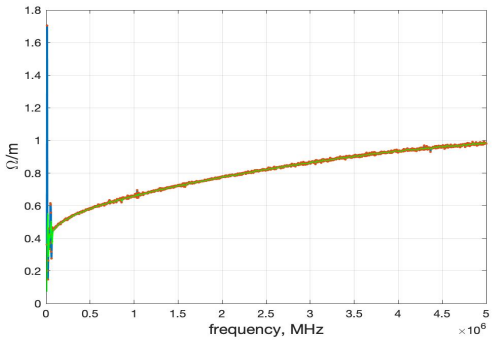

(c) Resistance per unit length $[\frac{\Omega}{m}]$.

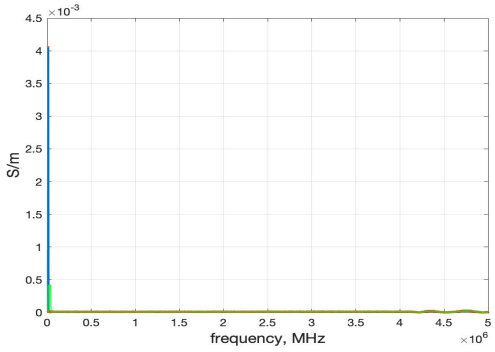

(d) Conductance per unit length $[\frac{S}{m}]$.

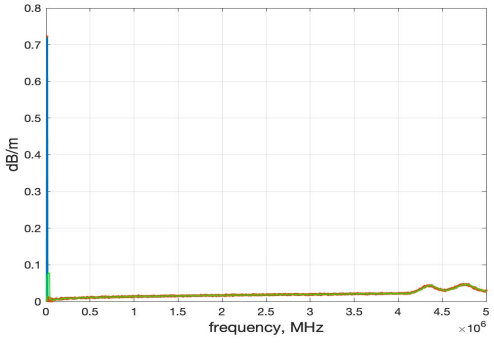

(e) Attenuation per unit length $[\frac{dB}{m}]$.

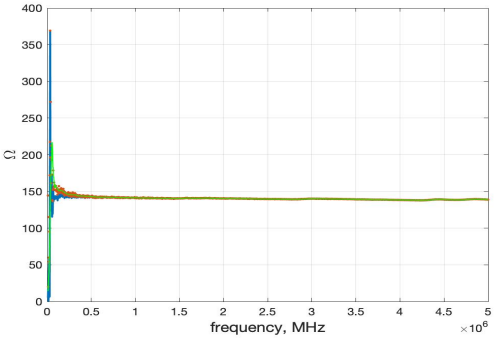

(f) Impedance $[\Omega]$.

Figure 3.19: Parameters in function of frequency for a LUMIREP-E coaxial cable in a Phase-Phase configuration.

3.10.2.3 SENOREP-3G Phase-Ground configuration

The second cable geometry examined was the SENOREP-3G three wires cable with a section of $(10mm^2)$. It consists of three symmetric conductors made by stranded plain anealed copper and with a radius of $a = 1.78mm$, each of which having a first insulation screen made by HEPR (Hard Grade Ethylene Propylene Rubber), a second one made by PVC (Polyvinyl Chloride), a first outside conductor screen made by extruded semi-conductor compound (copper) and a second screen made by plain annealed copper wires with tight watersmelling material. By inserting a hard plastic wire in the middle to the three cables and three more wires made of a material similar to that used for the strings and placing them at the sides, the symmetry is preserved. Everything is inserted inside an outer sheat made of reinforced PVC according to Normative HD 620, which guarantees not only insulation but also great mechanical strength. From the datasheet is possible to obtain the Resistance per unith length $R' = 0.00208\frac{\Omega}{m} = 2.08\frac{\Omega}{km}$ as an average between its maximum value at $20°$ and its maximum value at $90°$, the Capacitance per unith length between the phase and the neutral $C' = 0.22\frac{nF}{m} = 220\frac{nF}{Km}$ and the Inductance per unith length $L' = 0.53\frac{\mu H}{m} = 530\frac{\mu H}{Km}$. These values, as was also true for Low Voltage cables, refer to a working frequency of $50Hz$, far below the range of frequencies studied $(9kHz - 5MHz)$. The obtained parameters L', C', R', G', α_{dB} and Z_0 obtained are (**Figure3.20**).
It is possible to note that, also in this case, at low frequencies there are some due oscillations dependent on the fact that the line used to determine the line parameters must be shorted. Resonance phenomena appears again in the transmission near $5MHz$, higher with respect to the LUMIREP-E cable. Despite all the conductors are shielded, this is probably due to the presence of higher cross-talk interference between cables, that all lives togheter in an outer sheat. In fact, in certain ways, they exist on the graphs for the same parameters, for the same frequency range and with the same shape as they did in the LV cables, where the two conductors are joined in an outer sheat.
The characteristic impedance Z_0 and the other results at $133kHz$ are shown in the **Tab3.6**:

	Measured	**Calculated**
Inductance per unit-length (L') $[\frac{\mu H}{m}]$	1.009	0.301
Capacitance per unit-length (C') $[\frac{nF}{m}]$	0.259	0.103
Resistance per unit-length (R') $[\frac{\Omega}{m}]$	0.458	0.186
Conductance per unit-length (G') $[\frac{\mu S}{m}]$	5.446	0.260
Attenuation per unit-length (α_{dB}) $[\frac{dB}{m}]$	0.029	0.014
Characteristic impedance (Z_0) $[\Omega]$	60.740	54.072

Table 3.6: The characteristic impedance Z_0 and the other results L', C', R', G', α_{dB} at $133kHz$ measured and calculated.

From the simulation it is possible to notice how, also in this case, the error between the graphs obtained through the formulas as a function of frequency and those obtained through measurements is not neglegible. From the results obtained through the measurements, it is possible to notice, as for the LUMIREP-E cable in the Phase-Ground configuration, a lowering of the characteristic impedance of the line $(Z_0 = 60.7406\Omega)$ with respect to LV cables and therefore a clear improvement in terms of matching between the line itself and the transmitter/receivers, thus reducing the power lost due to reflections.
However it is clear from the analysis of the loss coefficient (α_{dB}) that this is still excessively high for a line that is several kilometers long. For instance, the attenuation is $29.3dB$ with a transmitter and a receiver positioned $1km$ apart.

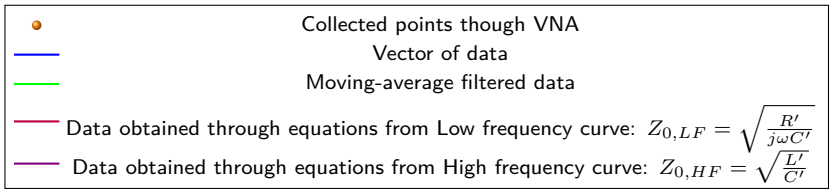

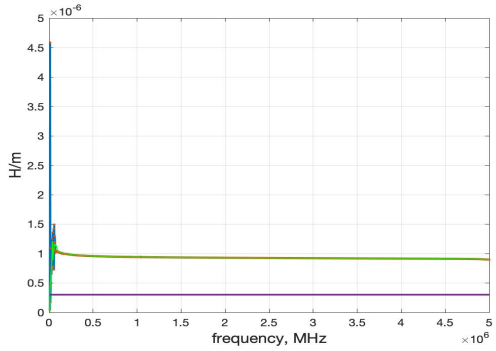

(a) Inductance per unit length $[\frac{H}{m}]$.

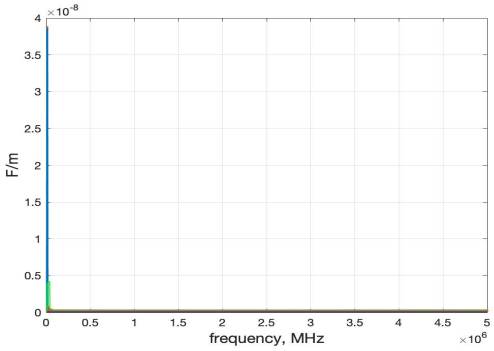

(b) Capacitance per unit length $[\frac{F}{m}]$.

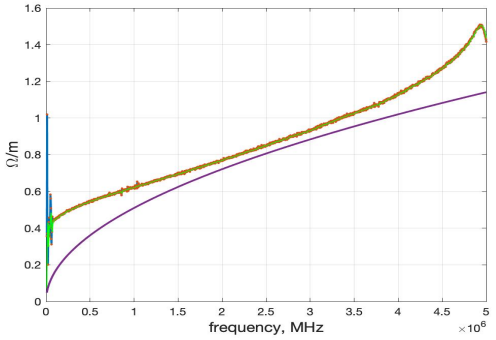

(c) Resistance per unit length $[\frac{\Omega}{m}]$.

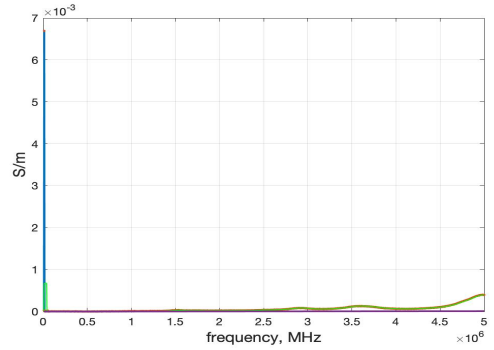

(d) Conductance per unit length $[\frac{S}{m}]$.

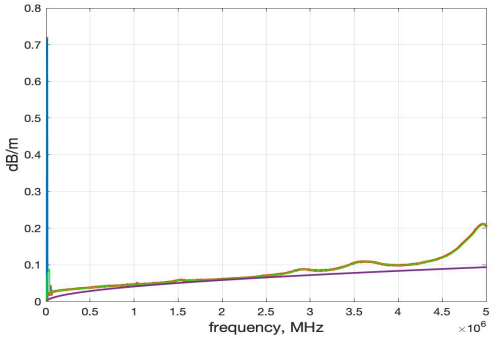

(e) Attenuation per unit length $[\frac{dB}{m}]$.

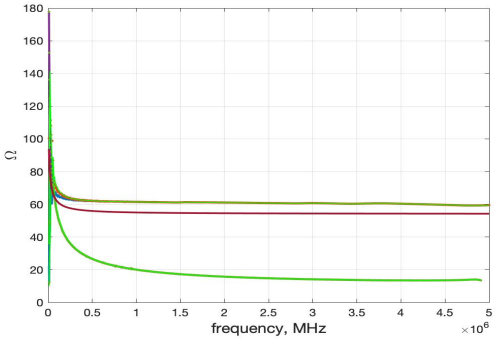

(f) Impedance $[\Omega]$.

Figure 3.20: Parameters in function of frequency for a SENOREP-3G three-wire cable in a Phase-Ground configuration.

3.10.2.4 SENOREP-3G Phase-Phase configuration

To perform the simulations below, two SENOREP-3G coaxial cable with a section of $(10mm^2)$, previously studied, were taken with the signal injected on two different phases present in the outer sheat of the cable for the three-phase system.
As for the LUMIREP-E cable in the Phase-Phase configuration, also here was not possible to compare the measurements' results with formulas **3.11**, **3.12** in function of frequency on Matlab used for a two-wire transmission line. This is due to the fact that, as was already said, a two-wire transmission line approximates the behaviour of two distinct unshielded cables, joined together in an outer protective sheath, which exhibit considerable electromagnetic interference and cross-talk.
Instead, two coaxial cables in parallel were each carrying a portion of the differential signal and able to minimises crosstalk and electromagnetic interference were ex- amined in this instance.
The obtained parameters L', C', R', G', α_{dB} and Z_0 acquired with the VNA in the form of S-parameters and adapted on Matlab, are shown in **Figure3.21**. It is possible to note that also in this case at low frequencies, there are some oscillations dependent on the fact that the line used to determine the line parameters must be shorted. Small resonance phenomena are present in the transmission near $5MHz$, larger than those present in the LUMIREP-E cable with the same configuration, although they are not significant.
The characteristic impedance Z_0 and the other results at $133kHz$ are shown in the **Tab3.7**:

	Measured
Inductance per unit-length (L') $[\frac{\mu H}{m}]$	1.302
Capacitance per unit-length (C') $[\frac{nF}{m}]$	0.127
Resistance per unit-length (R') $[\frac{\Omega}{m}]$	0.448
Conductance per unit-length (G') $[\frac{\mu S}{m}]$	5.387
Attenuation per unit-length (α_{dB}) $[\frac{dB}{m}]$	0.0165
Characteristic impedance (Z_0) $[\Omega]$	98.374

Table 3.7: The characteristic impedance Z_0 and the other results L', C', R', G', α_{dB} at $133kHz$ measured.

It is interesting to notice how the attenuation coefficient (α_{dB}) has significantly decreased. Positioning a transmitter and a receiver $1km$ apart, the attenuation is $16.5dB$, very small compared to the Phase-Ground configuration. Instead, it is possible to notice how the characteristic impedance (Z_0) of the line has worsened, reaching a value of 98.374Ω.
This certainly creates an higher mismatch between the characteristic impedance of the transmitter, of the line and of the receiver, increasing the losses for reflections.
Despite the worsening, this confirms that the data exchange techniques in the Phase-Phase configuration is more efficient in therms of attenuation-efficient and is preferable to the Phase-Ground one also for this geometry.
This because it is always possible to add an impedance coupler between the line and the MASTER/SLAVE to reduce the reflection losses, whereas the attenuation coefficient is a parameter intrinsic to the cable that, once present, cannot be modified, making the Insertion Loss very high and so the signal, after a certain distance, no longer usable.
As will be analyzed in detail in the next section, this geometry with a higher section presents the best behavior in terms of cost-benefits for PLC communication without distorting its peculiar characteristics.

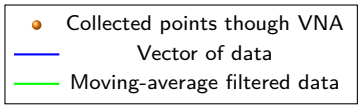

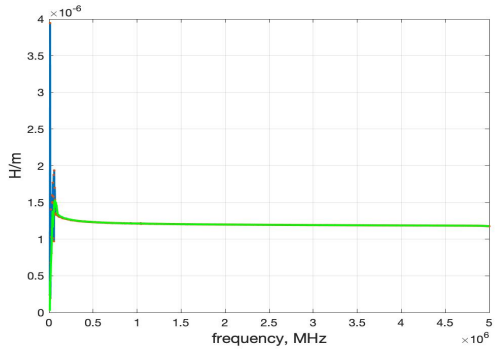

(a) Inductance per unit length $[\frac{H}{m}]$.

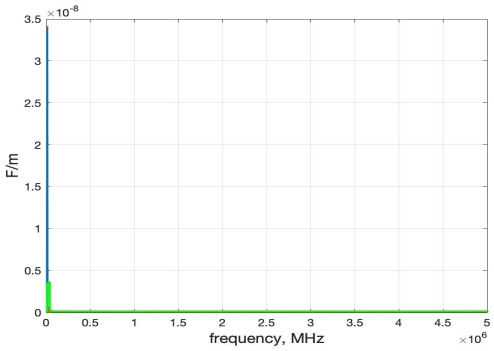

(b) Capacitance per unit length $[\frac{F}{m}]$.

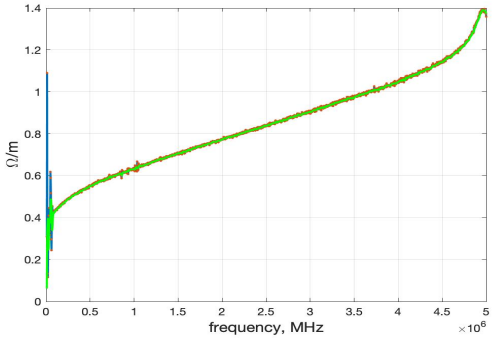

(c) Resistance per unit length $[\frac{\Omega}{m}]$.

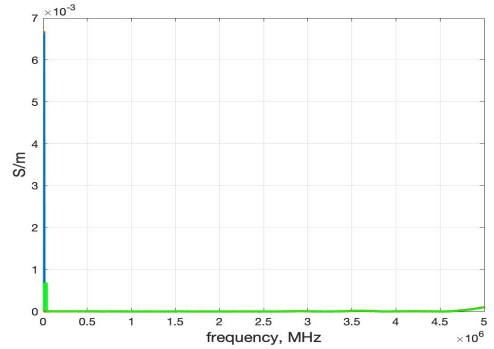

(d) Conductance per unit length $[\frac{S}{m}]$.

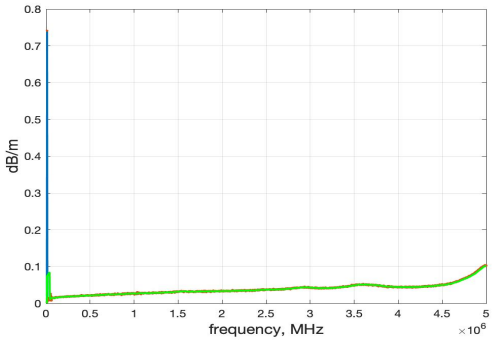

(e) Attenuation per unit length $[\frac{dB}{m}]$.

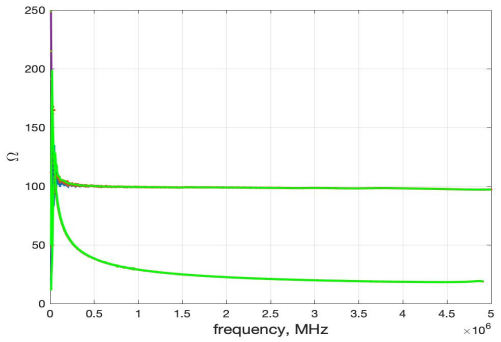

(f) Impedance $[\Omega]$.

Figure 3.21: Parameters in function of frequency for a SENOREP-3G three-wire cable in a Phase-Phase configuration.

3.10.2.5 Cost-Benefit analysis

For data exchange at Medium-Voltage, entering the differential signal between two phases of the three-phase system causes it to experience a lower attenuation coefficient (α_{dB}) than a configuration in which it travels in the Phase-Ground configuration, but that the value of the cable's characteristic impedance (Z_0) is higher and, as a result, the reflections caused by the mismatch. A three-wires cable Senorep-3G with a cross section of $10mm^2$, a Phase-Ground configuration shows a characteristic impedance $Z_0 = 60.740\Omega$ and at $133kHz$, a loss coefficient in dB, $\alpha_{dB} = 29.3\frac{dB}{km}$. Instead the same cable in a Phase-Phase configuration shows a characteristic impedance $Z_0 = 98.3743\Omega$ and always at $133kHz$, a loss coefficient in dB, $\alpha_{dB} = 16.5\frac{dB}{km}$. For a single-wire coaxial cable, with a cross section of $25mm^2$, a Phase-Ground configuration shows a characteristic impedance $Z_0 = 59.084\Omega$ and at $133kHz$, a loss coefficient in dB, $\alpha_{dB} = 27.9\frac{dB}{km}$. Instead the same cable in a Phase-Phase configuration shows a characteristic impedance $Z_0 = 140.002\Omega$ and always at $133kHz$, a loss coefficient in dB, $\alpha_{dB} = 6.2\frac{dB}{km}$. Since it is always possible to build an impedance coupler that reduces impedance mismatch and because a higher attenuation coefficient drastically increase the Insertion Loss and so the maximum transport distance, it is generally preferred to have a configuration with a lower attenuation coefficient than with higher impedances. It has been observed that larger sections generally perform better in both Medium and Low Voltage. The LUMIREP-E cable, which has a conductor section of $25mm^2$, responds to line losses better than the SENOREP-3G cable, which has a conductor section of $10mm^2$.This result in much more difficult handling, significantly more complex weights, and transport challenges.
From the datasheet, the weight of the SENOREP-3G three-wire cable with a section of $10mm^2$ is $1240\frac{kg}{km}$, whereas the weight of the same cable with a section of $25mm^2$ is $1980\frac{kg}{km}$. Or even the LUMIREP-E unarmored cable, which weighs $490\frac{kg}{km}$, with a cross section of $10mm^2$ and $870\frac{kg}{km}$ with a section of $25mm^2$, which for a three-phase line become $1470\frac{kg}{km}$ and $2610\frac{kg}{km}$ respectively. It is clear that these values for MV cables, which need to be kilometers long to transfer power, have a significant influence on the choice of the cable. For instance, the LUMIREP-E with a section of $10mm^2$ and one with a section of $16mm^2$ cost, respectively, $10446.480\frac{eur}{km}$ and $13108.920\frac{eur}{km}$. Although the second option has significant performance advantages as it is possible to deduce from the simulations above, it is not always viable to select this geometry because the cables are primarily intended for the transportation of power and are therefore more concerned with cost-cutting.
A three-phase system for MV data transport made up of three-wire cables has typically performed better in terms of losses along the line, characteristic impedance, overall weigth, and costs than a single-wire coaxial cable line constructed with a three of them, with the same section. In fact, as demonstrated above, a three-wire cable with a section of $10mm^2$, for instance, weighs $1240\frac{kg}{km}$ overall, compared to $490\frac{kg}{km}$ for a single wire, and $1470\frac{kg}{km}$ for three linked wires. Higher sections also fit the same difference. A coaxial single-wire cable performs better, but only because a section more than double the size of the three-wire cable has been tested. Their values in therms of characteristic impedance (Z_0) and attenuation coefficient (α_{dB}) are not too far, and if it is taken a SENOREP-3G cable having the same section as the LUMIREP-E one, it is possible to see how one works better than the other. Finally, the cost for a SENOREP-3G with a cross-section of $16mm^2$ is $19463.880\frac{eur}{km}$ instead, only one LUMIREP-E with the same cross section costs $13108.920\frac{eur}{km}$ for a total price of $39326.760\frac{eur}{km}$ (three phase system),more than double that of the other three-wires geometry.

4 Transformers

A transformer is a static electrical device with no moving or rotating components. It converts AC voltage at constant power (minus losses) without changes in frequency between input and output, with a consequent change in current levels, hence enhancing the security and effectiveness of power networks as and when necessary. Transformers only use AC power signals to run on the mutual induction concept. They transfer electrical power between two systems that are electrically insulated expecially in a wide range of residential and industrial applications, primarily and perhaps most importantly in the distribution and regulation of power across long distances. Transformers are mainly used for:

- management of transmission and distribution power at 50/60Hz;
- safety electrical separation;
- measurement circuits;
- supply of electric and electronic circuits.

4.1 Transformer Structure

Three-phase systems are used to generate and transmit electrical power because, it is possible to demostrate, that using a three-phase transport method enables the use of cables with a section that is twice as small as a single-phase line while maintaining the same power and line length. Three-phase power transformers are used to connect the different voltage levels. They can be realized using 3 single-phase transformers, connecting each line to each transformers.Therefore, it is much simpler to think about a single-phase transformer in order to comprehend how they are constructed, their behaviour, characteristic parameters and its non-idealities. The behaviour of a three-phase transformer will directly follow from its operation once it is understood.
A monophase transformer is composed of three main components:

- ferromagnetic core;
- primary winding;
- secondary winding.

The primary winding is the part that is connected to an electrical source, from where Magnetic Flux (a measurement of the total magnetic field which passes through a given area) is initially produced. These coils are insulated from each other and the main flux, induced in the primary winding from where it pass to the magnetic core, is linked to the transformer's secondary winding (the one connected to the load) through a low Reluctance path.

In this way the windings are magnetically coupled as shown in figure **Figure4.1**. The role of the two windings can be inverted because transformers are bidirectional.
The ferromagnetic core is used to increase the coupling between the windings because has a Reluctance (opposition offered by a magnetic circuit to the production of magnetic flux) lower than air, so the flux is concentrated in it. It can be calculated as:

$$\Re = \frac{l}{\mu_0 \mu_r A} = \frac{l}{\mu A}[H^{-1}] \tag{4.1}$$

Where:

- l is the length of the circuit in metres;
- μ is the permeability of the material ($\mu = \mu_0 \mu_r$);
- μ_0 is the permeability of vacuum, equal to $\mu_0 = 4\pi \times 10^{-7} \left[\frac{H}{m}\right]$;
- μ_r is the relative magnetic permeability of the material (dimensionless), for a ferromagnetic core of a transformer $< 1400\mu_r < 20000$;
- A is the cross-sectional area of the circuit in square metres.

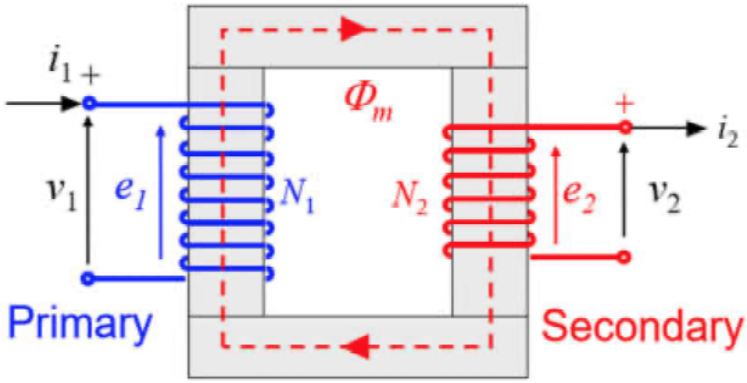

Figure 4.1: Scheme of a single phase transformer.

4.1.1 Lamination of the Ferromagnetic Core

All types of transformers have a magnetic core that is built by stacking laminated steel sheets with the minimum air-gap between each one to maintain the magnetic path's continuity. Instead of being made from a single solid block, it is constructed from a number of metal insulated plates through thin layer of varnish or enamel, glued together and compressed into a single solid core as shown in figure **Figure4.2**. This is done for two main reasons:

- to reduce Eddy Currents (Foucault's currents);
- to create various core geometries, a much more complex goal from a single block of ferrite.

In accordance with Faraday-Lenz law, to generate a Magnetic Field and consequently a Magnetic Flux, an emf (electromotive force) is applied to the primary winding, which results in the production of currents that are not wanted in the core of the transformer and are known

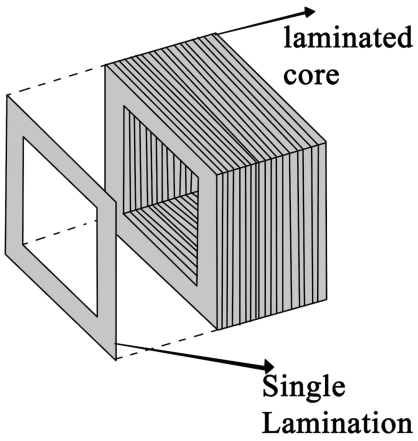

Figure 4.2: Laminated Ferromagnetic Transformer Core.

as Eddy Currents. The Joule effect, caused by Eddy Currents in conductors with resistivity greather than zero, increase the heat in the core difficult to dissipate, decrease the useful power and the transformer efficiency and consequently, increase the power loss. In order to increase the performances and therefore improve the efficiency of the transformers, it is necessary that the power dissipated in heat is lowered as much as possible. The Dissipated Power (P_d), is given by the relation below (**4.2**):

$$P_d \propto \frac{\omega^2 \hat{B}}{R} \tag{4.2}$$

Where:

- ω is the field pulsation;
- $\hat{B}$ is the peak value of the magnetic flux density;
- R is the equivalent ohmic resistance "seen" by Eddy Currents.

Therefore, high resistivity materials must be selected, and lamination must be carried out, in order to reduce P_d in the core as much as possible. In fact, the expected result of laminating the material with insulated layers perpendicular to the planes results in an increase in electrical resistance within the core, which reduces the flow of current as it circulates in smaller paths.

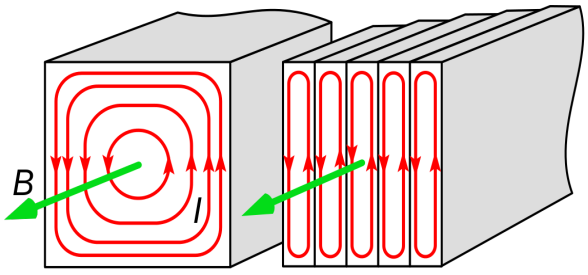

Figure 4.3: Non laminated and laminated Laminated Ferromagnetic Transformer Core.

However, it is not the only one: ferrite does exactly the same thing, but with particles of sintered ferromagnetic material. This allows to have much smaller cores with the same power, as well as transformers that can work at frequencies of the order of hundreds of kHz or even MHz. This technology has been developing a lot in recent years, especially with the advent of energy storage systems (batteries) and the related inverters.
Materials with a not very high resistivity can be chosen, since then the lamination itself will increase the coefficient of the electrical resistance. Varnish or enamel, which act as electrical and thermal insulators in turn, has the drawback of making it more difficult to remove the heat that is naturally created. However, in light of the advantages that lamination offers, this effect is insignificant. Small transformers usually have a c-type core that is a rectangular geometry with rounded sharp edges. Usually it is not a single block of ferromagnetic material but composed of two pieces then joined together, to facilitate the assembly of the primary and secondary windings. To create the final core, usually two different cores are paired together. The below (**Figure4.4**) shows the geometry described before:

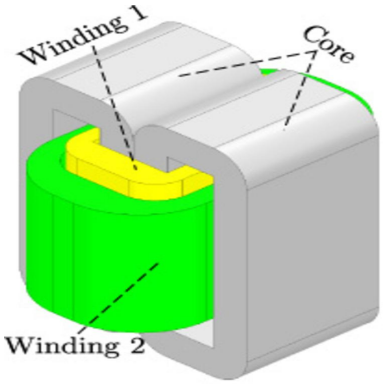

Figure 4.4: C-type ferromagnetic core.

Larger transformers, instead, always have a rectangular geometry, but the sharp edges are usually not rounded. In these, it is possible to distinguish between vertical parts called colums and horizontal ones named yokes. Depending on the the kind of joint between the colums and the yonkes it is possible to distinguish two different profiles:

- Planed;
- Intersected.

Planed geometries are not produced anymore since are less efficient: increase the amount of dissipated power and the effect of Eddy Currents.

4.1.2 Galvanic Insulation

Galvanic isolation is the separation of electrical systems/subsystems by which non direct current can flow and may possess different ground potentials, so no direct conduction path is permitted.The two most common reasons for creating isolation are:

- safety from fault conditions in industrial grade products;
- wired communication between devices is needed but each device regulates its own power.

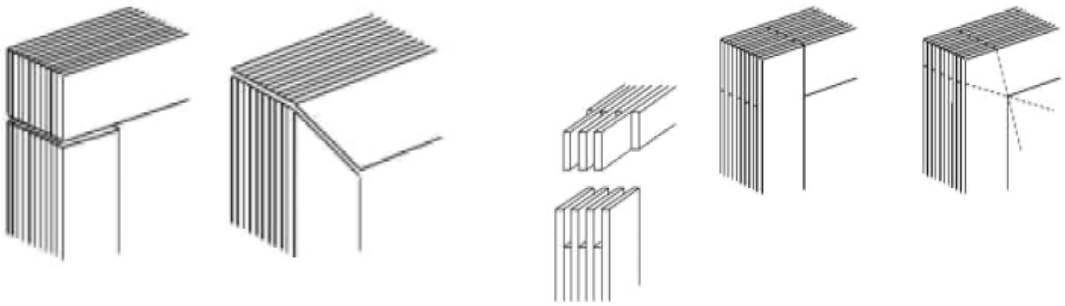

(a) Planed **(b)** Intersected

Figure 4.5: Types of joints.

As alrady explained, transformers couple by magnetic flux. The primary and secondary windings of a transformer are not connected to each other, so while transformers are usually used to change voltages, isolation transformers with a 1:1 ratio are used in safety applications. If two electronic systems have a common ground, they are not galvanically isolated. The common ground might not normally and intentionally have connection to functional poles, but might become connected. For this reason isolation transformers do not supply a GND/earth pole.Transformers guaratee galvanic insolation as an intrinsic behaviour so they are the most widespread galvanic insolators. Energy or information can still be exchanged between the sections without any problems.

4.2 Real Transformers

Real transformers are not linear, have losses due to non-idealities of the construction elements and are not perfectly coupled. These usually work at low frequencies (50-60Hz) as they are mainly used in the field of power distribution. They are able to convert electrical power into electrical power but at different voltage and, consequently, current levels with no change in frequency. In the range of frequencies used by power distribution networks non idealities that must be taken into account are:

- non zero Reluctance of the magnetic circuit ($\mu_{Fe} \neq \infty$);
- primary and secondary leakage fluxes;
- Joule losses in the windings ($R_{wind} \neq 0$);
- iron losses.

4.2.1 Non zero Reluctance $\mathfrak{R}$ of the magnetic circuit

Considering in the primary winding a time varying current i_1 (magnetizing current), it generates a variable flux (Φ_m) in the transformer's core thanks to the Ampère's law:

$$\oint_{\partial S} \vec{H} \cdot \vec{dl} = \int_S \vec{J_f} \cdot \vec{dS} = JS = Ni_1 \tag{4.3}$$

Where:

- Ni_1 is the net current since the path of integration cuts the coil N times and each wire carries the current i_1;
- $\vec{dl} = l_c$ since the magnetic field remains inside the transformer's core due to its less Reluctance with respect to the air, the path of integration of Ampere's law is the length of the core;
- $\Phi_m = \int_S \vec{B} \cdot \vec{dS}$ is the Magnetic Flux (a measurement of the total magnetic field which passes through a given area) knowing that the magnetic field in materials ($\vec{B}$) is equal to the magnetic field in vacuum ($\vec{H}$), multiplied by the medium permeability $\mu \Rightarrow \vec{B} = \mu\vec{H} = \mu_r\mu_0\vec{H}$.

Thanks to the Faraday-Lenz law:

$$\oint_{\partial S} \vec{E} \cdot \vec{dl} = -\frac{d}{dt}\int_S \vec{B} \cdot \vec{dS} = -\frac{d\Phi_m}{dt} \tag{4.4}$$

The flux Φ_m self-induces an emf e_1 (electromagnetic force), that impose a supply voltage v_1. Using the load convention, the Faraday-Lenz law has a $+$ sign:

$$v_1 = e_1 = +\frac{d\lambda_1}{dt} = +N_1\frac{\Phi_m}{dt} \tag{4.5}$$

Where:

- $\lambda_1 = N_1\Phi_m$ is the total flux linked with the coil since each turn is crossed by the same flux.

Using for the secondary winding the generator convention (the Faraday-Lenz law has $-$ sign), it is possible to obtain:

$$v_2 = e_2 = +\frac{d\lambda_2}{dt} = +N_2\frac{\Phi_m}{dt} \tag{4.6}$$

Since the transformer's core has the relative magnetic permeability $\mu_{Fe} \neq \infty$, it is possible to model the single-phase transformer as a magnetic circuit (**Figure4.6**):

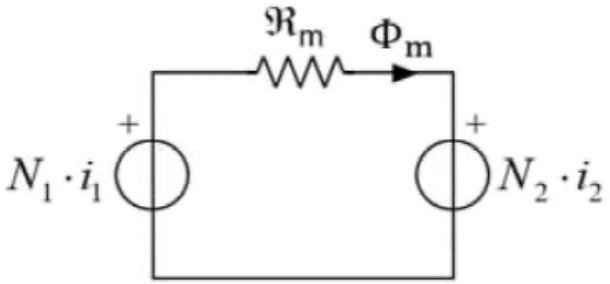

Figure 4.6: Equivalent magnetic circuit due to the non zero Reluctance of the transformer's core.

For this kind of circuit it is possible to apply the Hopkinson's law:

$$\oint_{\partial S} \vec{H} \cdot \vec{dl} = Ni \Rightarrow \oint_{\partial S} \frac{\Phi_m}{\mu A(l)} \cdot \vec{dl} = Ni \tag{4.7}$$

Knowing that the Reluctance of the ferromagnetic material is $\mathfrak{R} = \oint_{\partial S} \frac{\Phi_m}{\mu A(l)} \cdot \vec{dl}$, the Hopkinson's law for the studied case is:

$$N_1 i_1 - N_2 i_2 = \mathfrak{R}_\mathfrak{m} \Phi_m \neq 0 \tag{4.8}$$

To sustain the magnetic flux Phi_m imposed by the voltage, is required a magnetizing current i_m and considering for semplicity that the magnetization depends only by the primary winding, the Hopkinson's law became:

$$N_1 i_1 - N_2 i_2 = N_1 i_m \tag{4.9}$$

To obtain the equivalent component in which flow this current:

$$\mathfrak{R}_\mathfrak{m} \Phi_m = N_1 i_m \Rightarrow \Phi_m = \frac{N_1 i_m}{\mathfrak{R}_\mathfrak{m}} \tag{4.10}$$

And applying again the the Faraday-Lenz law at the primary winding since it has been considered that all the flux Φ_m is generated by the primary winding:

$$v_1 = e_1 = N_1 \frac{\Phi_m}{dt} = \frac{N_1^2}{\mathfrak{R}_\mathfrak{m}} \frac{di_m}{dt} = L_m \frac{di_m}{dt} \tag{4.11}$$

Where $L_m = \frac{N_1^2}{\mathfrak{R}_\mathfrak{m}}$ is the magnetizing inductance of the transformer. The figure below depics the obtained result (**Figure4.7**):

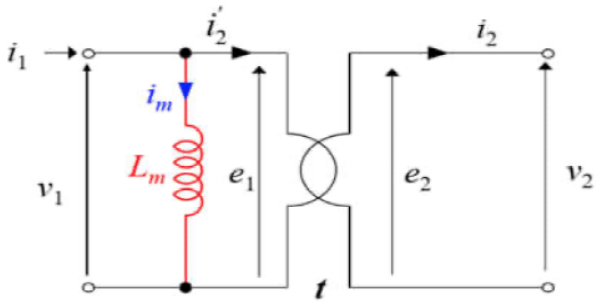

Figure 4.7: Equivalent magnetizing inductance inserted in a single-phase transformer scheme.

4.2.2 Primary and secondary leakage fluxes

Real transformers are not perfectly coupled, in fact part of the flux is not bounded in the magnetic core, but propagate in air. Since it is linked to only one coil at time, it cannot be used for magnetic coupling. This behaviour is shown in the **Figure4.8**.
The total flux is given by:

$$\lambda = N(\Phi_m + \Phi_d) = \lambda_m + \lambda_d \tag{4.12}$$

In the primary winding the Faraday-Lenz law becomes:

$$v_1 = \frac{d\lambda_1}{dt} = N_1 \frac{\Phi_m}{dt} + N_1 \frac{\Phi_{d1}}{dt} \tag{4.13}$$

Where $\lambda = N_1(\Phi_m + \Phi_{d1})$ and Φ_m is used to couple the secondary winding while the flux Φ_{d1} is lost. Knowing that $\Phi_{d1} = \frac{N_1 i_1}{\mathfrak{R}_{d1}}$, where $\mathfrak{R}_{d1}$ is the Reluctance of the leakage flux

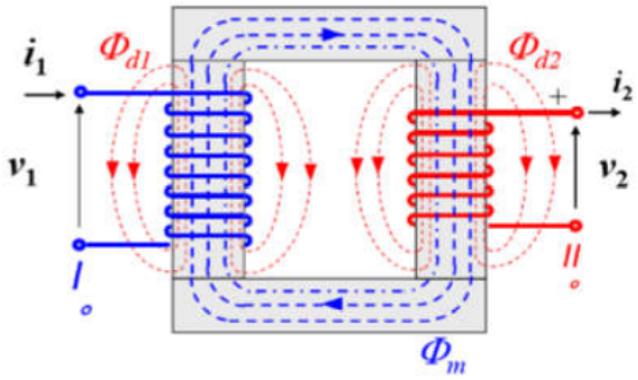

Figure 4.8: Main flux and dispersed fluxes in the real transformers.

(Reluctance of the air), it is possible to obtain the equivalent component to insert in the magnetic circuit that is the primary leakage inductance (L_{d1}):

$$v_1 = \frac{d\lambda_1}{dt} = N_1 \frac{\Phi_m}{dt} + \frac{N_1^2}{\mathfrak{R}_{\mathfrak{d}1}} \frac{di_1}{dt} = e_1 + L_{d1} \frac{di_1}{dt} \tag{4.14}$$

It is possible to do the same thing also for the secondary winding:

$$v_2 = -\frac{d\lambda_2}{dt} = N_2 \frac{\Phi_m}{dt} - N_2 \frac{\Phi_{d2}}{dt} \tag{4.15}$$

And obtain the reluctance of the secondary leakage inductance (L_{d2}):

$$v_2 = -\frac{d\lambda_2}{dt} = N_1 \frac{\Phi_m}{dt} - \frac{N_2^2}{\mathfrak{R}_{\mathfrak{d}2}} \frac{di_2}{dt} = e_2 - L_{d2} \frac{di_2}{dt} \tag{4.16}$$

It is possible to add to the obtained circuit shown in the **Figure4.7**, the new two parassitic components (**Figure4.9**):

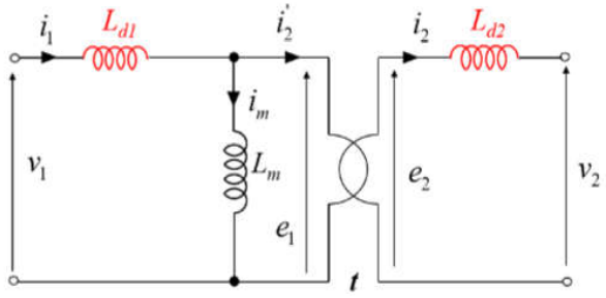

Figure 4.9: Equivalent leakage inductances inserted in a single-phase transformer scheme.

Leakage reactances are small with respect to magnetization reactance.

4.2.3 Joule losses in the windings

Current flowing through a winding's conductor causes joule heating due to the resistance of the material of the wire. They can be added as a resistance components (R_1 and R_2), in

series to the primary and secondary leakage inductances as follow:

$$v_1 = e_1 + L_{d1}\frac{di_1}{dt} + R_1 i_1, \quad v_2 = e_2 - L_{d2}\frac{di_2}{dt} - R_2 i_2 \tag{4.17}$$

Usually the value of the primary resistance is very high with respect to the secondary one since the voltage values are much smaller.
The equivalent circuit that takes into account the parassitic contribute of the non zero Reluctance of the magnetic circuit, primary and secondary leakage fluxes and the Joule losses in the windings is shown in **Figure4.10**:

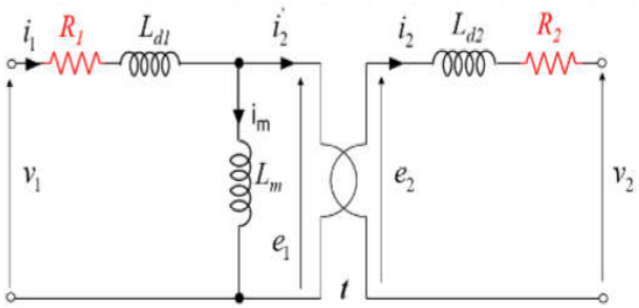

Figure 4.10: Equivalent resistances due to Joule effect inserted in a single-phase transformer scheme.

4.2.4 Non zero iron losses

The ferromagnetic core is interested by losses due to time varying magnetization:

- hysteresis losses;
- eddy current losses.

It is possible to approximate power loss in the ferromagnetic core due to this two contributes as proportional to the square of the flux density $\vec{B}$ and, consequently, to the square of the main flux flowing through the core Φ_m:

$$P_{fe} \propto B^2 \propto \Phi_m^2 \tag{4.18}$$

Since it was considered for semplicity that the flux is generated only by the primary coil, losses are proportional to the also to the square of the voltage of the first coil:

$$P_{fe} \propto B^2 \propto \Phi_m^2 \propto e_1 \tag{4.19}$$

Iron losses can be modelled as a resistive component R_{fe}, placed in parallel to the magnetizing inductance only in the primary side as shown in **Figure4.11**.
From the above picture it is possible to see that actually the power dissipated in the resistance R_{fe} is proportional to the square of the voltage drop:

$$P_{fe} = \frac{e_1}{R_{fe}} \tag{4.20}$$

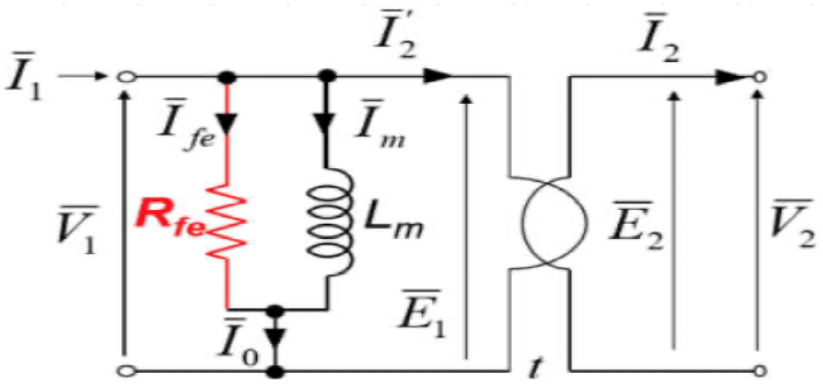

Figure 4.11: Equivalent resistance due to the non zero iron losses in a single-phase transformer scheme.

4.2.5 Equivalent circuit

Taking into account all the parassitic components due to the non idealities present into transformers, it is possible to obtain an equivalent circuit at $50Hz$:
The non linearity of the transformer due to magnetic saturation is represented by a variation of the magnetizing inductances with respect to the magnetizing current I_m:

$$L_m = f(I_m) \tag{4.21}$$

The circuit obtained is called T-shape and it is possible to describe it in the phasor domain:

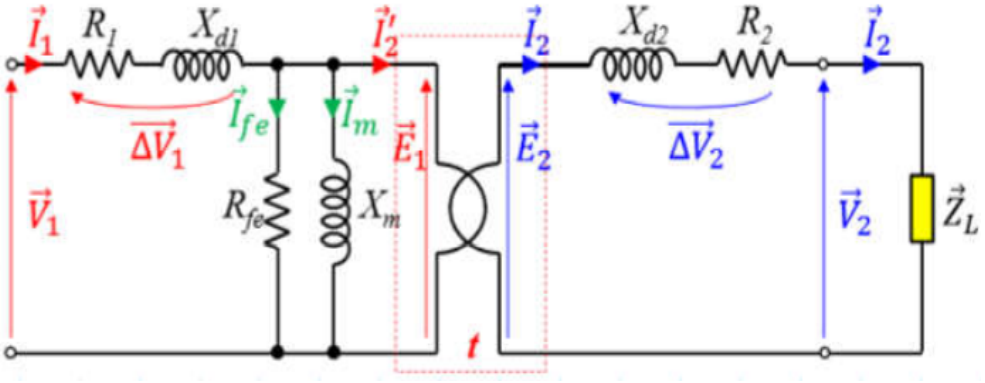

Figure 4.12: Single-phase transformer equivalent circuit with parassitic components at $50Hz$.

Where:

- $\overline{Z_1} = R_1 + jX_{d1}$ is the primary winding impedance;
- $\overline{Z_2} = R_2 + jX_{d2}$ is the secondary winding impedance;
- $\overline{Z_0} = R_{fe}//X_m = \frac{R_{fe}jX_m}{R_{fe}+jX_m} = R_0 + jX_0$ is the no load impedance.

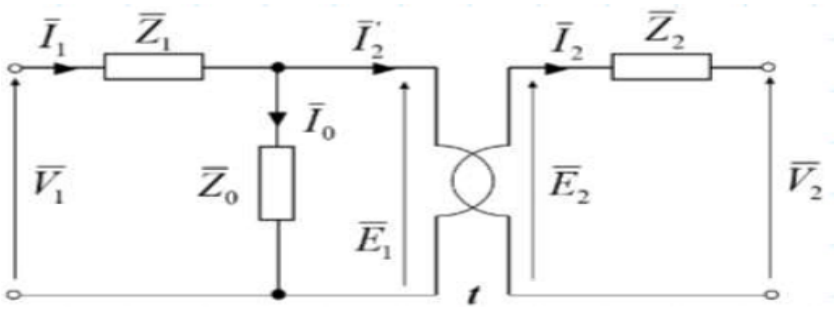

Figure 4.13: Single-phase transformer equivalent circuit with parassitic components at $50Hz$ in the phasor domain.

The above equivalent circuit can be modified in a simplify model, called L-shape model, in order to be easier to analyse. Despite this benefit, the new shape introduce some errors and, to be as close as possible to the real behaviour, it has been not considered.

4.2.6 Characterisation of the parassitic parameters

In order to understand the frequency behaviour of the studied transformers, it is necessary ro determine the values of the equivalent circuit parameters. They can be evaluated in two ways:

- computed from the design data, considering the geometrical dimensions;
- obtained from experimental measurements.

The second method is the most accurate since the analysis is not performed during construction but a posteriori, in such a way as to have more precise parameters conforming to what is the real behavior of the transformers.
The four performed tests are:

- Turns Ratio test;
- Winding resistance measurement;
- No load test (NLT);
- Short circuit test (SCT)

Usually, a Device Undre Test (DUT) is characterised by nominal values reported on the datasheets within some tollerances ($5 - 10\%$):

- Rated/Nominal voltage (V_N);
- Rated/Nominal power (S_N);
- Rated/Nominal current (I_N);
- Rated/Nominal frequency (f_N).

These values are the working parameters to which the DUT is usually used. The side on which the test is performed can be exchange since the machine is symmetric, while the frequency is also tested $10 - 100$ times higher than the nominal one for up to 30 seconds, in order to understand the robustness of the transformer under study.

4.2.6.1 Turs Ratio test

Power transformer turns ratio test is an AC Low Voltage test which determines the ratio of the High Voltage winding (t) to all other windings at no-load. The turns ratio test is performed on all taps positions of every winding and calculated by dividing the induced voltage reading into the applied voltage value.. The transformer turns ratio tester (TTR) is a device used to measure the turns ratio between the windings. Measured ratio variations should be within 0.5% of nameplate markings, otherwise the transformer under test presents some problems. A typical Turns Ratio Tester (TRT) for a single-phase transformer is shown in **Figure4.14**. In order to perform it, all the equipment must be isolated, must be applied working grounds to all incoming and outgoing cables and disconnected all incoming and outgoing cables from the transformer bushing terminals connections. It could be used a nylon rope to hold cables away from incoming and outgoing terminals. Given that the searched value is unknown, the process is iterative. On a central screen, the panel displays a non-zero value that can be modified by turning the testing knobs. The LCD will display a number that becomes closer and closer to zero as it is turned the knobs, indicating that it is discovering the true turns ratio. The screen will tell that the turns ratio has been found once the knobs have indicated the searched value up to the third decimal place at the end.

Figure 4.14: Example of single-phase hand cranked TTR.

4.2.6.2 Winding resistance measurement

It is used the the Volt-Ampère method, obtaining the resistance from current and voltage. A known voltage value (V_{test}) is applied on one side of the transformer at a time, leaving the other disconnected. In this way, through the relation **4.22**, it is possible to directly obtain the value of the parasitic resistance at time caused by the resistivity (ρ) of the windings made by copper, since the tool is also able to measure the corrispective current.

$$R_{wind} = \frac{V_{test}}{I} \tag{4.22}$$

The measurement are done with a cold DUT, when is not working for a sufficient time, in the way to consider the copper temperature equal to the environment one. The resistance value are referred to environment temperature and not at the working temperature when

the transformer has already been active for some time. This test must be performed with a current 10 times lower of the nominal one, to avoid the heating of the winding.

4.2.6.3 No Load Test (NLT)

This test is performed to evaluate the value of the parassitic resistance due to the non zero iron losses (R_{fe}) and the value of the parassitic inducatance due to the non zero Reluctance $\mathfrak{R}_\mathfrak{m}$ of the magnetic circuit (L_m). These enable to obtain the no load impedance $Z_0 = R_{fe}//X_m$. Since the voltage and the current values involved are high, the test is carried out inside an insulated and controlled cabinet from outside, with access prohibited during the test, all for ensure its safety. The side on which the test is performed can be exchange since the machine is symmetric, but usually the measurement is performed on the Low Voltage side so as not to have to reach nominal voltages even in the order of $\sim kV$, to increase the safety and reduce the test consumption.
The figure **Figure4.15** shows, schematically, how the test is done. An input voltage test value (V_{NL}) is applied on the input with no load attached to the output of the transformer, thus obtaining an open circuit.

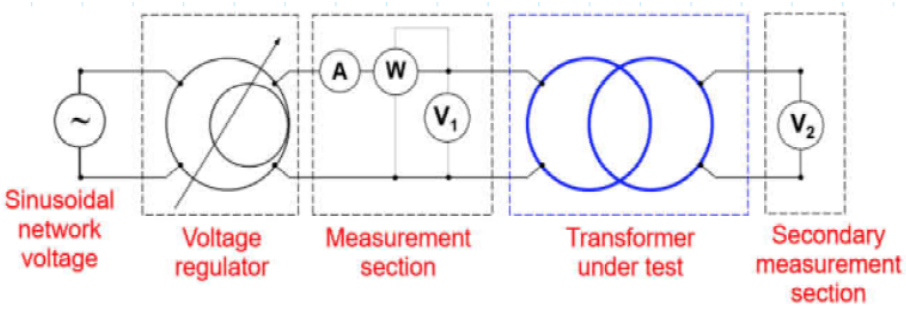

Figure 4.15: Schematic view of the NLT.

By imposing this input voltage with a value approximately 3% higher than the nominal one on the Low Voltage side of the transformer, it is evaluate the corresponding current value (I_{NL}) injected into the transformer and the corrisponding power dissipated (P_{NL}) on the equivalent impedance $Z_{0,LV} = R_{fe}//X_m$.
In fact considering the open circuit configuration, it is possible to think approximately ~ 0 the values of the primary and secondary winding impedances ($\overline{Z_1} = R_1 + jX_{d1}$, $\overline{Z_2} = R_2 + jX_{d2}$). Once obtained the value of the active power dissipated into the transformer circuit (P_{NL}), it is possible to get the apparent power and the reactive power as follow:

$$S_{NL} = V_{NL} I_{NL}, \quad Q_{NL} = \sqrt{S_{NL}^2 - P_{NL}^2} \tag{4.23}$$

Knowing that the V_{NL} is applied on the LV side, it is possible to get the corresponding $R_{fe,LV}$ and $X_{m,LV}$ values on the LV side:

$$R_{fe,LV} = \frac{V_{NL}^2}{P_{NL}}, \quad X_{m,LV} = \frac{V_{NL}^2}{Q_{NL}} \tag{4.24}$$

Once the values on the Low Voltage side have been found and knowing that the value of the resistance due to the non zero iron losses and the value of the parasitic reactance due to the non zero Reluctance $\mathfrak{R}_\mathfrak{m}$ of the magnetic circuit X_m are considered only for the High Voltage side, they can be transposed knowing the turns ratio t, obtaining R_{fe}, X_m and the equivalent impedance $\overline{Z_0} = R_0 + jX_0$ as follow:

$$R_{fe} = R_{fe,LV} t^2, \quad X_m = X_{m,LV} t^2 \quad \Rightarrow \quad \overline{Z_0} = R_{fe}//X_m = \frac{R_{fe} j X_m}{R_{fe} + j X_m} \tag{4.25}$$

Knowing that the test has been performed at $50Hz$ frequency value, it is possible to finally obtain the value of the parasitic inductance due to the non zero Reluctance $\mathfrak{R}_{\mathfrak{m}}$ of the magnetic circuit L_m as:

$$L_m = \frac{X_m}{2\pi f} \tag{4.26}$$

4.2.6.4 Short Circuit Test (SCT)

This test is performed to evaluate the value of series parameters composed by the resistances due to the resistivity (ρ) of the primary (R_1) and secondary (R_2) windings and the values of the primary (L_{d1}) and secondary (L_{d2}) inductances due to the leakage fluxes. These enable to obtain the primary and secondary winding impedances $Z_1 = R_1 + jX_{d1}$ and $Z_2 = R_2 + jX_{d2}$. Since the voltage and the current values involved are high, the test is carried out inside an insulated and controlled cabinet from outside, with access prohibited during the test, all for ensure its safety. The side on which the test is performed can be exchange since the machine is symmetric, but for this type of measurement, it is usually done on the High Voltage side, as the value of the rated current is much lower than that on the Low Voltage side.
The figure **Figure4.16** shows, schematically, how the test is done. The test can be performed at ambient temperature, but results must be rescaled at rated temperature.

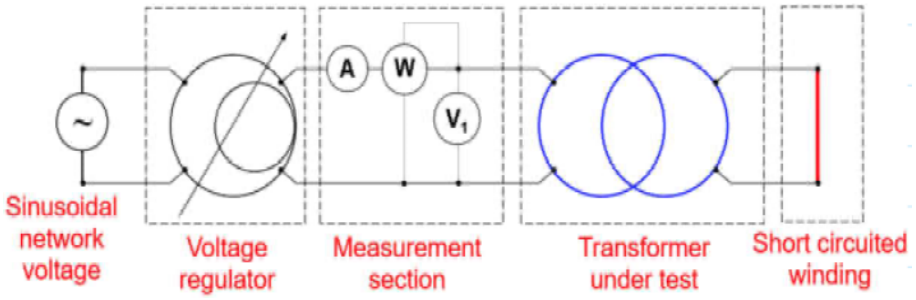

Figure 4.16: Schematic view of the SCT.

An input voltage test value (V_{SC}) is applied on the input with the output of the transformer shorted, thus obtaining an short circuit. V_{SC} (usually much lower than the nominal one V_N) is applied on the High Voltage side such that allows the achievement of the nominal current value on both sides and corresponding total power lost P_{SC} on the impedances $Z_1 = R_1 + jX_{d1}$ and $Z_2 = R_2 + jX_{d2}$. In fact considering the short circuit configuration, it is possible to think approximately ~ 0 the values of the resistance due to the non zero iron losses and the value of the parasitic inductance due to the non zero Reluctance $\mathfrak{R}_{\mathfrak{m}}$ of the magnetic circuit L_m, thus approximately ~ 0 the value of the equivalent impedance $\overline{Z_0} = R_{fe}//X_m$. From the winding resistance measurement, it is also possible to get the values of the primary and secondary resistances due the Joule losses in the windings and, knowing the value of the nominal current on both the sides, it is possible to obtain:

$$P_{SC1} = R_1 I_{N1}^2, \quad P_{SC2} = R_2 I_{N2}^2 \tag{4.27}$$

By adding the two contributions, it is possible to obtain power dissipated in the transformer circuit in the short circuit configuration:

$$P_{SC} = P_{SC1} + P_{SC2} = R_1 I_{N1}^2 + R_2 I_{N2}^2 \tag{4.28}$$

With this step it is also possible to compare the value obtained from the SCT with that measured, having taken into account the resistance values previously obtained (R_1 and R_2). Usually, the one calculated through the sum of the two powers tends to understimate what is the power actually lost. However, the error is usually around $2-3\%$ with a difference of $3-4[W]$. That makes clear that it is strainghtforward to consider the contribution of the impedance $\overline{Z_0}$ almost zero, but that in any case the parasitic effects due to the non zero iron losses and the value of the parasitic inductance due to the non zero Reluctance $\mathfrak{R}_\mathfrak{m}$ of the magnetic circuit L_m have a contribution also in this condiguration, absorbing a small percentage of power.
Anyway, from now ont, the power values obtained by taking into consideration R_1 and R_2 (obtained through the winfing resistance measurement) will be considered for the below relations, since for semplicity and as a first approximation, the contribution of $\overline{Z_0}$ in the SCT is considered null.
From the value of the input voltage applied (V_{SC}), the one of the nominal current (I_{N1}) on the HV side and the one of the power loss P_{SC1} due to the Joule loss in the primary winding, it is possible to get the apparent power and the reactive power for the first side as follow:

$$S_{SC1} = V_{SC} I_{N1}, \quad Q_{SC1} = \sqrt{S_{SC1}^2 - P_{SC1}^2} \tag{4.29}$$

The obtained reactance (X_{d1}), inductance (L_{d1}) at $50Hz$ and impedance (Z_1) on the HV side are:

$$X_{d1} = \frac{V_{SC}^2}{Q_{SC1}} \quad \Rightarrow \quad L_{d1} = \frac{X_{d1}}{2\pi f}, \quad \overline{Z_1} = R_1 + jX_{d1} \tag{4.30}$$

Now it is possible to evaluate the value of the Voltage on the LV side, knowing the turns ratio (t):

$$E_{SC1} = V_{SC} - (I_{N1} Z_1), \quad E_{SC2} = \frac{E_{SC1}}{t} \tag{4.31}$$

From that values, remembering that in the circuit is flowing the nominal current I_{N2} and is dissipated the power P_{SC2} due to the Joule loss in the secondary winding , it is possible to get the apparent power and the reactive power for the second side as follow:

$$S_{SC2} = |E_{SC2}|\, I_{N2}, \quad Q_{SC2} = \sqrt{S_{SC2}^2 - P_{SC2}^2} \tag{4.32}$$

The obtained reactance (X_{d2}), inductance (L_{d2}) at $50Hz$ and impedance (Z_2) on the HV side are:

$$X_{d2} = \frac{Q_{SC2}}{I_{2N}^2} \quad \Rightarrow \quad L_{d2} = \frac{X_{d2}}{2\pi f}, \quad \overline{Z_2} = R_2 + jX_{d2} \tag{4.33}$$

4.3 Studied transformers

AUGIER works with PLC communication as well as the building of single and three-phase transformers at various power levels. It will be essential to investigate transformers and all of their parasitic effects in order to analyze their frequency behaviour and attempt to simplify the existing PLC line. Furthermore, AUGIER builds two different transformer models: the TEE MODULO and the TER, as shown in **Figure4.17**. As will be clear from the study of the Transfer Function of the TER, this results in better performance in terms of attenuation at $133kHz$ as well as having the great advantage of being able to be connected directly to the three-phase Medium Voltage line without adding wires and connection components, making it much leaner, easier to maneuver, less prone to failure, able to adapt the output voltage $\pm 5\%$ and less expensive than the MODULO.
Although it has these great advantages, it is not possible to connect this transformer model to the current PLC line as it uses a signal coupler (MCEP), capable of adapting the LV modulated signal to the MV line. This requires the addition of external cables that the TER does

not have, making this model unusable. The study and research of the TF of transformers with the degree of attenuation they introduce along the line in the exchange of data, will also have the advantage of being able to modify the current line, allowing the use of these transformers as well for PLC communication.
Two distinct models of monophase transformers with different rated powers have been evaluated and studied in order to simplify the study:

- TER MM with a $S_N = 5kVA$ and $V_N = 3.2kV$;
- TEE MT MODULO with a $S_N = 3kVA$ and $V_N = 5.5kV$.

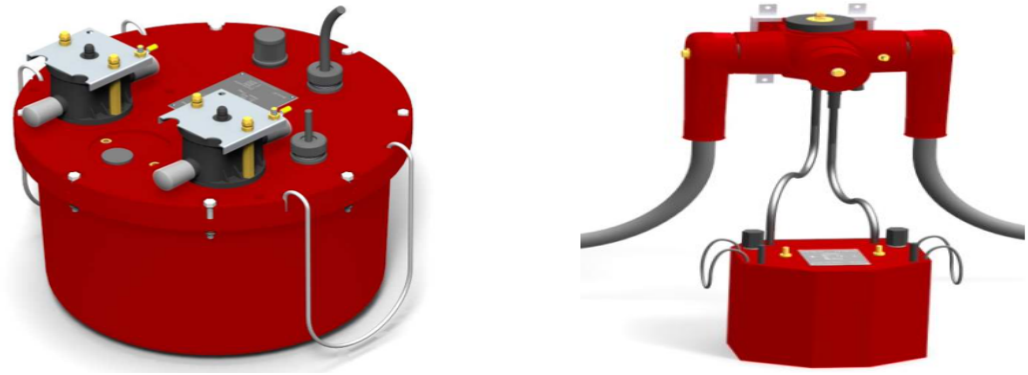

(a) TER MM. **(b)** TEE MT MODULO.

Figure 4.17: Studied transformers.

4.3.1 TER MM

A single-phase TER MM for single-phase network with a Nominal Power $S_N = 5kVA$ and Nominal Voltage $V_N = 3.2kV$, weighs $120kg$ as reported on the datasheet. The external structure is made the external structure is made by low density dielectric epoxy, while the core made of ferrite and the windigs made by copper are immersed in a low density organic dielectric oil, to ensure better insulation of the coils and also better dissipation of the heat produced during work. The transformer is equipped with a tap-changer switch. This allows the adjustment of the transformer output voltage within the $\pm 5\%$. It is accessible after having unscrewed the switch plug.
It is comes with a H07RN-F $6mm^2$ cable $4m$ long on the LV side and with a H07RN-F $1.5mm^2$ cable $4m$ long for the thermal probe.
The earthing terminal is made up of brass, $20mm$ diameter, with a threaded shaft $M10$, length $20mm$, equipped with a brass nut. The earthing terminal has to be connected to the earth network of the pit.
At $50Hz$, the transformer can be approximated from the scheme shown in **Figure4.12**, adding to the diagram of a real transformer, only the inductive and resistive components that take into account non zero Reluctance of the magnetic circuit ($\mu_{Fe} \neq \infty$), the primary and the secondary leakage fluxes, the Joule losses in the windings ($R_{wind} \neq 0$) and the iron losses. The results obtained through the Turns ratio test, the Winding resistance measurement, the NLT and the SCT and then developed through the formulas **4.22**, **4.25**, **4.26**, **4.30** and **4.30** are shown in the table **Tab4.1**.

	Measured
$R_1[\Omega]$	10.319
$X_{d1}[\Omega]$	49.234
$L_1[H]$	0.1567
$Z_1 = R_1 + jX_{d1}[\Omega]$	$10.319 + j49.234$
$R_2[\Omega]$	0.070
$X_{d2}[\Omega]$	0.3295
$L_2[H]$	0.001
$Z_2 = R_2 + jX_{d2}[\Omega]$	$0.070 + j0.001$
$R_{fe}[k\Omega]$	241.370
$X_m[k\Omega]$	118.490
$L_m[H]$	377.157
$Z_0 = R_{fe}//jX_m = R_0 + jX0[k\Omega]$	$46.870 + j95.4790$

Table 4.1: Values of all the parasitic components for the TER MM single-phase transformer at $50Hz$.

The low frequency transformer model was created on LTspice once the data were acquired, and its In/Out behaviour and frequency response were verified. This was mostly done to create models for unstudied transformers in order to forecast their behaviour after the prasitic parameters have been discovered. For this to work, there must be a $3-5\%$ maximum error between the simulation and the real transformer behaviour and it must also be sufficiently robust to follow any modifications made to the real transformer without increasing the error between the two outcomes and hence not deviate too far from reality. The simulated In/Out characteristic on LTspice is shown in the figure below (**Figure4.18**):

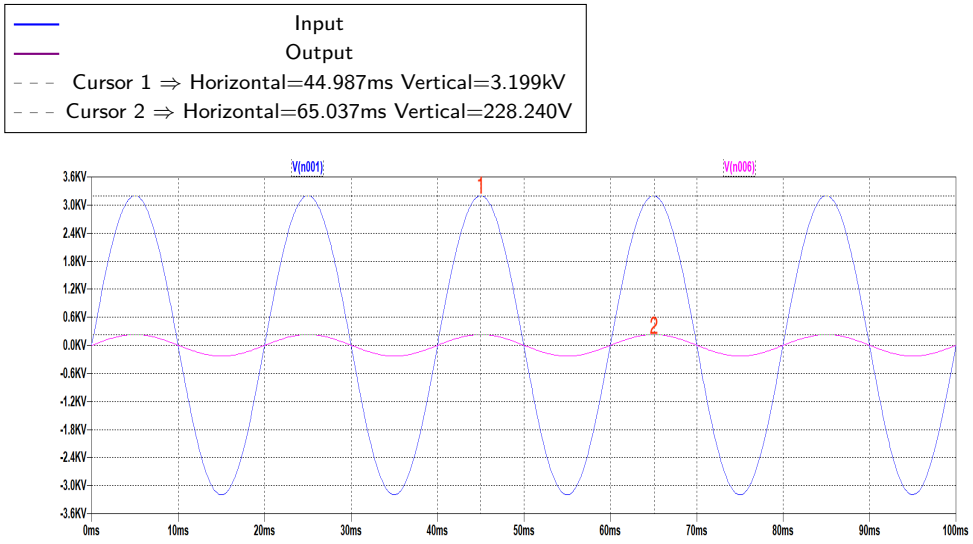

Figure 4.18: In/Out characteristic of the TER MM single-phase transformer.

On LTspice, in order to find the real coupling factor that takes into account the non idealities due to due to an imperfect coupling between primary and secondary, the fallowing relation has been used:

$$k = \frac{tL_m}{\sqrt{(L_{d1} + L_m)(L_{d2} + t^2 L_m)}} \tag{4.34}$$

It has been found that the obtained result for the TER MM single-phase transformer is $k = 0.9998$. Comparing the simulation on LTspice with respect to the real behaviour, the In/Out simulation have an error of 3.278% on the output voltage, which shows an error between real and simulated transformer in an acceptable range, thus being able to consider accurate the model for the description of the In/Out characteristic.
To obtain the TF of the transformer, the frequency response of the model on LTspice was simulated in a frequency range between $9kHz$ and $5MHz$. This interval was chosen as it was done for the frequency response of the cables studied in Chapter 3, since the result will be compared with the TF obtained through the Keysight/Agilent VNA just used. This interval contains the working frequency used by AUGIER for data exchange with PLC communication ($133kHz$) and moreover, it is large enough to be able to characterize the entire frequency response of the transformer, identifying how each parasitic effect affects the frequency response.
In order to have clear and consistent results without ambiguity and knowing that the VNA has a characteristic impedance of 50Ω, it was decided to use a resistance of 50Ω as the transformer's load (both during the simulation than during the testing), rather than 10Ω when the characteristic impedance of the transmitter and receiver was taken into account. This allowed for a directly comparison between the TF simulated on LTspice and the one obtained through the VNA's measurements. It results to be not a issue since scaling the TF will be enough to enable it to be adjusted to the actual impedance value. The obtained TF is shown in the **Figure4.19**:

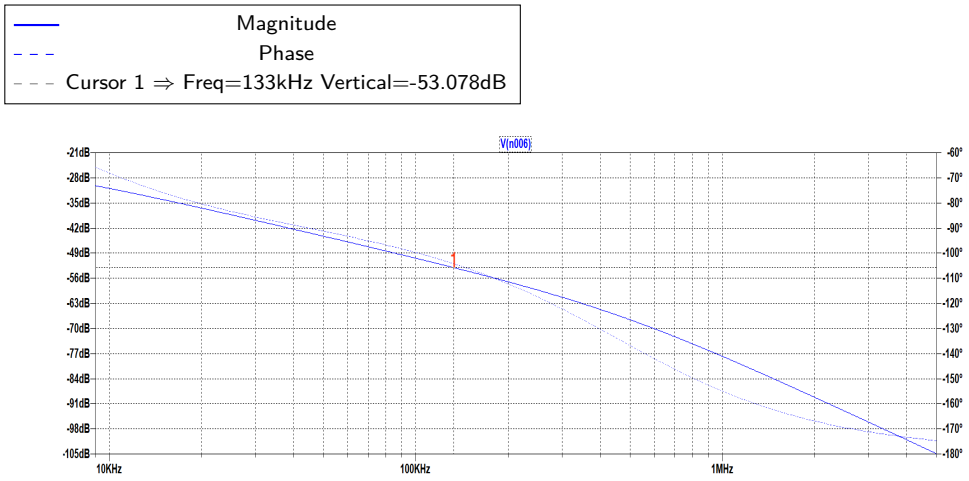

Figure 4.19: Frequency response of the TER MM single-phase transformer.

The actual behaviour of the transformer differs significantly from the results of the LTspice simulation and the error between the two performances are not in an acceptable range. In fact, some parasitic effects that can be approximated with capacitive components, which are notably prominent at high frequencies and cannot be ignored as at $50Hz$, must be taken into account in order to produce an accurate model.
From the study of the frequency response obtained with the VNA, it will be clear how the two results are very far apart and how, luckily, at $133kHz$ the attenuation is about $20dB$ lower than that obtained by this simulation.

4.3.2 TEE MT MODULO

A single-phase TEE MT MODULO for single-phase network with a Nominal Power $S_N = 3kVA$ and Nominal Voltage $V_N = 5.5kV$, weighs $58kg$ as reported on the datasheet. As it is possible to notice, it turns out to be much less heavy than the TER MM model, even if the nominal power involved is lower. At the same power, it is the same lighter with an overall weight of $66kg$. The external structure is made the external structure is made by low density dielectric epoxy, while the core made of ferrite and the windigs made by copper are immersed in a low density organic dielectric oil, to ensure better insulation of the coils and also better dissipation of the heat produced during work. The transformer is equipped with a tap-changer switch but only from the $8kVA$ rated power model.
It is comes with a H07RN-F $6mm^2$ cable $4m$ long on the LV side, with a H07RN-F $1.5mm^2$ cable $4m$ long for the thermal probe and with two LUMIREP-SOUPLE coaxial cables $1.5m$ long on the HV side with pins as terminations to be able to easily and safely connect the transformer to the medium voltage line with an equipment provided by AUGIER.
The earthing terminal is made up of brass, $20mm$ diameter, with a threaded shaft $M10$, length $20mm$, equipped with a brass nut. The earthing terminal has to be connected to the earth network of the pit. The big advantage of this transformer is that it is completely insulated and equipped with high voltage cables which are also insulated with a connection to the electrical HV network through the pins that does not allow the infiltration of dirt or water. This allows it to be used also in submarine applications or in the presence of water without the risk of short circuits.
At $50Hz$, the transformer can be approximated from the scheme shown in **Figure4.12**, adding to the diagram of a real transformer, only the inductive and resistive components that take into account non zero Reluctance of the magnetic circuit ($\mu_{Fe} \neq \infty$), the primary and the secondary leakage fluxes, the Joule losses in the windings ($R_{wind} \neq 0$) and the iron losses. The results obtained through the Turns ratio test, the Winding resistance measurement, the NLT and the SCT and then developed through the formulas **4.22**, **4.25**, **4.26**, **4.30** and **4.30** are shown in the table below (**Tab4.2**):

	Measured
$R_1[\Omega]$	56.423
$X_{d1}[\Omega]$	215.447
$L_1[H]$	0.686
$Z_1 = R_1 + jX_{d1}[\Omega]$	$56.423 + j215.447$
$R_2[\Omega]$	0.119
$X_{d2}[\Omega]$	0.475
$L_2[H]$	0.001
$Z_2 = R_2 + jX_{d2}[\Omega]$	$0.119 + j0.001$
$R_{fe}[k\Omega]$	669.110
$X_m[k\Omega]$	207.500
$L_m[H]$	660.503
$Z_0 = R_{fe}//jX_m = R_0 + jX0[k\Omega]$	$58.705 + j18.930$

Table 4.2: Values of all the parasitic components for the TEE MT MODULO single-phase transformer at $50Hz$.

The model on LTspice was also created for this transformer to simulate its In/Out behavior and frequency response. The simulated In/Out characteristic on LTspice is shown in the figure below (**Figure4.20**):

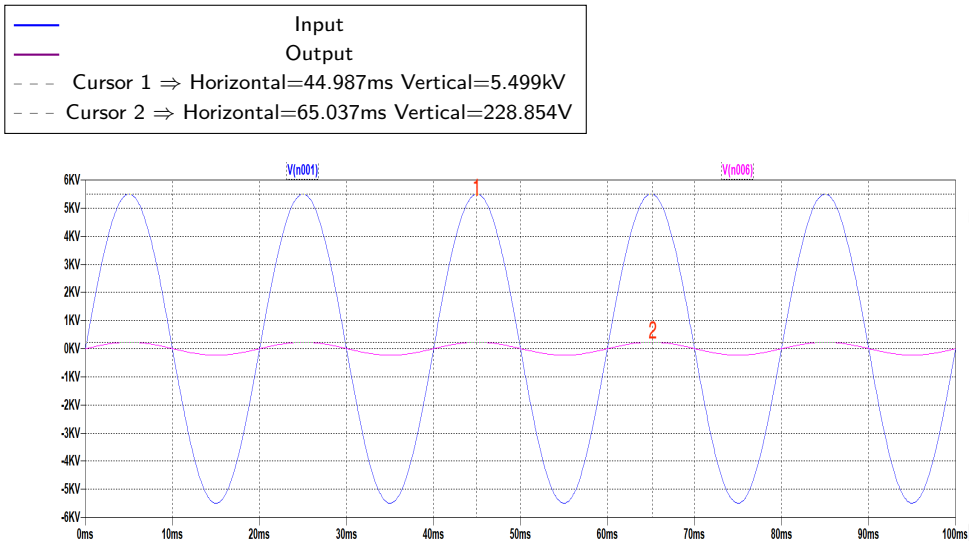

Figure 4.20: In/Out characteristic of the TEE MT MODULO single-phase transformer.

In order to find the real coupling factor that takes into account the non idealities due to due to an imperfect coupling between primary and secondary it was used the (**4.34**) relation, obtaining $k = 0.995$, less compared to the previous transformer, but always acceptable.
Also fo the TEE MT MODULO has been obtained the simulated TF on LTspice always with a 50Ω load and in the $9kHz - 5MHz$ range, as shown in the figure below (**Figure4.21**):

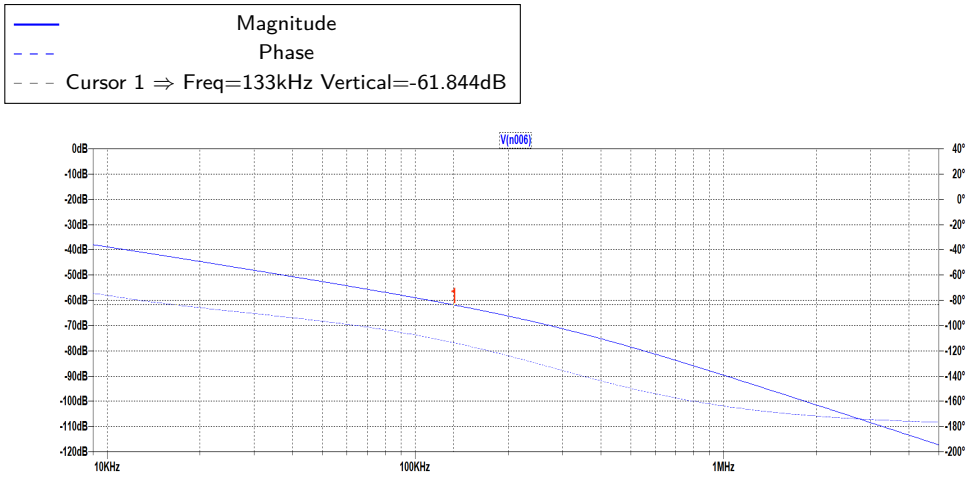

Figure 4.21: Frequency response of the TEE MT MODULO single-phase transformer.

Also in this case, the actual behaviour of the transformer differs significantly from the results of the LTspice simulation and the error between the two performances are not in an acceptable range. In fact, some parasitic effects that can be approximated with capacitive components, which are notably prominent at high frequencies and cannot be ignored as at $50Hz$, must be taken into account in order to produce an accurate model. Despite this, it can be seen that the attenuation at $133kHz$ is greater in the simulation, this case will also be confirmed by the real TF.

4.4 Augmented model

The frequency response of real transformers, in reality, is very different from that obtained previously on LTspice. In fact, their behaviour is affected by parasitic components not considered in the $50Hz$ model, which greatly change its dynamism. These parasitic effects can be approximated as capacitive components which, in fact, at low frequencies behave like an open circuit and make a negligible contribution to the characteristics of the transformers. By increasing the frequency, these capacitive effects affect the real behaviour of the transformers, becoming dominant and instead making the effect of the inductive components less predominant.
The figure **Figure4.23** shows, for example, the real TF of the TER MM transformer studied previously obtained through thr VNA in a $9kHz - 5MHz$ range. It is possible to note how actually the behavior with respect to the simulation on LTspice is completely different and how elements must be added so that the simulation can be considered correct.

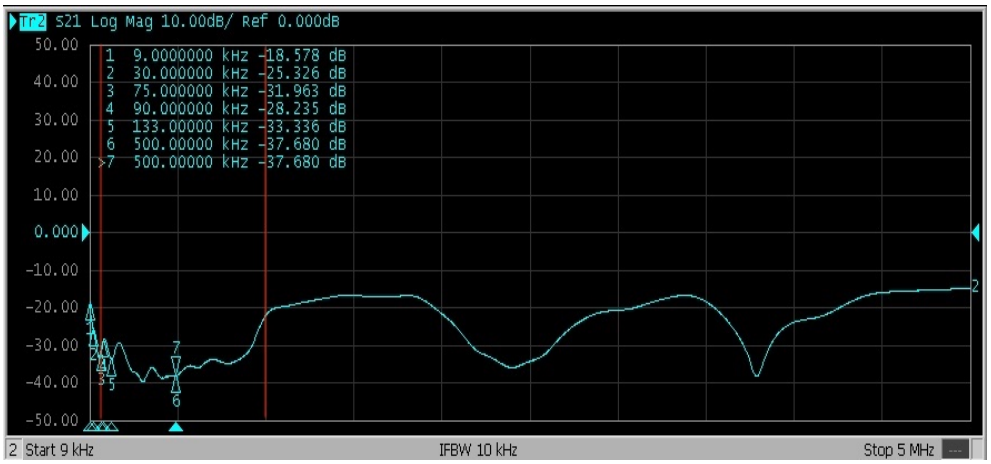

Figure 4.22: Real TER MM Transfer Function.

Four major areas of the frequency response can be distinguished where a parasite effect predominates:

- **Core Effect:** the response in low frequency range (from low frequencies to $2kHz$), is dominated by the core magnetizing inductances and the bulk capacitances of the transformer (capacitance between windings and ground), and the response follows a falling magnitude trend across the frequency range with a linearly decreasing slope of approximately $-20dB$ per decade. It is not possible to see this region in the image above since the VNA's frequency range is between $9kHz - 5MHz$;
- **Interaction between windings:** the response in the intermediate frequency region (from $2kHz$ to $10kHz$), is mostly affected by the interaction between windings, which depends significantly on the arrangement and connections of the windings, for example, delta connection, auto-transformer winding connection, single-phase or three-phase transformer configurations, as well as how the neutrals are connected;
- **Effect of winding structure:** in the winding structure influence region (from $10kHz$ to $1MHz$), the response is determined by the winding leakage inductances together with the winding series and ground capacitances. In this region, the series capacitance is the most influential factor in determining the shape of the response. Typically, the response

of the HV winding of large power transformers with a high winding series capacitance shows a generic rising amplitude trend with few resonances and anti-resonances. On the other hand, the LV winding with low series capacitance generally shows a flat amplitude trend and superimposed by a series of anti-resonances and resonances;

- **Effect of winding structure:** at higher frequencies (above 1 MHz), the response is less repeatable and it is influenced by the measurement set-up, tap leads, especially by the earthing connections, which effectively rely on the length of the bushing.

It can be seen from the frequency response obtained how, fortunately, the attenuation at $133kHz$ of the transformer with a load of 50Ω, is $A = 33.336dB$, far below that obtained on LTspice. The behaviour of the TF of the TEE MT MODULO transformer is almost the same with only some differences, in terms of attenuation, at the frequencies highlighted with the markers on the VNA and, for example at $133kHz$ always with a load of 50Ω, the attenuation is $A = 39.037dB$. This attenuation turns out to be greater than the TER MM model as expected but the difference is not excessive between the two. The interesting discovery made is that the $133kHz$ frequency falls perfectly (TER MM) or almost perfectly (TEE MT MODULO) in a valley of the TF, thus having a well defined Bandwidth by nature. This will be a very useful key step in the proposed modification of the PLC line to make it leaner.
In order to take into accout all this parassitic effects, an Augmented Model of the trasformer has been studied, as shown in the figure below (**Figure4.23**):

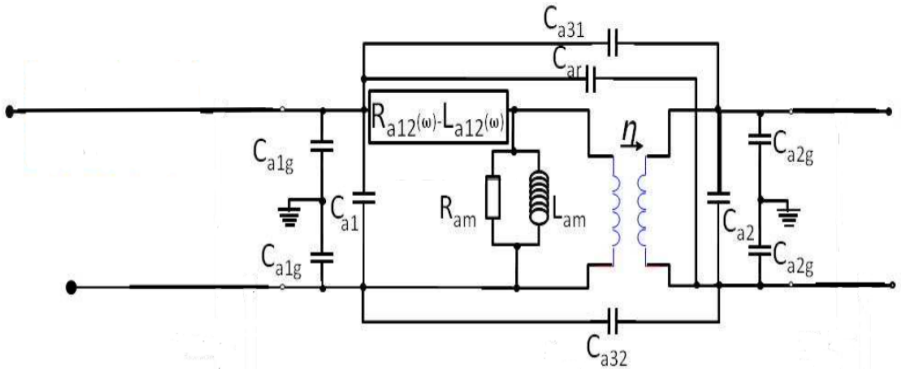

Figure 4.23: Transformer augmented model.

Where:

- C_{a1} and C_{a2} are the turn-to-turn capacitance of the primary and secondary windings;
- C_{a31} and C_{a32} are the capacitances between windings (divided in two capacitances);
- C_{ar} is the capacitance between the input of the primary winding and the output of the secondary;
- C_{a1g} and C_{a2g} are the capacitances between the winding and the ground.

The VNA has been utilized to carry out the measurements in **Figure4.24** in order to determine the values of the seven unknown capacitances for both the transformers.

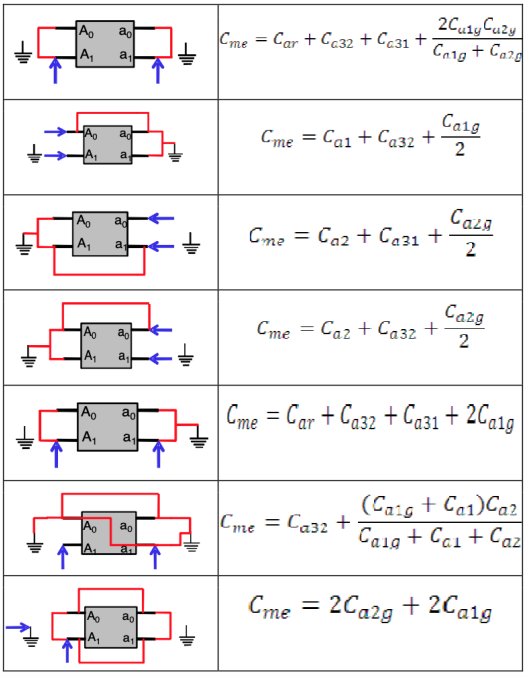

Figure 4.24: Measurement configurations used for determining unknown capacitances.

The Levenberg-Marquardt approach has been used in Matlab to solve the nonlinear system of 7 equations with 7 unknowns, providing us with the parasitic capacity' values. It is possible to see their values for the TER MM transformer in the tab below (**Tab4.3**):

	C_{a1}	C_{a2}	C_{a31}	C_{a32}	C_{ar}	C_{a1g}	C_{a2g}
$[nF]$	1.25	0.6	0.8	0.5	0.1	0.11	0.03

Table 4.3: Obtained values of parasitic capacitance for the transformer TER MM.

In the same way, through the measurements reported in the figure **Figure4.24** and performed the Levenberg-Marquardt approach in Matlab to solve the nonlinear system of 7 equations with 7 unknowns, it was possible to obtain the values of the parassitic capacitances for the TEE MT MODULO transformer, reported in the tab below (**Tab4.4**):

	C_{a1}	C_{a2}	C_{a31}	C_{a32}	C_{ar}	C_{a1g}	C_{a2g}
$[nF]$	2.23	0.9	1.0	0.2	0.5	0.9	0.09

Table 4.4: Obtained values of parasitic capacitance for the transformer TEE MT MODULO.

When the capacitance values are added to the LTspice model, it becomes clear that, even with a smaller frequency range $(9 - 500kHz)$, the simulation was unable to reproduce the real behaviour of the TF despite the non-linear system's resolution. This is mostly because the testers were placed on the Medium and Low Voltage cables exiting the transformer rather than directly accessing the transformer core, which without a doubt bias the results obtained with the VNA by introducing an unwanted inductive and capacitive component. Additionally, if the frequency value is increased, even the inductive components, which were computed for

the low frequency model ($f = 50Hz$) experience variations, rendering their modelling inaccurate. The model was not physically accurate enough due to all of these aspects, as well as the fact that LTspice is not a software performing enough to return a dynamism as great as that demanded by the TF. It is possible to find these values and simulate a model transformer circuit using more efficient algorithms and simulation environment, which are in any case outside the scope of the thesis. In fact, the main scope was to find the degree of attenuation that the studied transformers introduce in the data exchange at $133kHz$ in a PLC communication, in order to understand if it is possible to make the existent architecture leaner and this goal has been achived.

5 AUGIER's PLC architecture

This chapter will show a typical architecture utilised by AUGIER for data exchange via PLC communication based on the topics treated in the earlier Chapters, having a clear understanding of PLC idea. It will be possible to understand the limits of the existent configurations suggesting optimal solutions with advantages in terms of cost-benefits, by critically analysing the many core components and the different effects they have on the lines.

5.1 Generalities

A typical line consists of a single AUGIER MASTER, placed in Low Voltage and powered at $230V$, which is capable of sending an high frequency ($133kHz$) and Low Voltage ($5V/10mA$) signal on a Medium Voltage ($3.2 - 5.5 - 6.6kV$) and low frequency electrical power line ($50 - 60Hz$) through a signal coupler (MCEP) placed between the two voltage levels.
A single MASTER can talk to up to 300 SLAVES modules and over long distances (several tenth of km) through the G3-PLC communication standard, since the line being bidirectional and each SLAVE being a repeater. The working temperature range for correct operation goes from $-20C°$ to $+55C°$. The **Figure5.1** shows a typical AUGIER's PLC architecture. A MASTER is installed into a cabinet that is tipically a transformer substation while the SLAVES, as it is possible to notice from **Figure5.1**, are installed into cabinets located after the step-down transformers. A MASTER monitors permanently the status of modules on the field (e.g. contact position) to identify any anomaly on the electrical network.
It can send automatically either unitary commands or group commands, if it is connected to a timer or a supervision and in case of an event occurring on a SLAVE, the information is sent automatically to it, for this reason the dialogue is bidirectional. The information sent is capable of activating two relays mounted directly on the different SLAVES, allows to implement lighting (for example they can send to turn on all the lamps into a tunnel) to activate pumps, electrical motors or a videosurveillance system. Currently, the projects allow a total extension of the line of up to $40km$, with a maximum distance of $2km$ between the various modules before the Insertion Loss becomes so high that the information cannot be decoded. This means that on nowdays PLC line 20 receivers with related transformers and MCEPs are mounted. The main goals of the study are:

- **network optimization:** trying to increase the maximum distance between 2 transformers to be able to carry the signal even for a longer distance, if required, without the noise canceling it;
- **network streamlining:** trying to eliminate all the MCEPs from the line by passing the signal directly through the various transformers, thus reducing the overall costs.

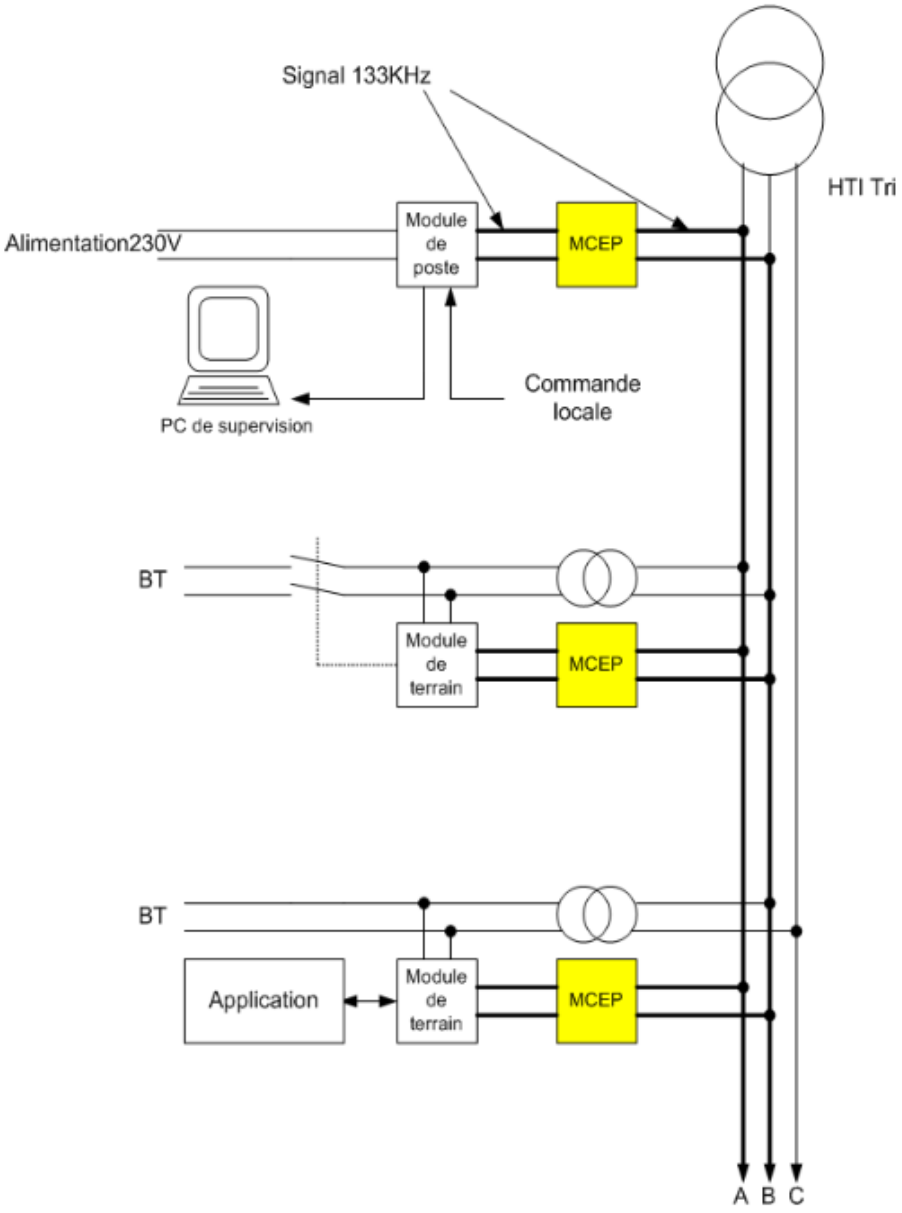

Figure 5.1: AUGIER's PLC architecture.

5.2 Link Budget Determination

A Link Budget is an accounting of all of the power gains and losses that a communication signal experiences during the data exchange; from a transmitter, through a communication medium (in this case MV/LV cables) and MCEPs to the receiver. It can be expressed by the relation below (**5.1**):

$$Link\,Budget[dB] = Transmitted\,power[dB] + Gains[dB] - Losses[dB] \tag{5.1}$$

An experimental approach was employed to determine the maximum Link Budget between the transmitter and the receiver. An $O-Pad$ attenuator made up of 9 cells built to work well with a characteristic impedance $Z_0 = 10\Omega$ (corresponding to the source impedances of the MASTER and of the SLAVES) and that could each create a separate attenuation between input and output for a total of $99dB$ was made as in **Figure5.2**:

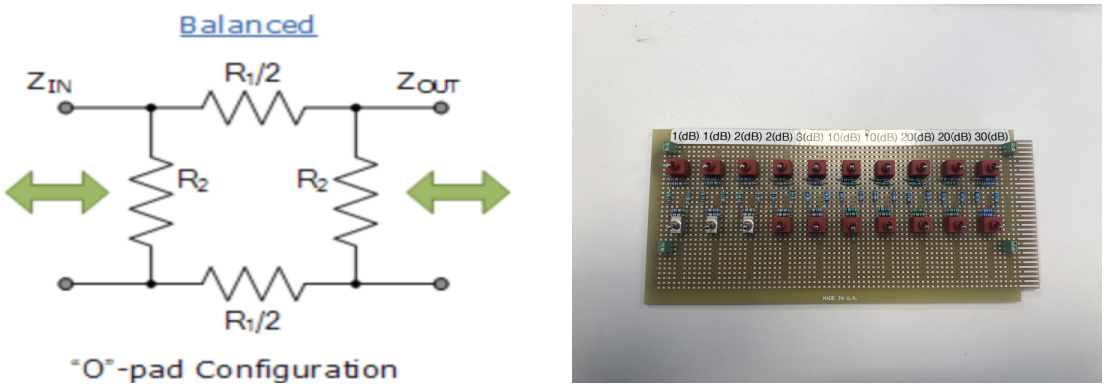

(a) **(b)**

Figure 5.2: O-Pad attenuator.

In order to characterize the Link Budget between transmitter and receiver (without the influence of cables), the attenuator was mounted between an MASTER and an SLAVE with 4 cables having a short length $(20cm)$ as shown in the figure below (**Figure5.3**):

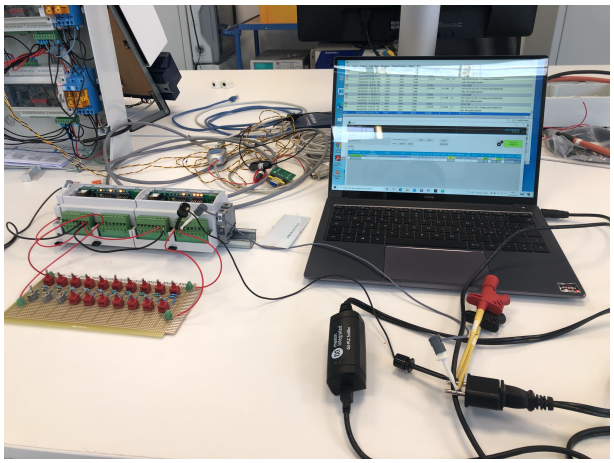

Figure 5.3: Testing the Budget-Link between the transmitter and the receiver.

The approach was pretty straightforward: after matching the frequency ranges on both MASTER and SLAVE (Cenelec-C, $133kHz$), an oscilloscope was attached to both sides, to observe the signal exchange between the transmitter and the receiver.
Polling between the two began with no attenuations inserted. Two signals can be seen in the image below (**Figure5.4**): one of which corresponds to the transmitter's "call" and the other to the correct receiver's "answer".
After verifying that the communication occurs as expected, several levels of attenuation have been added into the communication, activating the different cells of the $O-Pad$ attenuator

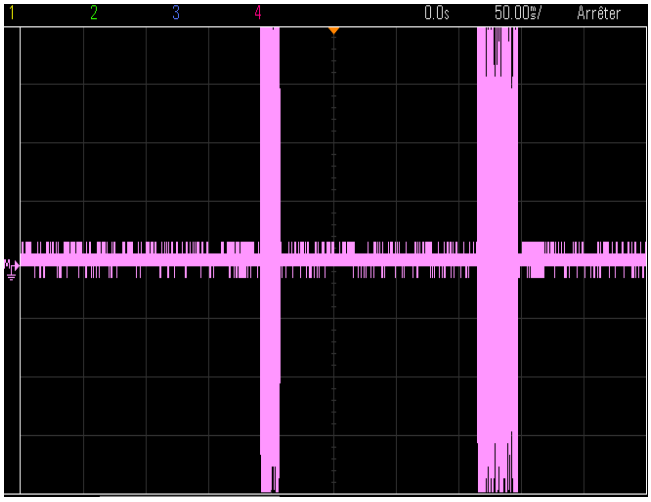

Figure 5.4: Polling successful.

until the highest attenuation that the line can support is attained. When the amount of noise on the line is greater than the signal being exchanged and so the SNR is very small, polling between the transmitter and receiver fails. In this situation, when the slave is "called" by the master, the communication breaksdown and the software interface error results. The figure below makes this clear (**Figure5.5**):

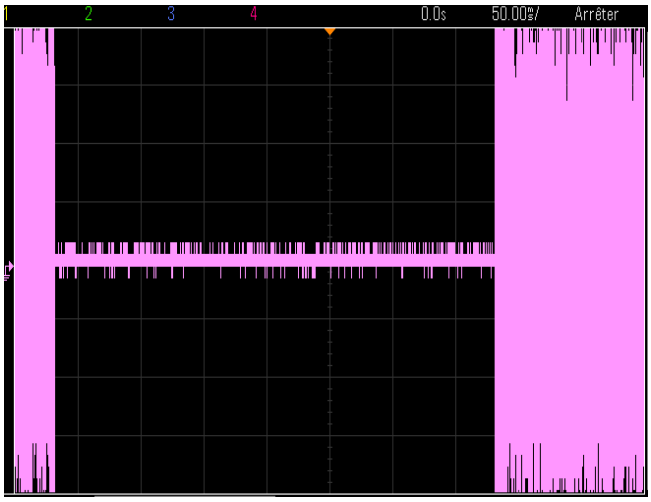

Figure 5.5: Polling failure.

After testing the insertion of different attenuation levels, it was found that the Link Budget of the line turns out to be $96dB$. By inserting a higher attenuation value, the communication is interrupted, making communication impossible. The choice of a differential attenuator was made to match the differential architecture of MASTER and SLAVE. It was experimentally verified that even with only one of the two differential lines connected, MASTER and SLAVE could communicate, as the signal travels between the remaining line and ground. In this experimental set-up, ground return is provided by measurement instruments sharing the same power socket. This made the use of a traditional $\Pi - Pad$ attenuator simply useless.

5.3 MCEP

An MCEP is a signal coupler used to modulate the signal at high frequency ($133kHz$) and Low Voltage ($5V/10mA$) on a Medium Voltage ($3.2-5.5-6.6kV$) and low frequency wave of the electrical power line ($50-60Hz$), which is the carrier. The electrical diagram is shown in the figure below (**Figure5.6**):

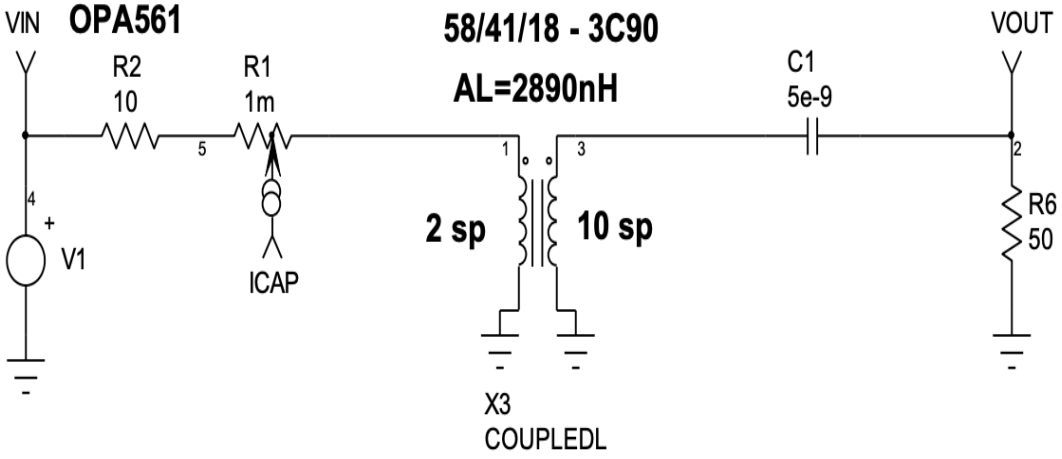

Figure 5.6: MCEP electrical scheme.

An MCEP is composed by a toroidal core in ferrite 58/41/8-3C90, coated with a white epoxy resin, flame retardant, able to work with a maximum temperatures of $200C^{\circ}$.
It has a relative magnetic permeability $\mu_r = 2300$, that guarantees a core inductance of $A_L = 2890 \pm 25\%[nH]$. The transformation ratio is $1:5$, with 2 and 10 windings per side and its behaviour is bidirectional. As it is possible to see from the figure above (**Figure5.6**), its electrical scheme also includes a $5nF$ capacitor and 3 resistors.
A 50Ω resistor was used as load, as well as for transformers, always because the VNA has a characteristic impedance of 50Ω, rather than 10Ω which turned out to be that of the MASTER and the SLAVES. This allowed for a comparison between the TF simulated on LTspice and the one obtained through measurements through the VNA.
This doesn't seem to be a problem because scaling the TF will be enough to enable it to be adjusted to the actual impedance value.
The capacitor is an High Voltage Class 1 Ceramic AC and DC disc capacitor with a tolerance of $\pm 20\%$, molded in a epoxy resin. Adding these additional components to a classic transformer, allows to achieve the desired effect:

- obtain a frequency response of a band pass filter, capable of passing almost signals at the chosen resonant frequency ($133kHz$) and attenuating those outside the Bandwidth, expecially at low frequencies;
- maintain the In/Out characteristic almost unchanged, thus having a $V_{Out,pk-pk} \simeq V_{In,pk-pk}$. In truth, as it is possible to see from the simulation on LTspice (**Figure5.7**), the output voltage is slightly lower and out of phase with respect to the input one, but as the signal passes through two MCEPs (when it is transformed from Low to High Voltage and vice versa) which have an opposite effect, the phase shift is canceled, returning an almost intact signal to the SLAVE albeit slightly attenuated.

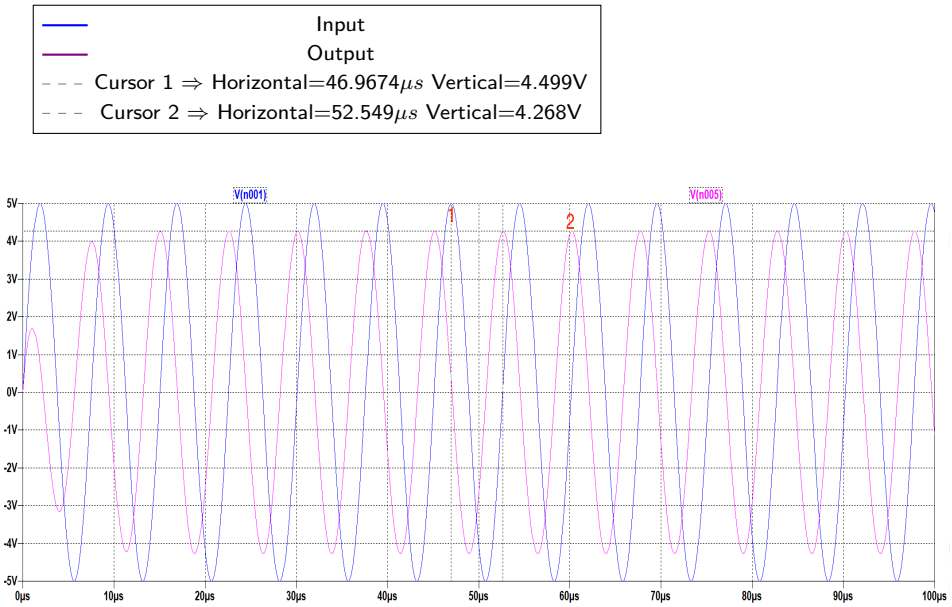

Figure 5.7: In/Out characteristic of the MCEP.

The MCEP mounts as a Low Voltage cable an H07RN-F $6mm^2$ of length $3m$ while at high voltage two LUMIREP-SOUPLE $6mm^2$ of length $1.5m$, so as to be able to carry the differential signal. The whole circuit is contained inside a rigid plastic box and isolated in a hardening epoxy resin to ensure isolation at relative High Voltage. The frequency response was simulated on LTspice and compared with that obtained through the VNA in a frequency range between $9kHz$ and $5MHz$. In particular, the Montecarlo method was used on LTspice to take into account the $\pm 20\%$ tolerance of the capacitor and observe how the TF changes as a function of this. The obtained result is shown in the figure below (**Figure5.8**):

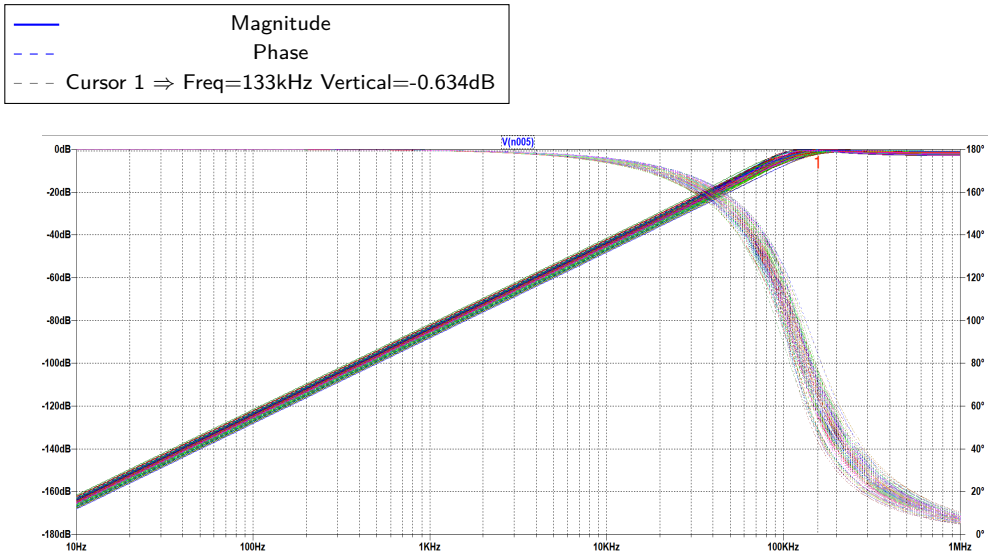

Figure 5.8: Frequency responce of the MCEP on LTspice with Montecarlo's method.

From the simulation it is possible to observe how for the resonant frequency ($133kHz$) and within the Bandwidth, the attenuation is very low, below $1dB$, while as the frequency decreases the signal disappears completely. It is also possible to observe, thanks to the Monte-carlo's method, that according to the tolerances of the capacitor the frequency response has a greater or lesser slope, but always remaining in a neighborhood of $\pm 1dB$, making the result acceptable. The newly obtained TF can be compared with that obtained through the VNA but in a smaller frequency range ($9 - 500kHz$), in order to have a better resolution of the behaviour. The measures made were two:

- one in which the pins of the VNA have been connected directly to the input and output of the circuit without any cables attouched and any dielectric resin around the circuit, as shown in the image below (**Figure5.9**):

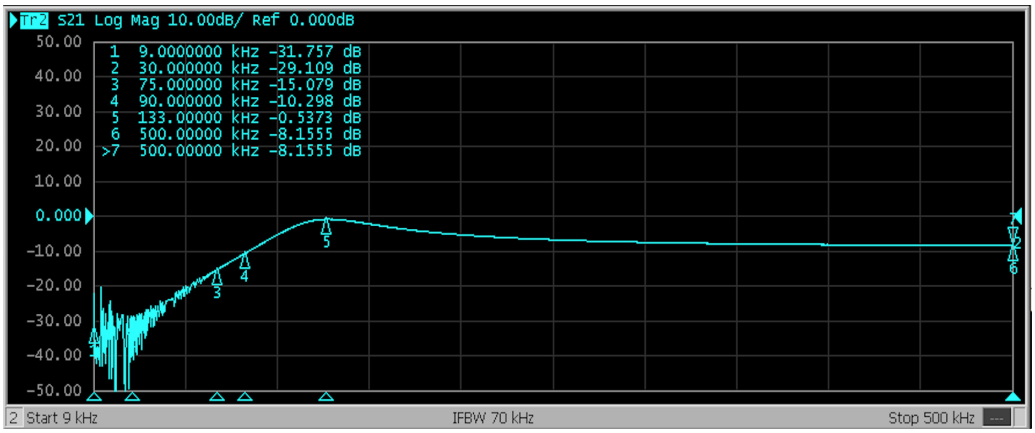

Figure 5.9: Frequency responce of the MCEP through the VNA direct connect to the circuit and with no resin.

- the other in which the pins of the VNA have been connected to the output cables and the circuit is surrounded by the dielectric resin, as shown in the image below (**Figure5.10**):

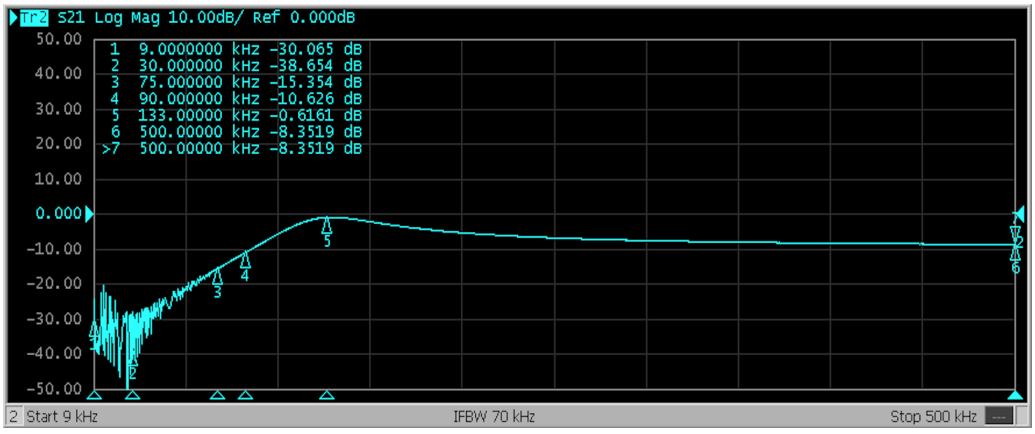

Figure 5.10: Frequency responce of the MCEP through the VNA direct to the cables and with the resin.

From the simulation it is possible to observe how oscillations are present in low frequencies, but this is the same problem that occurred even when cables were studied, which indicate that the line used to calculate the line parameters must be shorted.
Despite them, it can be seen that in this range the signal is practically non-existent, which is fundamental to guarantee safety in the event of short circuits along the line at relatively high voltages ($\simeq kV$). Comparing the results at $133kHz$, it can be seen that the simulation of the TF on LTspice with respect to the one obtained with the VNA directly connected to the circuit and without dielectric resin, has an error regarding the introduced attenuation of 17.992%. It can also be noted that the MCEP with the cables and the dielectric resin inside, introduces at the resonant frequency an attenuation 14.665% greater with respect to the bare one, as expected.
For the calculations carried out in the remainder of the Chapter, the data collected on the MCEP with the connected cables and with the dielectric resin will be used. This approach was followed to take into account the effects that the resin brings to the behaviour of the signal coupler and also because the cables should in any case have to be considered in the calculations and to have data that already take into account their effect, certainly introduces less error than to add them a-posteriori.

5.4 Studied Configurations

This section will examine various PLC communication setups for data exchange, illustrating which keeps the highest Link Budget and, consequently, which results in less power lost throughout the line (smaller IL). This will be accomplished by applying the knowledge learned in Chapter 3 regarding lossy transmission lines and the benefits and drawbacks of signal injection on Medium Voltage cables. Starting with **Figure5.1** and understanding the data of existing projects, solutions are proposed in order to optimise the current architectures.

5.4.1 Transmission with MV LUMIREP-E Phase-Ground configuration cables

The first architecture studied is the one in which the LUMIREP-E in the Phase-Ground configuration with a cross-section of $25mm^2$ are the Medium Voltage coaxial cables.
Currently, the projects allow a total extension of the line of up to $40km$ with a maximum distance of $2km$ between the various modules before the IL become to high and the information is lost. Starting with image **Figure5.1**, the first branch of the line is isolated (**Figure5.10**) noting that effectively, the introduced attenuations and reflections depend only on the Low Voltage and High Voltage cables and on the two MCEPs. The other components, such as the various transformers and breakers, participate in the transport of power and their contribution does not affect the attenuation that the signal experience. This is done while keeping in mind the Link Budget (LB) previously discovered ($96dB$) between the MASTER and a SLAVE (it is the same between SLAVE-SLAVE) which is the maximum degree of attenuation that can be introduced. From the datasheet it is possible to see that the Low Voltage cable that connects the MCEP to the MASTER or to the various SLAVES is a H07RN-F $6mm^2$, two-wires cable with phase and neutral and $3m$ long, while the two High Voltage cables are LUMIREP-Souple $6mm^2$ coaxial cables, $1.5m$ long. These deal with the exchange of data and guarantee the possibility to do it in a differential way. From **Figure5.1**, it is possible to notice that the injection of the signal on the Medium Voltage power line through the MCEP it always happens with the same two phases of the three-phase system, so as to reduce the losses and the number of bits lost during the exchange.

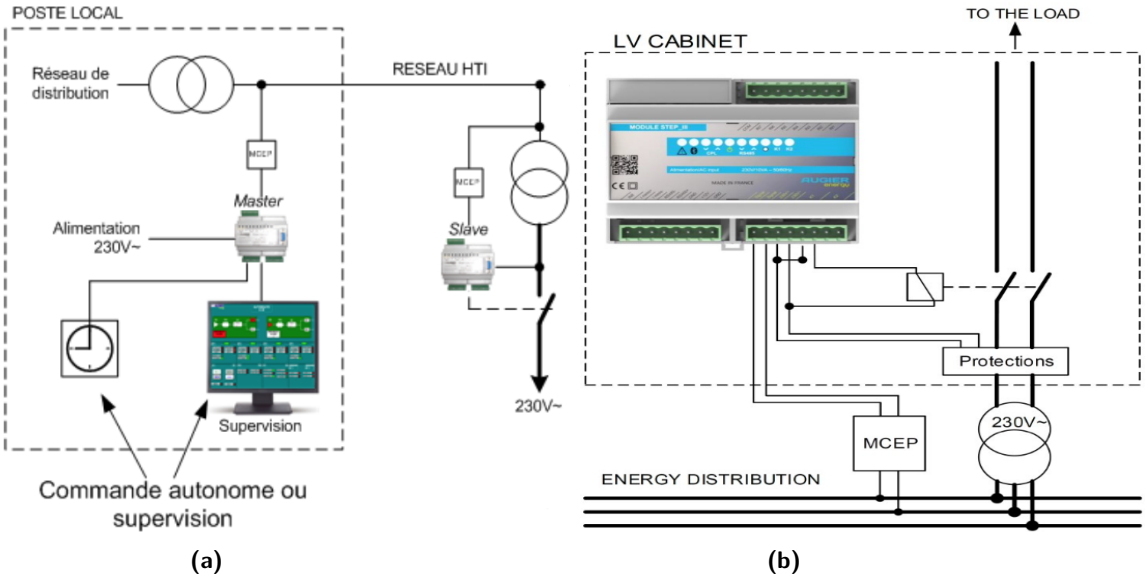

Figure 5.11: Isolation of the first branch.

What actually happens, however, is that even if the first branch of the line is disconnected from the rest, to study the exchange of data with relative losses the effect of the remaining part of the line cannot be completely neglected.
The big advantage, however, is that the whole system is linear and the superimposition principle can be applied: the losses that occur in each single branch can be evaluated neglecting the remaining, adding as an additional factor the remnants length of the line and the last impedance connected to it.
The figure below (**Figure5.11**) helps to clarify this point:

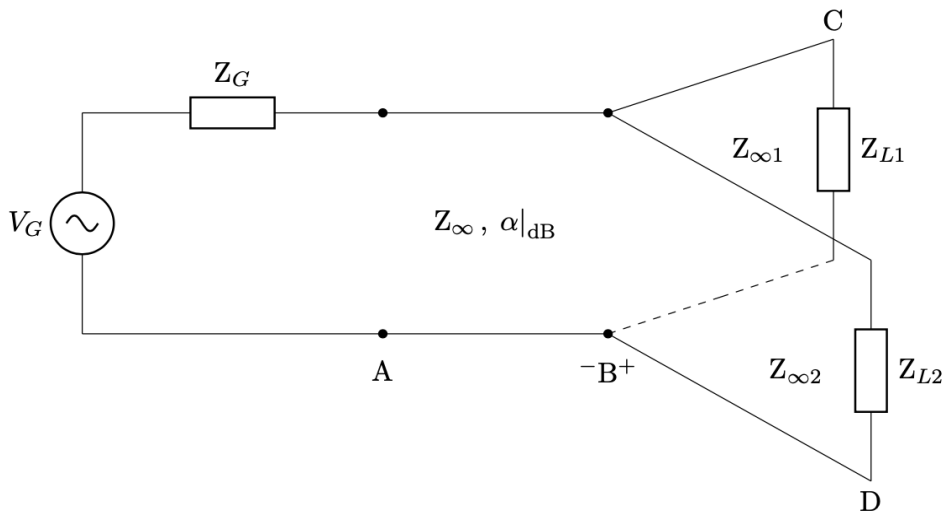

Figure 5.12: Parallel transmission line model.

For a total extension of the line of up to $40km$ with a maximum distance of $2km$ between the various modules it is possible to understand that:

- Z_G is the characteristic impedance of the generator, $Z_G = 10\Omega$;
- $\overline{AB}$ is the section that takes into account the $2km$ extension of the three phase Medium Voltage cables, the effect of the first MCEP which modulates the data signal wave with the carrier and the total extension of associated cables is about $4.5m$ long;
- $\overline{BD}$ is the section that takes into account the presence of the second MCEP, responsible for demodulating the signal wave from the carrier and the length of the associated cables with total extension of $4.5m$. Z_{L2} is the characteristic impedance of the SLAVE, equal to the one of the generator: $Z_{L2} = Z_G = 10\Omega$;
- $\overline{BC}$ is the section that takes into account the extension of the remaining $2km$ of Medium Voltage three-phase cables, the effect of the last MCEP responsible of the demodulation and associated cables (always $4.5m$ long). This is where the line closes and it is a section that cannot be overlooked in the discussion. As before, Z_{L2} is the characteristic impedance of the last SLAVE, equal to the one of the generator: $Z_{L2} = Z_G = 10\Omega$.

As can be seen, thanks to the superimposition principle, the presence of the other branches is not taken into account in the section $\overline{BC}$ for the calculation of the parameters in the first one, greatly simplifying the treatment.
In order to obtain the values of interest, the S-parameters collected in Chapter 3 on the cables and those collected to find the TF of the MCEP, in the previous Section, having the dielectric resin and the relative cables alrady connected, through the VNA were exploited.
Since the aim is to find the attenuations on the line A_{Line}, RL and consequently IL, thus discovering which configuration is capable of not consuming all the LB actually available at the working frequency of $133kHz$, S-parameters obtained in Chapter 3 become punctual at the chosen frequency only, thus being able to work with only matrices.
The S-parameters are a powerful tool especially because, for components in series, an equivalent one can be obtained with the relative parameters by doing a cascade of matrices of the single components among themselves.
Section $\overline{AB}$ can be effectively treated doing it with the Medium Voltage cables S-matrix and the first MCEP S-matrix, obtaining a new matrix. However, before doing this getting the correct values, the parameters relating to LUMIREP-E cable in the Phase-Ground configuration must be scaled. In fact these have been taken for a unit length of $1m$ while the interest is having the correspondent ones for a length of $2km$.
Knowing that the matrix at $133kHz$ for $1m$ length is:

$$S = \begin{pmatrix} 0.0046 + 0.0028j & 0.9960 - 0.0132j \\ 0.9960 - 0.0132j & 0.0046 + 0.0028j \end{pmatrix} \tag{5.2}$$

And remembering that the components are passive and reciprocal ($S_{11} = S_{22}$ and $S_{12} = S_{21}$), it is possible to demostrate that the entries of the corresponding matrix with an arbitray length are given by the following relations:

$$\begin{aligned} S_{11} &= \frac{Z_0 \frac{Z_\infty + jZ_0 tan(kl)}{Z_0 + jZ_\infty tan(kl)} - Z_\infty}{Z_0 \frac{Z_\infty + jZ_0 tan(kl)}{Z_0 + jZ_\infty tan(kl)} + Z_\infty} = S_{22} \\ S_{12} &= \frac{(1+S_{11})(1+\Gamma_L)e^{-jkl}}{1+\Gamma_L e^{-j2kl}} = S_{21} \end{aligned} \tag{5.3}$$

Where:

- β is the propagation constant and, at $133kHz$ for $1m$ length is: $\beta = 0.013\left[\frac{rad}{m}\right]$;
- α is the attenuation constant and, at $133kHz$ for $1m$ length is: $\alpha = 0.003\left[\frac{Np}{m}\right]$;
- k is the complex wavenumber and, at $133kHz$ for $1m$ length is: $k = \beta - j\alpha = 0.013 - 0.003j\left[\frac{rad}{m}\right] \epsilon \mathbb{C}$
- l is the length under interest and in this case: $l = 2km$;
- Z_0 is the characteristic impedance of the LUMIREP-E, $25mm^2$ MV coaxial cables in the Phase-Ground configuration: $Z_0 = 59.084\Omega$;
- Z_∞ is the characteristic impedance of the of the measuring instrument, that for the Keysight/Agilent VNA, Model E5071C with 2-ports is: $Z_0 = 50\Omega$;
- Γ_L is the reflaction coefficient between the load impedance and the line impedance given by: $\Gamma_L = \frac{Z_{inf} - Z_0}{Z_{inf} + Z_0} = -0.083$.

The corresponding $133kHz$ S-matrix scaled to $2km$ is:

$$S_{2km} = \begin{pmatrix} 0.0833 - 0.0000j & -0.0003 - 0.0013j \\ -0.0003 - 0.0013j & 0.0833 - 0.0000j \end{pmatrix} \tag{5.4}$$

And finally, making a cascade between the obtained matrix and the one of the first MCEP, it is possible to obtain for the section $\overline{AB}$ the corresponding S-parameters:

$$S_{\overline{AB}} = \begin{pmatrix} 0.0833 - 0.0000j & -0.0011 + 0.0006j \\ -0.0011 + 0.0006j & 0.0833 - 0.0000j \end{pmatrix} \tag{5.5}$$

This type of reasoning cannot be made between the $\overline{BD}$ and $\overline{BC}$ lengths as they are parallel to each other. What can be done is to obtain an equivalent impedance for each section at point B, make it parallel and finally treat the line as if it were a normal transmission line composed of the generator impedance Z_G, the newly found S-matrix $S_{\overline{AB}}$, and as load, the equivalent impedance $Z_{eq} = Z_{B,BD} // Z_{B,BC}$.
Starting from the $\overline{BD}$ section, this is composed of only the MCEP with attached cables and the impedance of the SLAVE set as a load of 10Ω. The equivalent S-matrix of the MCEP is:

$$S_{MCEP} = \begin{pmatrix} -0.1082 + 0.0458j & -0.2300 - 0.9076j \\ -0.2300 - 0.9076j & -0.1082 + 0.0458j \end{pmatrix} \tag{5.6}$$

Knowing that the reflection coefficient between the load and the line ($Z_0 = 132.262[\Omega]$) is:

$$\Gamma_{L2} = \frac{Z_{L2} - Z_0}{Z_{L2} + Z_0} = -0.859 \tag{5.7}$$

Referring to the figure below (**Figure5.13**) and with some calculations, it is possible to obtain the reflaction coefficient at the point B^+:

$$\Gamma_{in,2} = S_{11} + \frac{\Gamma_{L2} S_{21} S_{12}}{1 - S_{22}\Gamma_{L2}} = 0.695 - 0.444j \tag{5.8}$$

And finally getting the equivalent impedance at point B for the section $\overline{BD}$:

$$Z_{B,BD} = Z0\frac{1 + \Gamma_{in,2}}{1 + \Gamma_{in,2}} = 145.540 - 405.160j[\Omega] \tag{5.9}$$

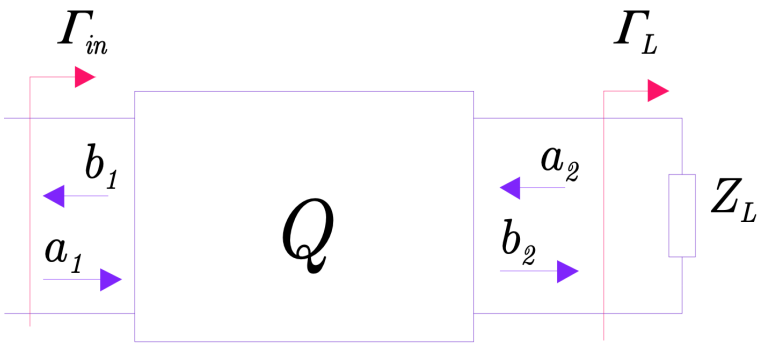

Figure 5.13: Two ports circuit with associated incident and reflected powers.

It is possible to proceed in the same way also for the section $\overline{BC}$. Starting from the transmission matrix $S_{\overline{AB}}$ obtained previously (**5.5**), it is possible to get the reflection coefficient of the line ($Z_0 = 59.084[\Omega]$) with respect to the SLAVE's load ($Z_{L1} = 10[\Omega]$):

$$\Gamma_{L1} = \frac{Z_{L1} - Z_0}{Z_{L1} + Z_0} = -0.710 \tag{5.10}$$

Also here with some calculations, it is getting the reflaction coefficient at the point B^+:

$$\Gamma_{in,1} = S_{11} + \frac{\Gamma_{L1} S_{21} S_{12}}{1 - S_{22}\Gamma_{L1}} = 0.083 + 0.000j \tag{5.11}$$

And finally the equivalent impedance at point B for the section $\overline{BC}$:

$$Z_{B,BC} = Z0\frac{1 + \Gamma_{in,1}}{1 + \Gamma_{in,1}} = 69.8170 + 0.0003j[\Omega] \tag{5.12}$$

Making the parallel between the two impedances just founded ($Z_{B,BD}, Z_{B,BC}$):

$$Z_{eq} = Z_{B,BD} // Z_{B,BC} = 64.831 - 9.380j[\Omega] \tag{5.13}$$

The equivalent impedance used as load has been obtained, now being able to treat the line in a simplified way like the one in the picture below (**Figure5.14**):

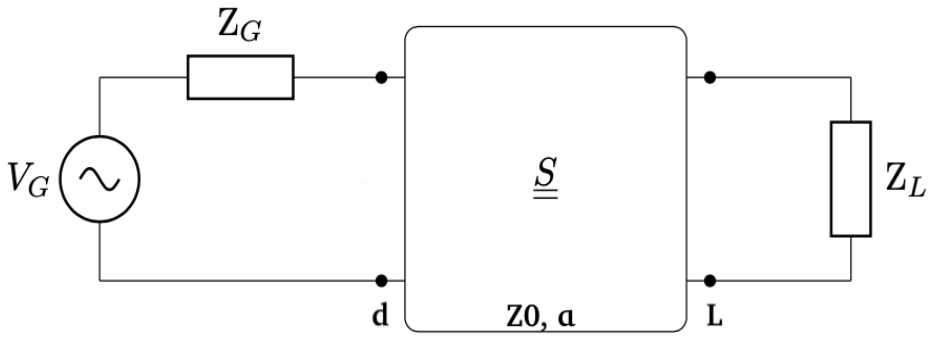

Figure 5.14: Obtained equivalent circuit.

Where:

- $\underline{\underline{S}} = S_{\overline{AB}}$ is the S-matrix just founded above (**5.5**);
- Z_G is the generator impedance: $Z_G = 10[\Omega]$;
- $Z_L = Z_{eq}$ is the load impedance: $Z_L = 64.835 - 9.382j[\Omega]$, founded previously (**5.13**).

As seen above, the Link Budget (LB) of the line was obtained experimentally. This value expresses in logarithmic scale the degree of maximum attenuation that can be introduced, beyond which communication is interrupted and data exchange cannot take place.
To understand if the studied configuration exceeds this parameter, it is necessary to find the actual IL due to reflections (caused by the impedance mismatch) and attenuation along the line: if their value is higher than the expendable Link Budget, communication cannot take place. Looking at the $S_{\overline{AB}}$-matrix and knowing that the S_{21} term express the direct transmission coefficient with matched output (for a passive and reciprocal component $S_{21} = S_{12}$), it is possible to get the total attenutaion of the $\overline{AB}$ length:

$$A_{line} = 20log_{10}(|S_{21}|) = 133.644dB \Rightarrow Attenuation\,over\,the\,line \tag{5.14}$$

In the same way as before (**5.8**) with some calculations, it was possible to obtain the reflaction coefficient at the point L^+:

$$\Gamma_L = S_{22} + \frac{\Gamma_S S_{21} S_{12}}{1 - S_{22}\Gamma_S} = -0.172 + 0.081j \tag{5.15}$$

Where Γ_S is the reflaction coefficient between the MASTER characteristic impedance ($Z_G = 10\Omega$) and the one of the line in the $\overline{AB}$ segment ($Z_0 = 59.084\Omega$):

$$\Gamma_S = \frac{Z_S - Z_0}{Z_S + Z_0} = -0.710 \tag{5.16}$$

Finally, with the results just obtained, it is possible to get the parameters under interest RL and IL as:

$$\begin{aligned} RL &= 10log_{10}((1 - |\Gamma_S|^2)(1 - |\Gamma_L|^2)) = 7.396dB \Rightarrow Return\,Loss \\ IL &= 10log_{10}((1 - |\Gamma_S|^2)|S_{21}|^2(1 - |\Gamma_L|^2)) = 141.040dB \Rightarrow Insertion\,Loss \end{aligned} \tag{5.17}$$

As it is possible to notice $IL > LB$, this makes possible to understand how communication cannot take place with this type of configuration at the chosen distance.Also confirms, as previously found in Chapter 3, that signal injection between the phase of a cable and its shield is not the optimal way to transmit data on a PLC technology, as the attenuations along the line are too high.
It also possible to understand that the existing lines already apply a different data transmission, making this solution unusable for lengths of $2km$ between a receiver and a transmitter. Instead, by trying the same configuration but with a distance of $1.5km$ between MASTER and SLAVE, it is possible to obtain the power dissipated (P_{line}) of the $S_{\overline{AB}}$-matrix in the segment $\overline{AB}$, due to the attenuation α:

$$A_{line} = 20log_{10}(|S_{21}|) = 100.414dB \Rightarrow Attenuation\,over\,the\,line \tag{5.18}$$

And than can get the parameters under interest RL and IL as:

$$\begin{aligned} RL &= 10log_{10}((1 - |\Gamma_S|^2)(1 - |\Gamma_L|^2)) = 7.396dB \Rightarrow Return\,Loss \\ IL &= 10log_{10}((1 - |\Gamma_S|^2)|S_{21}|^2(1 - |\Gamma_L|^2)) = 107.810dB \Rightarrow Insertion\,Loss \end{aligned} \tag{5.19}$$

Here too, as in the previous case, $IL > LB$, making communication not possible. It is clear that this configuration is practically not used for data exchange with PLC technology since the IL are exaggeratedly high. Although the line has low RL due to the small mismatch between the impedance of the generators/load and that of the line, the signal is too attenuated in the segment $\overline{AB}$ by the line losses, not bringing great advantages with this beneficial behaviour.

5.4.2 Transmission with MV LUMIREP-E Phase-Phase configuration cables

Now the same architecture as above is taken, but the PLC signal is injected between two phases of the LUMIREP-E coaxial cables $25mm^2$, in the three-phase system.
The total extension of the line is always up to $40km$ with a maximum distance of $2km$ between the various modules. Referring to the **Figure5.11** and isolating the first branch also here, it has been applied the superposition principle in order to not consider the other branches in the section $\overline{BC}$ for the calculation of the parameters in the first one, greatly simplifying the treatment. For sure, it is always valid the Budget-Link previously discovered ($96dB$) between the MASTER and a SLAVE (it is the same between SLAVE-SLAVE).
Since the aim is to find the attenuations on the line A_{Line}, RL and consequently IL, thus discovering which configuration is capable of not consuming all the LB actually available at the working frequency of $133kHz$, S-parameters obtained in Chapter 3 become punctual at the chosen frequency only, thus being able to work with only matrices. Section $\overline{AB}$ has been treated doing a cascade between the Medium Voltage cables S-matrix and the first MCEP S-matrix, obtaining a new one.
However, before doing this getting the correct values, also here the parameters relating to LUMIREP-E cable in the Phase-Phase configuration have been scaled for a length of $2km$.
Knowing that the matrix at $133kHz$ for $1m$ length is:

$$S = \begin{pmatrix} 0.0057 + 0.0098j & 0.9965 - 0.0123j \\ 0.9965 - 0.0123j & 0.0057 + 0.0098j \end{pmatrix} \tag{5.20}$$

The corresponding $133kHz$ S-matrix scaled to $2km$ is:

$$S_{2km} = \begin{pmatrix} 0.4583 - 0.0141j & -0.1727 - 0.0682j \\ -0.1727 - 0.0682j & 0.4583 - 0.0141j \end{pmatrix} \tag{5.21}$$

Where:

- β is the propagation constant and, at $133kHz$ for $1m$ length is: $\beta = 0.008 \left[\frac{rad}{m}\right]$;
- α is the attenuation constant and, at $133kHz$ for $1m$ length is: $\alpha = 7.195 \times 10^{-4} \left[\frac{Np}{m}\right]$;
- k is the complex wavenumber and, at $133kHz$ for $1m$ length is: $k = \beta - j\alpha = 0.008 - 7.195 \times 10^{-4} j \left[\frac{rad}{m}\right] \epsilon \mathbb{C}$
- l is the length under interest and in this case: $l = 2km$;
- Z_0 is the characteristic impedance of the LUMIREP-E, $25mm^2$ MV coaxial cables in the Phase-Phase configuration: $Z_0 = 140.003\Omega$;
- Z_∞ is the characteristic impedance of the of the measuring instrument, that for the Keysight/Agilent VNA, Model E5071C with 2-ports is: $Z_0 = 50\Omega$;
- Γ_L is the reflaction coefficient between the load impedance and the line impedance given by: $\Gamma_L = \frac{Z_{inf} - Z_0}{Z_{inf} + Z_0} = -0.474$.

And finally, making a cascade between the obtained matrix and the one of the first MCEP, it is possible to obtain for the section $\overline{AB}$ the corresponding S-parameters:

$$S_{\overline{AB}} = \begin{pmatrix} 0.4583 - 0.0148j & -0.0200 + 0.1715j \\ -0.0200 + 0.1715j & 0.4583 - 0.0148j \end{pmatrix} \tag{5.22}$$

As it was explained before, this type of reasoning cannot be made between the $\overline{BD}$ and $\overline{BC}$ lengths as they are parallel to each other. What can be done is to obtain an equivalent impedance for each section at point B, make it parallel and finally treat the line as if it were a normal transmission line composed of the generator impedance Z_G, the newly found S-matrix $S_{\overline{AB}}$, and as load, the equivalent impedance $Z_{eq} = Z_{B,BD}//Z_{B,BC}$.
It was started from the $\overline{BD}$ section, composed by the only MCEP with attached cables and the impedance of the SLAVE set as a load of 10Ω. The equivalent impedance at point B of the MCEP is the same founded before and is equal to: $Z_{B,BD} = 145.540 - 405.160j[\Omega]$.
It is possible to proceed in the same way also for the section $\overline{BC}$. Starting from the transmission matrix $S_{\overline{AB}}$ obtained previously (**5.5**), it is possible to get the reflection coefficient of the line ($Z_0 = 134.481[\Omega]$) with respect to the SLAVE's load ($Z_{L1} = 10[\Omega]$):

$$\Gamma_{L1} = \frac{Z_{L1} - Z_0}{Z_{L1} + Z_0} = -0.862 \tag{5.23}$$

Also here with some calculations, it is getting the reflaction coefficient at the point B^+:

$$\Gamma_{in,1} = S_{11} + \frac{\Gamma_{L1} S_{21} S_{12}}{1 - S_{22}\Gamma_{L1}} = 0.498 - 0.019j \tag{5.24}$$

And finally the equivalent impedance at point B for the section $\overline{BC}$:

$$Z_{B,BC} = Z0\frac{1 + \Gamma_{in,1}}{1 + \Gamma_{in,1}} = 416.680 - 20.867j[\Omega] \tag{5.25}$$

Making the parallel between the two impedances just founded ($Z_{B,BD}, Z_{B,BC}$), it is getting the equivalent one:

$$Z_{eq} = Z_{B,BD}//Z_{B,BC} = 206.110 - 149.500j[\Omega] \tag{5.26}$$

Once obtained the equivalent impedance, the line can be now in a simplified way like the one in the picture **Figure5.14**.
So, remembering that the Link Budget (LB) is:

$$LB = 96dB \tag{5.27}$$

Looking at the $S_{\overline{AB}}$-matrix and knowing that the S_{21} term express the direct transmission coefficient with matched output (for a passive and reciprocal component $S_{21} = S_{12}$), it is possible to get the total attenutaion of the $\overline{AB}$ length:

$$A_{line} = 20log_{10}(|S_{21}|) = 35.128dB \Rightarrow Attenuation\,over\,the\,line \tag{5.28}$$

And in the same way as before (**5.8**) with some calculations, it was possible to obtain the reflaction coefficient at the point L^+:

$$\Gamma_L = S_{22} + \frac{\Gamma_S S_{21} S_{12}}{1 - S_{22}\Gamma_S} = -0.484 + 0.243j \tag{5.29}$$

Where Γ_S is the reflaction coefficient between the MASTER characteristic impedance ($Z_G = 10\Omega$) and the one of the line in the $\overline{AB}$ segment ($Z_0 = 134.481\Omega$):

$$\Gamma_S = \frac{Z_S - Z_0}{Z_S + Z_0} = -0.752 \tag{5.30}$$

Finally, with the results just obtained, it is possible to get the parameters under interest RL and IL as:

$$\begin{gathered} RL = 10log_{10}((1 - |\Gamma_S|^2)(1 - |\Gamma_L|^2)) = 17.134dB \Rightarrow Return\,Loss \\ IL = 10log_{10}((1 - |\Gamma_S|^2)|S_{21}|^2(1 - |\Gamma_L|^2)) = 52.262dB \Rightarrow Insertion\,Loss \end{gathered} \tag{5.31}$$

From the reported data it is possible to notice how $LB > IL$, with a margin of $43.738dB$. This result is great as the signal is able to pass, arriving at the load with relatively low attenuation. Despite the impedance of the line being 134.481Ω, about $74,651\Omega$ more than the previous configuration, the RL increased by only $9,738dB$, not much compared to the increase in impedance. This worsening of RL is largely balanced by lower A_{line}, these being $35.128dB$, a much smaller value than before. It is important to choose cables with a low attenuation coefficient (α_{dB}), since the losses due to this are the predominant ones in a communication system. The use or not of all the available Link Budget to understand whether or not a signal can reach the SLAVE is not a binary behaviour. It is usually a good norm to consider a signal that is no longer usable below $3dB$. This is the minimum threshold below which communication can be considered interrupted. To take into account any effects not considered during the design or occasional and unpredictable events that may negatively affect the data exchange, it is good to widen this limit, taking a little margin. Doubling the $3dB$ limit and setting $6dB$ as the treshold after which the signal is no longer able to reach the load, it is possible to understand how the maximum value that the IL can reach is $90dB$, beyond which the communication is to be considered interrupted.
On the basis of the previous evaluations and, knowing that the attenuation introduced in the line are $52.262dB$, it is possible to modify the existing architecture by increasing the maximum distance traveled by the MASTER and SLAVE signal. Setting a length of $3km$, the results obtained in terms of A_{line}, RL and IL are:

$$\begin{gathered} A_{line} = 20log_{10}(|S_{21}|) = 49.749dB \Rightarrow Attenuation\,over\,the\,line \\ RL = 10log_{10}((1 - |\Gamma_S|^2)(1 - |\Gamma_L|^2)) = 16.107dB \Rightarrow Return\,Loss \\ IL = 10log_{10}((1 - |\Gamma_S|^2)|S_{21}|^2(1 - |\Gamma_L|^2)) = 65.856dB \Rightarrow Insertion\,Loss \end{gathered} \tag{5.32}$$

From the results obtained it can be seen that $LB > IL$ and how these do not exceed the minimum limit of $6dB$, making communication possible. In fact, it can be seen that there is still a margin of $24.135dB$ that can be spent on the line, making this change applicable where required. Also, given the margin still available, the distance can be further increased if required, bringing the limit to around $4km$
Maintaining a distance of $2km$ and imagining to use a 50Ω (as the internal impedance of the VNA) impedance couplers between the MASTER and the line and between the line and the SLAVE, the obtained results in terms of A_{line}, RL and IL are presente below:

$$\begin{gathered} A_{line} = 20log_{10}(|S_{21}|) = 35.128dB \Rightarrow Attenuation\,over\,the\,line \\ RL = 10log_{10}((1 - |\Gamma_S|^2)(1 - |\Gamma_L|^2)) = 5.630dB \Rightarrow Return\,Loss \\ IL = 10log_{10}((1 - |\Gamma_S|^2)|S_{21}|^2(1 - |\Gamma_L|^2)) = 40.758dB \Rightarrow Insertion\,Loss \end{gathered} \tag{5.33}$$

It can be noticed that the RL decreased by $10.477dB$, bringing the IL to $40.758dB$, compared to $65.856dB$ before. This allows to have a margin of $49.242dB$, which, although the previous configuration shows remarkable results, improves them even more, making it a valid option for higher performances. The table below **Tab5.1** summarizes the obtained results:

	Line without couplers		**Line with couplers**
	$2km$	$3km$	$2km$
Loss over the line $A_{line}[dB]$	35.128	49.749	35.128
Reflection Loss $RL[dB]$	17.134	16.107	5.630
Insertion Loss $IR[dB]$	52.262	65.856	40.758

Table 5.1: Obtained Results.

From the results obtained it can be seen that, in general, the data exchange takes place with high performances. In the configuration without the impedance coupler, it can be seen that there is a slight difference in the RL between the two distances taken into consideration. This happens because the line shows a slight decrease in impedance ($Z_{0,2km} = 134.481\Omega$, $Z_{0,3km} = 123.937\Omega$) which allows its improvement, but it is only $1.027dB$. The use of the impedance couplers is a valid option for higher performances as it further improves the results obtained by decreasing the RL. Despite the excellent results, this section of the LUMIREP-E cable is not much used for the energy transport given the high price and overall weight for a three-phase system that derives from it. Usually smaller sections are used while this is employed for short distances or as a bridge between different components in MV.

5.4.3 Transmission with MV SENOREP-3G Phase-Ground configuration cable

The next architecture studied is the one in which the SENOREP-3G in the Phase-Ground configuration with a cross-section of $10mm^2$ are the Medium Voltage three-wire cables. The total extension of the line always remain of up to $40km$ with a maximum distance of $2km$ between the various modules before the IL become to high and the information is lost. Referring to the **Figure5.11** and isolating the first branch also here, it has been applied the superposition principle in order to not consider the other branches in the section $\overline{BC}$ for the calculation of the parameters in the first one, greatly simplifying the treatment.
For sure, it is always valid the Budget-Link previously discovered ($96dB$) between the MASTER and a SLAVE (it is the same between SLAVE-SLAVE). Since the aim is to find the attenuations on the line A_{Line}, RL and consequently IL, thus discovering which configuration is capable of not consuming all the LB actually available at the working frequency of $133kHz$, S-parameters obtained in Chapter 3 become punctual at the chosen frequency only, thus being able to work with only matrices. Section $\overline{AB}$ has been treated doing a cascade between the Medium Voltage cables S-matrix and the first MCEP S-matrix, obtaining a new one. However, before doing this getting the correct values, also here the parameters relating to SENOREP-3G in the Phase-Ground configuration have been scaled for a length of $2km$. Knowing that the matrix at $133kHz$ for $1m$ length is:

$$S = \begin{pmatrix} 0.0048 + 0.0030j & 0.9957 - 0.0138j \\ 0.9957 - 0.0138j & 0.0048 + 0.0030j \end{pmatrix} \tag{5.34}$$

The corresponding $133kHz$ S-matrix scaled to $2km$ is:

$$S_{2km} = \begin{pmatrix} 0.0963 - 0.0000j & -0.0012 - 0.0001j \\ -0.0012 - 0.0001j & 0.0963 - 0.00002j \end{pmatrix} \tag{5.35}$$

Where:

- β is the propagation constant and, at $133kHz$ for $1m$ length is: $\beta = 0.014\left[\frac{rad}{m}\right]$;
- α is the attenuation constant and, at $133kHz$ for $1m$ length is: $\alpha = 0.003\left[\frac{Np}{m}\right]$;
- k is the complex wavenumber and, at $133kHz$ for $1m$ length is: $k = \beta - j\alpha = 0.014 - 0.003j\left[\frac{rad}{m}\right] \epsilon \mathbb{C}$
- l is the length under interest and in this case: $l = 2km$;
- Z_0 is the characteristic impedance of the SENOREP-3G, $10mm^2$ MV three-wire cable in the Phase-Ground configuration: $Z_0 = 60.652\Omega$;
- Z_∞ is the characteristic impedance of the of the measuring instrument, that for the Keysight/Agilent VNA, Model E5071C with 2-ports is: $Z_0 = 50\Omega$;
- Γ_L is the reflaction coefficient between the load impedance and the line impedance given by: $\Gamma_L = \frac{Z_{inf} - Z_0}{Z_{inf} + Z_0} = -0.096$.

And finally, making a cascade between the obtained matrix and the one of the first MCEP, it is possible to obtain for the section $\overline{AB}$ the corresponding S-parameters:

$$S_{\overline{AB}} = \begin{pmatrix} 0.0963 - 0.0000j & 0.0002 + 0.0011j \\ 0.0002 + 0.0011j & 0.0963 - 0.0000j \end{pmatrix} \tag{5.36}$$

As it was explained before, this type of reasoning cannot be made between the $\overline{BD}$ and $\overline{BC}$ lengths as they are parallel to each other. What can be done is to obtain an equivalent impedance for each section at point B, make it parallel and finally treat the line as if it were a normal transmission line composed of the generator impedance Z_G, the newly found S-matrix $S_{\overline{AB}}$, and as load, the equivalent impedance $Z_{eq} = Z_{B,BD}//Z_{B,BC}$.
It was started from the $\overline{BD}$ section, composed by the only MCEP with attached cables and the impedance of the SLAVE set as a load of 10Ω. The equivalent impedance at point B of the MCEP is the same founded before and is equal to: $Z_{B,BD} = 145.540 - 405.160j[\Omega]$.
It is possible to proceed in the same way also for the section $\overline{BC}$. Starting from the transmission matrix $S_{\overline{AB}}$ obtained previously (**5.5**), it is possible to get the reflection coefficient of the line ($Z_0 = 60.652[\Omega]$) with respect to the SLAVE's load ($Z_{L1} = 10[\Omega]$):

$$\Gamma_{L1} = \frac{Z_{L1} - Z_0}{Z_{L1} + Z_0} = -0.717 \tag{5.37}$$

Also here with some calculations, it is getting the reflaction coefficient at the point B^+:

$$\Gamma_{in,1} = S_{11} + \frac{\Gamma_{L1} S_{21} S_{12}}{1 - S_{22}\Gamma_{L1}} = 0.096 - 0.000j \tag{5.38}$$

And finally the equivalent impedance at point B for the section $\overline{BC}$:

$$Z_{B,BC} = Z0\frac{1 + \Gamma_{in,1}}{1 + \Gamma_{in,1}} = 73.5781 - 0.0002j[\Omega] \tag{5.39}$$

Making the parallel between the two impedances just founded ($Z_{B,BD}, Z_{B,BC}$), it is getting the equivalent one:

$$Z_{eq} = Z_{B,BD}//Z_{B,BC} = 67.987 - 10.338j[\Omega] \tag{5.40}$$

Once obtained the equivalent impedance, the line can be now in a simplified way like the one in the picture **Figure5.14**.
So, remembering that the Link Budget (LB) is:

$$LB = 96dB \tag{5.41}$$

Looking at the $S_{\overline{AB}}$-matrix and knowing that the S_{21} term express the direct transmission coefficient with matched output (for a passive and reciprocal component $S_{21} = S_{12}$), it is possible to get the total attenutaion of the $\overline{AB}$ length:

$$A_{line} = 20log_{10}(|S_{21}|) = 135.924dB \Rightarrow Attenuation\,over\,the\,line \tag{5.42}$$

And in the same way as before (**5.8**) with some calculations, it was possible to obtain the reflaction coefficient at the point L^+:

$$\Gamma_L = S_{22} + \frac{\Gamma_S S_{21} S_{12}}{1 - S_{22}\Gamma_S} = -0.172 + 0.081j \tag{5.43}$$

Where Γ_S is the reflaction coefficient between the MASTER characteristic impedance ($Z_G = 10\Omega$) and the one of the line in the $\overline{AB}$ segment ($Z_0 = 60.652\Omega$):

$$\Gamma_S = \frac{Z_S - Z_0}{Z_S + Z_0} = -0.717 \tag{5.44}$$

Finally, with the results just obtained, it is possible to get the parameters under interest RL and IL as:

$$\begin{aligned} RL &= 10log_{10}((1 - |\Gamma_S|^2)(1 - |\Gamma_L|^2)) = 7.629dB \Rightarrow Return\,Loss \\ IL &= 10log_{10}((1 - |\Gamma_S|^2)|S_{21}|^2(1 - |\Gamma_L|^2)) = 143.553dB \Rightarrow Insertion\,Loss \end{aligned} \tag{5.45}$$

As it is possible to notice $IL > LB$, this makes possible to understand how communication cannot take place with this type of configuration at the chosen distance. Compared to the Phase-Ground configuration of the LUMIREP-3G, the RL ($RL_{LUMIREP-E} = 7.396dB$, $RL_{LUMIREP-E} = 7.629dB$) and IL are slightly worse ($IL_{LUMIREP-E} = 141.040dB$, $IL_{SENOREP-3G} = 143.553dB$), this is the direct consequence of a little worse Z_0 ($Z_{0,LUMIREP-E} = 59.084\Omega$, $Z_{0,SENOREP-3G} = 60.651\Omega$) and a little worse α_{dB} ($\alpha_{dB,LUMIREP-E} = 57.835\Omega$, $\alpha_{dB,SENOREP-3G} = 59.231\Omega$.This also confirms, as previously found in Chapter 3, that signal injection between the phase of a cable and its shield is not the optimal way to transmit data on a PLC technology, as the attenuations along the line are too high and also that larger sections have better performances.
It also possible to understand that the existing lines already apply a different data transmission, making this solution unusable for lengths of $2km$ between a receiver and a transmitter. Instead, by trying the same configuration but with a distance of $1.5km$ between MASTER and SLAVE, it is possible to obtain the power dissipated (P_{line}) of the $S_{\overline{AB}}$-matrix in the segment $\overline{AB}$, due to the attenuation α:

$$A_{line} = 20log_{10}(|S_{21}|) = 102.912dB \Rightarrow Attenuation\,over\,the\,line \tag{5.46}$$

And than can get the parameters under interest RL and IL as:

$$\begin{aligned} RL &= 10log_{10}((1 - |\Gamma_S|^2)(1 - |\Gamma_L|^2)) = 7.629dB \Rightarrow Return\,Loss \\ IL &= 10log_{10}((1 - |\Gamma_S|^2)|S_{21}|^2(1 - |\Gamma_L|^2)) = 110.541dB \Rightarrow Insertion\,Loss \end{aligned} \tag{5.47}$$

The trend explained above is confirmed by the data just obtained and, as in the previous case, $IL > LB$, makingcommunication not possible. It is clear that this configuration is practically not used for data exchange with PLC technology since the IL are exaggeratedly high. Although the line has low RL due to the small mismatch between the impedance of the generators/load and that of the line, the signal is too attenuated in the segment $\overline{AB}$ by the line losses, not bringing great advantages with this beneficial behaviour.

5.4.4 Transmission with MV SENOREP-3G Phase-Phase configuration cable

The last architecture studied is the one in which the SENOREP-3G in the Phase-Phase configuration with a cross-section of $10mm^2$ are the Medium Voltage three-wire cables.
The total extension of the line always remain of up to $40km$ with a maximum distance of $2km$ between the various modules between the various modules before the IL become to high and the information is lost. Referring to the **Figure5.11** and isolating the first branch also here, it has been applied the superposition principle in order to not consider the other branches in the section $\overline{BC}$ for the calculation of the parameters in the first one, greatly simplifying the treatment.
For sure, it is always valid the Budget-Link previously discovered ($96dB$) between the MASTER and a SLAVE (it is the same between SLAVE-SLAVE). Since the aim is to find the attenuations on the line A_{Line}, RL and consequently IL, thus discovering which configuration is capable of not consuming all the LB actually available at the working frequency of $133kHz$, S-parameters obtained in Chapter 3 become punctual at the chosen frequency only, thus being able to work with only matrices. Section $\overline{AB}$ has been treated doing a cascade between the Medium Voltage cables S-matrix and the first MCEP S-matrix, obtaining a new one. However, before doing this getting the correct values, also here the parameters relating to SENOREP-3G in the Phase-Ground configuration have been scaled for a length of $2km$.
Knowing that the matrix at $133kHz$ for $1m$ length is:

$$S = \begin{pmatrix} 0.0048 + 0.0082j & 0.9958 - 0.0136j \\ 0.9958 - 0.0136j & 0.0048 + 0.0082j \end{pmatrix} \tag{5.48}$$

The corresponding $133kHz$ S-matrix scaled to $2km$ is:

$$S_{2km} = \begin{pmatrix} 0.3259 + 0.0001j & 0.0086 + 0.0166j \\ 0.0086 + 0.0166j & 0.3259 + 0.0001j \end{pmatrix} \tag{5.49}$$

Where:

- β is the propagation constant and, at $133kHz$ for $1m$ length is: $\beta = 0.011 \left[\frac{rad}{m}\right]$;
- α is the attenuation constant and, at $133kHz$ for $1m$ length is: $\alpha = 0.002 \left[\frac{Np}{m}\right]$;
- k is the complex wavenumber and, at $133kHz$ for $1m$ length is: $k = \beta - j\alpha = 0.011 - 0.002j \left[\frac{rad}{m}\right] \epsilon \mathbb{C}$
- l is the length under interest and in this case: $l = 2km$;
- Z_0 is the characteristic impedance of the SENOREP-3G, $10mm^2$ MV three-wire cable in the Phase-Phase configuration: $Z_0 = 98.197\Omega$;
- Z_∞ is the characteristic impedance of the of the measuring instrument, that for the Keysight/Agilent VNA, Model E5071C with 2-ports is: $Z_0 = 50\Omega$;

- Γ_L is the reflaction coefficient between the load impedance and the line impedance given by: $\Gamma_L = \frac{Z_{inf}-Z_0}{Z_{inf}+Z_0} = -0.326$.

And finally, making a cascade between the obtained matrix and the one of the first MCEP, it is possible to obtain for the section $\overline{AB}$ the corresponding S-parameters:

$$S_{\overline{AB}} = \begin{pmatrix} 0.3259 + 0.0001j & 0.0086 + 0.0166j \\ 0.0086 + 0.0166j & 0.3259 + 0.0001j \end{pmatrix} \tag{5.50}$$

As it was explained before, this type of reasoning cannot be made between the $\overline{BD}$ and $\overline{BC}$ lengths as they are parallel to each other. What can be done is to obtain an equivalent impedance for each section at point B, make it parallel and finally treat the line as if it were a normal transmission line composed of the generator impedance Z_G, the newly found S-matrix $S_{\overline{AB}}$, and as load, the equivalent impedance $Z_{eq} = Z_{B,BD}//Z_{B,BC}$.
It was started from the $\overline{BD}$ section, composed by the only MCEP with attached cables and the impedance of the SLAVE set as a load of 10Ω. The equivalent impedance at point B of the MCEP is the same founded before and is equal to: $Z_{B,BD} = 145.540 - 405.160j[\Omega]$.
It is possible to proceed in the same way also for the section $\overline{BC}$. Starting from the transmission matrix $S_{\overline{AB}}$ obtained previously (**5.5**), it is possible to get the reflection coefficient of the line ($Z_0 = 98.197[\Omega]$) with respect to the SLAVE's load ($Z_{L1} = 10[\Omega]$):

$$\Gamma_{L1} = \frac{Z_{L1} - Z_0}{Z_{L1} + Z_0} = -0.815 \tag{5.51}$$

Also here with some calculations, it is getting the reflaction coefficient at the point B^+:

$$\Gamma_{in,1} = S_{11} + \frac{\Gamma_{L1} S_{21} S_{12}}{1 - S_{22}\Gamma_{L1}} = 0.3261 - 0.0003j \tag{5.52}$$

And finally the equivalent impedance at point B for the section $\overline{BC}$:

$$Z_{B,BC} = Z0\frac{1 + \Gamma_{in,1}}{1 + \Gamma_{in,1}} = 193.560 - 0.114j[\Omega] \tag{5.53}$$

Making the parallel between the two impedances just founded ($Z_{B,BD}, Z_{B,BC}$), it is getting the equivalent one:

$$Z_{eq} = Z_{B,BD}//Z_{B,BC} = 148.000 - 54.437j[\Omega] \tag{5.54}$$

Once obtained the equivalent impedance, the line can be now in a simplified way like the one in the picture **Figure5.14**.
So, remembering that the Link Budget (LB) is:

$$LB = 96dB \tag{5.55}$$

Looking at the $S_{\overline{AB}}$-matrix and knowing that the S_{21} term express the direct transmission coefficient with matched output (for a passive and reciprocal component $S_{21} = S_{12}$), it is possible to get the total attenutaion of the $\overline{AB}$ length:

$$A_{line} = 20log_{10}(|S_{21}|) = 79.540dB \Rightarrow Attenuation\,over\,the\,line \tag{5.56}$$

And in the same way as before (**5.8**) with some calculations, it was possible to obtain the reflaction coefficient at the point L^+:

$$\Gamma_L = S_{22} + \frac{\Gamma_S S_{21} S_{12}}{1 - S_{22}\Gamma_S} = -0.357 + 0.184j \tag{5.57}$$

Where Γ_S is the reflaction coefficient between the MASTER characteristic impedance ($Z_G = 10\Omega$) and the one of the line in the $\overline{AB}$ segment ($Z_0 = 98.197\Omega$):

$$\Gamma_S = \frac{Z_S - Z_0}{Z_S + Z_0} = -0.661 \tag{5.58}$$

And than can get the parameters under interest RL and IL as:

$$\begin{aligned} RL &= 10log_{10}((1 - |\Gamma_S|^2)(1 - |\Gamma_L|^2)) = 7.515dB \Rightarrow Return\,Loss \\ IL &= 10log_{10}((1 - |\Gamma_S|^2)|S_{21}|^2(1 - |\Gamma_L|^2)) = 87.054dB \Rightarrow Insertion\,Loss \end{aligned} \tag{5.59}$$

From the reported data it is possible to notice how $LB > IL$, with a margin of $2.964dB$. This section ($10mm^2$) is widely used for the transport of the MV, making the results much closer to reality. It can be seen that the margin between the IL and the Link Budget is at the limit but always remaining above the $6dB$ treshold, thus being able to consider that the data exchange takes place. With this section, it is not possible to make changes to the network by placing the MASTER and SLAVE at a greater distance from each other, as it would go below the $6dB$ limit. Given the results, in order to reach greater distances, it is necessary to use impedance couplers. To begin with, a length of $2km$ was maintained and a 50Ω (as the internal impedance of the VNA) impedance couplers between the MASTER and the line and between the line and the SLAVE have been used.
The obtained results in terms of A_{line}, RL and IL are presente below:

$$\begin{aligned} A_{line} &= 20log_{10}(|S_{21}|) = 79.540dB \Rightarrow Attenuation\,over\,the\,line \\ RL &= 10log_{10}((1 - |\Gamma_S|^2)(1 - |\Gamma_L|^2)) = 2.874dB \Rightarrow Return\,Loss \\ IL &= 10log_{10}((1 - |\Gamma_S|^2)|S_{21}|^2(1 - |\Gamma_L|^2)) = 82.414dB \Rightarrow Insertion\,Loss \end{aligned} \tag{5.60}$$

As can be seen from the results, the RL decreased by $4.641dB$ making the line and the MASTER/SLAVE almost perfectly matched. Anyway, the signal continues to experience a large attenuation, as A_{line} is the predominant component, which cannot be changed. Despite this, the margin that can still be spent on the line is now $7.586dB$ and can be tested if, with the addition of the impedance couplers, the maximum distance between MASTER/SLAVE can be increased to $3km$. The obtined results in terms of A_{line}, RL and IL are:

$$\begin{aligned} A_{line} &= 20log_{10}(|S_{21}|) = 117.550dB \Rightarrow Attenuation\,over\,the\,line \\ RL &= 10log_{10}((1 - |\Gamma_S|^2)(1 - |\Gamma_L|^2)) = 2.874dB \Rightarrow Return\,Loss \\ IL &= 10log_{10}((1 - |\Gamma_S|^2)|S_{21}|^2(1 - |\Gamma_L|^2)) = 120.429dB \Rightarrow Insertion\,Loss \end{aligned} \tag{5.61}$$

From the results obtained it can be seen that the signal is not able to reach the load as $IL > LB$. The maximum limit in terms of length to which it can be pushed has been calculated and turns out to be $2.3km$. The obtined results in terms of A_{line}, RL and IL are:

$$\begin{aligned} A_{line} &= 20log_{10}(|S_{21}|) = 87.173dB \Rightarrow Attenuation\,over\,the\,line \\ RL &= 10log_{10}((1 - |\Gamma_S|^2)(1 - |\Gamma_L|^2)) = 2.874dB \Rightarrow Return\,Loss \\ IL &= 10log_{10}((1 - |\Gamma_S|^2)|S_{21}|^2(1 - |\Gamma_L|^2)) = 90.050dB \Rightarrow Insertion\,Loss \end{aligned} \tag{5.62}$$

It is noted that beyond this distance the $6dB$ treshold is exceeded and the signal crosses the safety limit. The table below **Tab5.2** summarizes the obtained results:

	Line without couplers	**Line with couplers**		
	$2km$	$2km$	$2.3km$	$3km$
Loss over the line $A_{line}[dB]$	79.540	79.540	87.173	117.550
Reflection Loss $RL[dB]$	7.515	2.874	2.874	2.874
Insertion Loss $IR[dB]$	87.054	82.414	90.050	120.429

Table 5.2: Difference between a line without and with impedance couplers.

The results show how, with the current configuration, it is not possible to go beyond $2km$ as the maximum distance between MASTER/SLAVE as the Insertion Loss introduced by the network are just above the safety treshold limit before the signal can be considered completely attenuated. this is due to the high values of the attenuations along the line that the data experience ($A_{line} = 79.540$). With the introduction of impedance couplers, the effect of reflection losses can be mitigated, even if these are not the predominant factor. Using a $50\ Omega$ impedance couplers, the line is almost matched with the generator/load, the $RL = 2.874$ and a maximum distance of $2.3km$ can be reached. Using an adjusted impedance of $\simeq 100\Omega$, the minimum Reflection Loss is achieved ($1.756dB$), thus having a margin of 8.704. This would allow to reach a maximum distance of $2.5km$ the furthest length hat can be pushed with this type of cable having $10mm^2$ as cross-section..

5.4.5 Comparison of the results

From the results obtained in the previous sections, it is clear that architectures that use a Phase-Ground configuration, regardless of the Medium Voltage cables utilised, are not used for data exchange with PLC communication, except for very short distances between MASTER-SLAVEs ($l < 1km$). These in fact, as had been found from the analysis made also in Chapter-3, although they present a lower characteristic impedances of the cables ($Z_{0,LUMIREP-E} = 59.084\Omega$,$Z_{0,SENOREP-3G} = 98.197\Omega$), have attenuation values that are too high for a channel able to accomodate the data exchange ($\alpha_{LUMIREP-E} = 27.9\frac{dB}{km}$, $\alpha_{SENOREP-3G} = 29.3\frac{dB}{km}$). And, since this is an intrinsic parameter of the cables which cannot be modified once the configuration has been chosen, it is not the smartest way to choose, also considering the amount of losses due to reflections for the mismatch between the characteristic impedance of the line and the one of the MASTER/SLAVEs are not negligible. The Phase-Phase configuration is the right choice to make for the injection of the signal on a power line and the one, therefore, currently used.
The cables in this configuration, however, present the problem of having a much higher characteristic impedance ($Z_{0,LUMIREP-E} = 140.004\Omega$, $Z_{0,SENOREP-3G} = 98.197\Omega$) than the previous one, increasing Reflection Losses due to the mismatch ($RL_{LUMIREP-E} = 17.134dB$, $RL_{SENOREP-3G} = 7.515dB$) with the characteristic impedance of the receivers and transmitters which is very low ($Z_G = Z_L = 10\Omega$). In any case, these do not appear to be the overwhelming losses on the line, not affecting too much the final yield. Moreover, for the LUMIREP-E cable, even if they turn out to be $17dB$, this one has $A_{line} = 35.128dB$, obtaining $IL = 52.262dB$ that leaves a margin of over $37.738dB$ before the signal exceeds the treshold safety of $6dB$. Instead for the SENOREP-3G one, the reflections losses turn out to be really low ($IL = 7.515dB$) compared to the line ones ($A_{line} = 79.540dB$) and even by adapting the generator/load to the line as much as possible, the IL does not fall below

$81.296dB$ having a maximum margin of $8.704dB$. The obtained results are summarized in the table below **Tab5.3**:

Configuration	Cable	mm^2	Impedance Coupler	km	$A_{line}[dB]$	$RL[dB]$	IL	Margin
Phase-Ground	LUMIREP-E	25	No	2	133.64	7.396	107.810	0
Phase-Ground	LUMIREP-E	25	No	1.5	100.414	7.396	107.810	0
Phase-Phase	LUMIREP-E	25	No	2	35.128	17.134	52.262	37.738
Phase-Phase	LUMIREP-E	25	No	3	49.749	16.107	65.856	40.251
Phase-Phase	LUMIREP-E	25	Yes	2	35.128	5.630	40.758	49.242
Phase-Ground	SENOREP-3G	10	No	2	135.924	7.629	143.553	0
Phase-Ground	SENOREP-3G	10	No	1.5	102.912	7.629	110.541	0
Phase-Phase	SENOREP-3G	10	No	2	79.540	7.515	87.054	2.946
Phase-Phase	SENOREP-3G	10	Yes	2	79.540	2.874	82.414	7.586
Phase-Phase	SENOREP-3G	10	Yes	2.3	87.173	2.874	90.050	$\simeq 0$
Phase-Phase	SENOREP-3G	10	Yes	3	117.550	2.874	120.429	0

Table 5.3: Comparison of the obtained results.

From the data it is possible to note the excellent performances provided by the LUMIREP-E cable with a cross-section of $25mm^2$ but it is not much used for the energy transport given the high price and overall weight for a three-phase system that derives from it.
Usually smaller sections are used while this is employed for short distances or as a bridge between different components in MV. The studied one does not require the use of impedance couplers given the intrinsic excellent results. This happens, however, because the LUMIREP-E shows a section that is more than twice larger than the one of the SENOREP-3G, which obviously affects performances. However, it is possible to note from Chapter 3, how the SENOREP-3G and the LUMIREP-E, do not have attenuation (α_{dB}) and impedance values (Z_0) far from each other, making it clear that with the same section and length the second returns letter results. Therefore, in order to have good performances in data exchange, taking into account the prices and not forgetting that the big advantage of the PLC is to be able to connect to existing power cables without having to add others, a fair margin that allows with respect to the security treshold of $6dB$ and the possibility of being able to introduce significant changes in the line by increasing the maximum distance between MASTER/SLAVEs if required, the SENOREP-3G three-wire cable, in the Phase-Phase configuration, having a section of $16mm^2$ with a $19463.880\frac{eur}{km}$ cost, is the best geometry for the data exchange.

6 Future Works

In the previous Chapter, a complete analysis of a typical architecture used by AUGIER for data exchange with PLC technology was made. It was studied which configuration is better for the injection of data on the MV cables, the attenuation of the various lines (A_{line}) and losses due to reflections RL, what margin thay can take with respect to a treshold safety limit and, with the existing set-up, if the maximum distance between the various MASTER and SLAVEs could be increased. It has been founded that the use of impedance couplers improves the performances in terms of smaller RL, but that they are not always necessary. In the existing configuration, however, the modulation between the carrier wave at $50Hz$ and the one containing the signal at $133kHz$, occurs through the use of the MCEP and the working principle has been explained in Chapter 5, Section 5.3. They are mounted in parallel to each transformers that adapts the Medium Voltage signal to the Low Voltage carrier, that is currently every $2km$. On an existing $40km$ long architecture, that means 20 are being fitted, each MCEP has a cost of $600euros$ for a total of $12,000euros$, increasing the final price of thre PLC system. Also if the signal is able to reach the distance of $3km$, 14 should still be installed, with a total cost of $8400euros$. Furthermore, the MCEP can only be used with TEE MM (MODULE) transformer models as it requires the addition of cables between the Medium Voltage and the transformers, which the TER MT transformer model does not mount, being directly connected to the line. This limits the use of a technology produced by AUGIER and also very efficient, restricting the field of transformers that can be utilized to a single model. To overcome this problem and to try to lower the total price of PLC technology to be sold to buyers, it is possible to use the results obtained in Chapter 4, when the augmented model of the transformers was presented and the TFs of the TER MT and of TEM MM (MODULE) through the VNA were obtained. Referring to the **Figure5.1**, what can actually be done is to eliminate all the MCEPs from the line (except the one connected to the MASTER since there is no transformer between it and the Medium Voltage) and to pass the data signal directly into the transformers by exploiting the attenuations that this introduce at $133kHz$ and knowing that the Budget Link of the line is always $96dB$.
As can be understand from the TFs of the transformers studied in Chapter 4, at $133kHz$ the TER MT transformer introduces an attenuation of $33.336dB$, while that TEE MM (MODULE) $39.037dB$. In order to introduce this modification in the existing line, regardless of the Medium Voltage cable present in the architecture, the signal must be injected in the Phase-Phase configuration, a breaker must be considere placed before transformers (as shown in **Figure5.11**) and, depending on the mounted cable, it is necessary to mount impedance couplers, otherwise the signal will pass the treshold safety limit, completely deleting the signal and making the changement useless. The study was carried out on LUMIREP-E cables with and without impedance couplers, as they return excellent results. It was done even on the SENOREP-3G with the couplers mounted, in order to have an idea of how possible is to apply this modification even to real situations. If it turns out to be files, it is possible to reduce the distance between the various MASTER/SLAVEs and see what is the operation

limit.The TF of the TER MT transformer at $133kHz$ has an attenuation of $33.336dB$, while that of the TEE MT transformer (MODULE) has one of $39.037dB$. Above all it must be said that if in the first branch the communication is affected by the strong attenuation of a single transformer since the signal from the MASTER is modulated to the carrier through the only one MCEP present on the line, in the other branches this is affected by the attenuation of two transformers, erasing it completely. This makes it clear that the idea adopted can be pursued but provided that some changes must be made to the line:

- use impedance couplers not of 50Ω but with values more inherent to what is the real mismatch between line and the generator/load;
- studying the TF of the transformers it possible to see that, lickely, the frequency of $133kHz$ falls within the valley having a fairly wide Bandwidth with a good Quality factor. What can been done is to keep the same Bandwidth, but try to reduce the attenuation that the signal experience at $133kHz$ ($33.336dB$ for the TER MT transformer and $39.037dB$ for the TEM MM (MODULO)) trying to bring the attenuation around $20dB$.

The two ideas can be used together to be able to pass the signal without experience so much attenuations and leave the IL not to high. In order to develop further the second one, a capacitive tap can used to exchange data through the grid. This capacitive tap is installed at the cable insulation and reads the data from a PLC MASTER. This system can be retrofitted to an existing grid. Though, with the potential-free capacitive tap a signal can be taken from the mid voltage grid without any electric potential problems.
The signal is extracted in the mid voltage grid by a capacitive tap and injected in the low voltage grid with a direct connection.A bidirectional transmission between two voltage levels and a transformer is shown in **Figure6.1**. The signal is extracted on both sides with a capacitive tap and directly injected on the opposite side. With this type of data transmission over the transformer the floating potential of the two coils is kept because the signal extraction on each side is potential free. A possible approach for a capacitive tap is shown in **Figure6.2**.

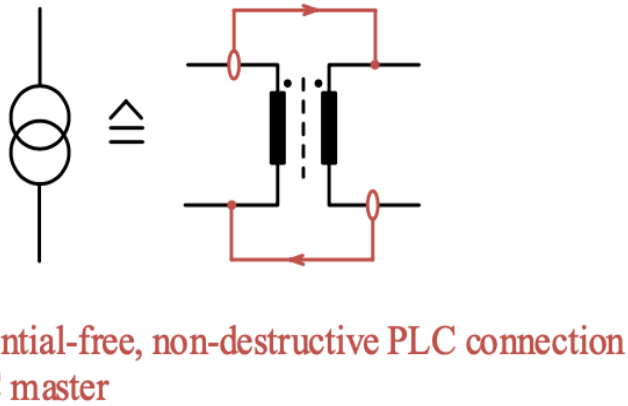

Figure 6.1: Bridging a transformer with direct coupling and capacitive tapping.

Since a capacity is made up of two parts, one part is the power line and the other one is an electrode around the cable. The geometry of the electrode depends on the force distribution of the electromagnetic field around the cable. The geometry also defines the coupling capacity, which matters in the filter design.

The capacity of the resulting capacitor can be calculated by **6.1**:

$$C = \frac{2 * \pi \epsilon l}{ln \frac{r_2}{r_1}} \tag{6.1}$$

Where:

- ϵ is the permittivity;
- l is the length of the electrode;
- r_1 is the radius of the inner cable;
- r_2 is the radius of the circular electrode.

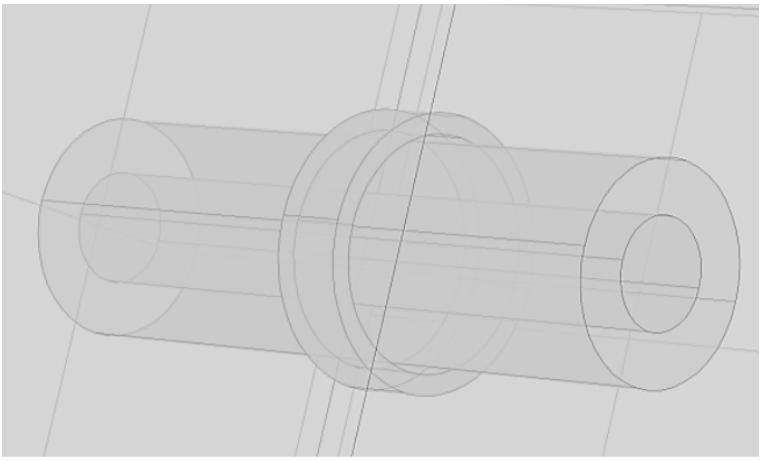

Figure 6.2: Geometry of the cable surrounded by a cylindrical electrode.

Once the value of the capacity to be applied has been discovered, the tap can be mounted directly on the connections of the transformers under construction, thus being able to have it mounted intrinsically. What should be create is a filtering system that at $133kHz$ is able to experience less attenuation to the signal, so as to allow the exchange of data. In any case, the operation, the guarantee that the transformer maintains the galvanic isolation and how much it actually brings a beneficial effect to the system are entirely experimental and future more in-depth research will confirm this idea.

7 Conclusions

Power Line Communication (PLC) can be used to create a communication system across Medium/Low Voltage electrical systems. It enables establishing digital communications without the need for extra wires allowing transmission of data and electricity over the same media. The system, which is made up of a transmitter and a receiver, ensures monitoring and control of electrical distribution installations over long distances, particularly in situations where maintenance is challenging. Despite its benefits, PLC channel is quite harsh and presents a number of challenges. With respect to frequency, location, environment and the sort of equipment connected to it, a channel's characteristics and properties change.
This is primarily due to the fact that the power grid was not initially intended to be used for communications and also is optimised to work at a super low frequency band ($50 - 60Hz$). The communication is differential, the band spans between $10kHz$ and $500kHz$ and in particular, the working frequency at which the data exchange takes place is $133kHz$.
The goals of the master thesis was to define, from the normative and through the least square fit, the characteristic impedance of the receivers/transmitters placed on the PLC line, find the Link Budget of the communication and study the various components that constitute the distribution system in order to understand the causes of loss and their magnitude, developing strategies to mitigate them. In particular, attention was paid to the Medium/Low Voltage cables typically used in France, on which the signal travels, which can be approximated as lossy transmission lines, and the characteristic parameter (Z_0) and the ones that describe them as a function of frequency (C', L', G', R' and α_{dB}), were obtained with experimental formulas using Matlab. A Keysight/Agilent Vector Network Analyzer (VNA), Model E5071C with 2-ports and a frequency range that goes from $9KHz$ to $8,5GHz$ has been used to get a comparison between real parameters and simulated ones. Taking into consideration an existing architecture with a total extension of up to $40km$ and with a maximum distance of $2km$ between the various modules before the Insertion Losses IL become to high and the information is lost, knowing that the power distribution system of the Medium Voltage cables is three-phase, it was studied which signal injection (Phase-Ground or Phase-Phase) and which geometry (coaxial or three-wire cables) was the best for the data exchange and whether the maximum distance between MASTER and SLAVES could be increased.
The PLC class under interset is the Narrowband (NB) one: a standard that operate in the frequency bands VLF/LF/MF ($3 - 500kHz$). This range includes the European CENELEC band ($3 - 148.5kHz$), the American FCC band ($10 - 490kHz$), the Japanise ARIB band ($10 - 450kHz$) and the Chinese EPRI band ($3 - 500kHz$) **[3]**.
NB-PLC can be further divided between:

- Low Data Rate (LDR): single-carrier technology with capacity data rate of a few $kbps$;
- High Data Rate (HDR): multicarrier technology capable of data rates ranging from tens of $kbps$ to $500kbps$.

The **Tab7.1** shows all the frequencies made avaible from the organisations mentioned before.

REGION	*ORGANIZATION*	*FREQUENCY RANGE [kHz]*
EUROPE		3-9
	CENELEC A	9-95
	CENELEC B	95-125
	CENELEC C	125-140
	CENELEC D	140-148.5
JAPAN	ARIB	10-450
CHINA	EPRI	3-90
		3-500
USA	FCC	100-490

Table 7.1: Summary of all the frequency ranges and their sub-bands made avaible from the different world organisations.

PLC network access impedance varies with time, frequency, location and whether the transmitter and receiver are turned on or off. The impedance matching technique utilised considers only the impedance magnitude ($|Z|$), which simplify the circuit construction (the phases are not considered). The **Tab7.2** shows a standard overview of the access impedance measurements for narrowband and broadband PLC **[8]**.

FREQUENCY BANDS	*FREQUENCIES*	$\|Z\|$ **or R/X**
Narrowband	5-20kHz	$0\Omega<R<4\Omega$
		$1\Omega<X<12\Omega$
	10-170kHz	$3\Omega<\|Z\|<17\Omega$ for rural;
		$1\Omega<\|Z\|<17\Omega$ for urban;
		$1\Omega<\|Z\|<21\Omega$ for industrial;
	0-500kHz	$1\Omega<\|Z\|<90\Omega$
BroadBand	20kHz-30MHz	$0.3\Omega<\|Z\|<800\Omega$
		$0\Omega<R<598\Omega$, $-800\Omega<X<686\Omega$
	1–100 MHz	$0\Omega<R<250\Omega$, $-175\Omega<X<150\Omega$

Table 7.2: The overview of the access impedance measurements for narrowband and broadband PLC.

Furthermore, knowing that the transmission frequency chosen by AUGIER falls within the CENELEC-C range and is $133kHz$, the absolute value of a transmitter/receiver impedance has been determined with the least squared fit method **[8]**:

$$|Z| = 0.005 * f^{0.63} = 8.45[\Omega] \tag{7.1}$$

This falls into the range for urban application ($1\Omega<|Z|<17\Omega$) indicated in **Tab7.2**. It was decided to use $|Z| = 10\Omega$ as a suitable approximation for the transmitter/receiver's imput impedance (AUGIER MASTER/SLAVEs).
The MV/LV cables studied that deal with power transport and therefore, in a PLC system, with data exchange, can be treated as lossy transmission lines. They can be modeled with L' (inductance per unit length $[\frac{H}{m}]$), C' (capacitance per unit length $[\frac{F}{m}]$) parameters,

which describe their lossless operation, and in addition, the parameters R' (resistance per unit length $\left[\frac{\Omega}{m}\right]$), G' (conductance per unit length $\left[\frac{S}{m}\right]$) which describe the losses **[9]**. The characteristic impedance of the cable, even in the presence of losses ($R' \neq 0, G' \neq 0$), is a real parameter defined as:

$$Z_0 = \sqrt{\frac{L'}{C'}}\,\epsilon\,\mathbb{R} \tag{7.2}$$

Although this is a purely real parameter, due to the presence of the losses (α), a wave that travel through them will be attenuate in its propagation. The attenuation parameter (α) can be divided into two different contributions, each of which dependent on a parameter of the line: the resistance and conductance per unit length, R' and G'. These two attenuation coefficients due to conductor and dielectric losses, are then expressible in terms of characteristic impedance Z_0, and α can be obtained as the sum of these contributions:

$$\alpha_c = \frac{R'}{2Z_0}, \quad \alpha_d = \frac{1}{2}G'Z_0 \quad \Rightarrow \quad \alpha = \alpha_c + \alpha_d \tag{7.3}$$

The attenuation in $\frac{dB}{m}$ will be $\alpha_{dB} = 8.686\alpha$. This expression tend to somewhat underestimate the actual losses, but it is generally a good approximation. Usually the α_c term grows in frequency like $\sqrt{f}$ and the α_d, like f. Since the communication between MASTER and SLAVEs occurs in a differential way, to get the parameters characterizing the cables studied and to be able to compare them with those obtained through the experimental formulas as a function of the frequency on Matlab, data have been acquired through the VNA in the form of S-parameters, that completely defines the behaviour of the quadripole. They are an expression of the incident power wave a and the reflected one b as a function of the voltage along the line with a characteristic impedance Z_0. The relationships is linear and it is possible to express the reflected power waves as a function of the incident ones:

$$\begin{cases} b_1 = S_{11}a_1 + S_{12}a_2 \\ b_2 = S_{21}a_1 + S_{22}a_2 \end{cases} \tag{7.4}$$

Since all the analyzed components were found to be passive and reciprocal, the scattering matrix turns out to be symmetric and dependent on only two independent parameters (S_{11} and S_{21}):

$$\begin{bmatrix} S_{11} & S_{21} \\ S_{21} & S_{11} \end{bmatrix} \tag{7.5}$$

Where:

- $S_{11} = \left(\frac{b_1}{a_1}\right)_{a_2=0} \Rightarrow$ is the reflection coefficient at the input with matched output;
- $S_{21} = \left(\frac{b_2}{a_1}\right)_{a_2=0} \Rightarrow$ is the direct transmission coefficient with matched output.

Elandcables' H07RN-F cables are mostly utilised for Low Voltage applications into the industrial field (for this reason unshielded) in France. Since they are involved into the transport of the signal from and to the various transmitters/receivers, do not carry too much power and therefore the analysis was focused only on single-phase cables. An outer sheath holds the two insulated phases inside, making it possible to approximate their behaviour as a two-wire transmission line.
Two sections were examined: the $1.5mm^2$ and the $6mm^2$ ones, since they are the most used and also because, by comparing the obtained results, it was possible to understand the trend

of the various parameters that describe their behaviour. The obtained data at $133kHz$ are shown in the **Tab7.3**:

	$1.5mm^2$		$6mm^2$	
	Measured	Calculated	Measured	Calculated
Inductance per unit-length (L') $[\frac{\mu H}{m}]$	1.181	0.562	1.120	0.456
Capacitance per unit-length (C') $[\frac{nF}{m}]$	0.111	0.059	0.134	0.073
Resistance per unit-length (R') $[\frac{\Omega}{m}]$	0.567	0.150	0.464	0.118
Conductance per unit-length (G') $[\frac{\mu S}{m}]$	1.282	0.099	0.591	0.123
Attenuation per unit-length (α_{dB}) $[\frac{dB}{m}]$	0.022	0.006	0.021	0.006
Characteristic impedance (Z_0) $[\Omega]$	99.444	97.286	88.538	78.947

Table 7.3: Obtained results measured and calculated for two different sections of the H07RN-F LV cable.

As can be seen from the values obtained, the results calculated through the formulas are understimated compared to those measured. Although larger section has some benefits in terms of data exchange compared to smaller one, these are much less manageable, heavier and more expensive. In fact, comparing the prices per meter of the H07RN-F $1.5mm^2$ $(0.610\frac{eur}{m})$ and of the H07RN-F $6mm^2$ $(1.776\frac{eur}{m})$, it is possible to find that one is more than two times expensive than the other.
It is understood that as the section increases there is a general improvement trend of the various parameters but it would need huge sections with exaggerated costs before it is possible to see acceptable benefits, therefore trying to use LV cables with larger sections to enhance PLC communication was discovered to be not the right way to proceed. Prysmian Group is one of the largest suppliers of MV cables in France, which is why two different geometries have been studied: the LUMIREP-E coaxial cable with a section of $25mm^2$ and the three-wire SENOREP-3G cable, with a section of $10mm^2$.
Knowing that a three-phase system is used for MV applications, two different methods of signal injection have been studied: Phase-Ground and Phase-Phase one. The obtained data only get through measurements at $133kHz$ are reported in the **Tab7.4**:

	LUMIREP-E		SENOREP-3G	
	Phase-Ground	Phase-Phase	Phase-Ground	Phase-Phase
Inductance per unit-length (L') $[\frac{\mu H}{m}]$	0.964	1.3222	1.009	1.302
Capacitance per unit-length (C') $[\frac{nF}{m}]$	0.207	0.057	0.259	0.127
Resistance per unit-length (R') $[\frac{\Omega}{m}]$	0.441	0.484	0.458	0.448
Conductance per unit-length (G') $[\frac{\mu S}{m}]$	4.143	10.851	5.446	5.387
Attenuation per unit-length (α_{dB}) $[\frac{dB}{m}]$	0.027	0.006	0.029	0.0165
Characteristic impedance (Z_0) $[\Omega]$	59.084	140.002	60.740	98.374

Table 7.4: Obtained results measured for both the LUMIREP-E and SENOREP-3G MV cables.

From the obtained data it is possible to understand that the Phase-Phase configuration experience a lower attenuation coefficient (α_{dB}) than the Phase-Ground one but at the expense of an increase in the characteristic impedance (Z_0).
The total weight of the SENOREP-3G with a cross-section of $10mm^2$ is $1240\frac{kg}{km}$ while that of the LUMIREP-E, with the same section, for a three-phase line is $1470\frac{kg}{km}$.
The cost for a SENOREP-3G with a cross-section of $16mm^2$ is $19463.880\frac{eur}{km}$ instead the total

one for the LUMIREP-E with the same cross section in a three-phase system is $39326.760\frac{eur}{km}$, more than double that the previous geometry. These trends of differences on weights and costs can also be appied to other sections. The LUMIREP-E cable in the Phase-Phase configuration responds to line losses better than the SENOREP-3G cable but only because has a section more than double the size of the three-wire cable. Their values in terms of Z_0 and α_{dB} are not too far, and if it is taken a SENOREP-3G cable having the same section as the LUMIREP-E one, one works better than the other, preferring the SENOREP-3G as a MV cable for data exchange with PLC communication. Currently, the projects allow a total extension of the line of up to $40km$ with a maximum distance of $2km$ between the various MASTER/SLAVEs. Starting with **Figure7.1**, the first branch of the line is isolated noting that the introduced attenuations and reflections depend only on the LV and HV cables and on the two signal couplers (MCEPs). They are used to modulate the signal at high frequency and LV on a MV and low frequency wave of the electrical power line, which is the carrier.

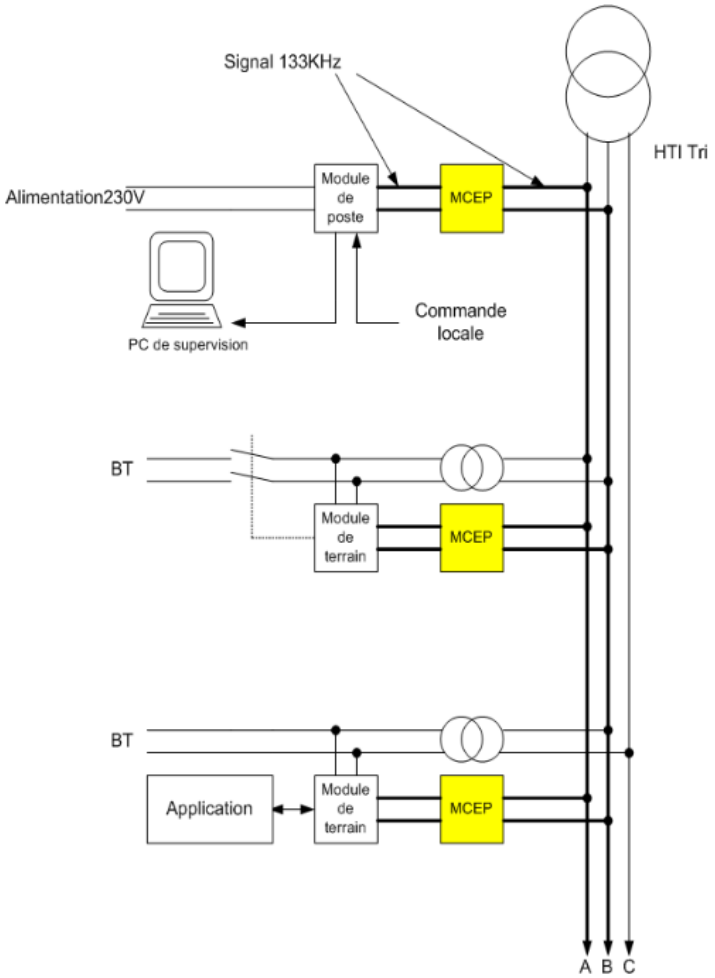

Figure 7.1: AUGIER's PLC architecture.

The big advantage, however, is that the whole system is linear and the superimposition principle can be applied: the losses that occur in each single branch can be evaluated neglecting the remaining, adding as an additional factor the remnants length of the line and the last impedance connected to it.

The Link-Budget (LB) between the MASTER and a SLAVE has been estimated in an experimental way and results to be $96dB$: it is the maximum degree of attenuation that can be introduced before the data signal is no longer avaible.
A safety margin of $6dB$ was then considered in order to take into account factors not considered during the design occasional and unpredictable events. The Attenuations on the line A_{line}, the Return Loss RL and the Insertion Loss IL have been evaluated through the following relations **7.6**:

$$A_{line} = 20log_{10}(|S_{21}|)$$

$$RL = 10log_{10}((1 - |\Gamma_S|^2)(1 - |\Gamma_L|^2)) \tag{7.6}$$

$$IL = 10log_{10}((1 - |\Gamma_S|^2)|S_{21}|^2(1 - |\Gamma_L|^2))$$

The obtained result for both the cables in the Phase-Ground and Phase-Phase configurations are reported in **Tab7.5**: To have good performances in data exchange over MV cables, taking

Cable	Coupler	km	$A_{line}[dB]$	$RL[dB]$	IL	Margin
LUMIREP-E, P-G	No	2	133.64	7.396	107.810	0
LUMIREP-E, P-G	No	1.5	100.414	7.396	107.810	0
LUMIREP-E, P-P	No	2	35.128	17.134	52.262	37.738
LUMIREP-E, P-P	No	3	49.749	16.107	65.856	40.251
LUMIREP-E, P-P	Yes	2	35.128	5.630	40.758	49.242
SENOREP-3G, P-G	No	2	135.924	7.629	143.553	0
SENOREP-3G, P-G	No	1.5	102.912	7.629	110.541	0
SENOREP-3G, P-P	No	2	79.540	7.515	87.054	2.946
SENOREP-3G, P-P	Yes	2	79.540	2.874	82.414	7.586
SENOREP-3G, P-P	Yes	2.3	87.173	2.874	90.050	$\simeq 0$
SENOREP-3G, P-P	Yes	3	117.550	2.874	120.429	0

Table 7.5: Comparison of the obtained results.

into account the prices and not forgetting that the big advantage of the PLC is to be able to connect to existing power cables without having to add others, a fair margin that allows with respect to the security treshold of $6dB$ and the possibility of being able to introduce significant changes in the line by increasing the maximum distance between MASTER/SLAVEs if required, the SENOREP-3G three-wire cable, in the Phase-Phase configuration, having a section of $16mm^2$ with a $19463.880\frac{eur}{km}$ cost, is the best geometry for the data exchange. MCEPs are mounted in parallel to each transformers and on an existing $40km$ long architecture means that 20 are being fitted, each of which with a cost of $600euros$. Furthermore, the MCEP can only be used with TEE MM (MODULE) transformer models, produce by AUGIER, as it requires the addition of cables between the MV and the transformers, which the TER MT transformer model does not mount. In order to streamline the existing architecture, data can pass directly into the transformers knowing the attenuations that these introduce at $133kHz$ through their Tansfer Fuctions. The effectiveness, the calculations and the experimentation of this idea are left to furure studies.

Bibliography

[1] Florence Chelangat; *"Power Line Communication Impendance Profiling and Matching for Broadband Applications"*, University of Kwazulu-Natal, School of Engineering, Departement of Electronic Engineering, June 2018.

[2] Giovanni Artale, Antonio Cataliotti, Valentina Cosentino, Dario Di Cara, Riccardo Fiorelli, Salvatore Guaiana, Nicola Panzavecchia and Giovanni Tinè; *"A New Coupling Solution for G3-PLC Employment in MV Smart Grids"*, Department of Engineering, Università degli Studi di Palermo, 90128 Palermo, Italy, June 2019.

[3] G. Bucci, F. D'Innocenzo, S. Dolce, E. Fiorucci, F. Ciancetta; *"Power Line Communication, Overview of Standard and Applications"*, Dip. di Ing. Industriale, dell'Informazione e di Economia, Università degli Studi dell'Aquila Via G. Gronchi, 18–Loc. Campo di Pile, 67100 L'Aquila, Italy, September 2015.

[4] Khurram Hussain Zuberi; *"Powerline Carrier (PLC) Communication Systems"*, Departement of Microelectronics and Information Technology, IMIT Royal Institute of Technology, KTH IT-Universitet, Kista, Stockholm, Sweden, September 2003.

[5] P.A. Janse Rensburg, Supervisor Prof. H. C. Ferreira; *"Effective Coupling for Power-Line Communications"*, D.Ing (Electrical and Electronic), University of Johannesburg, January 2008.

[6] Electricité Réseau Distribution France (eRDF); *"PLC G3 Physical Layer Specification"*; Specification.

[7] Candidato: Massimo Rocchi, Relatore: Prof. Luca Roffia; *"Sistemi di comunicazione a onde convogliate: Studio e analisi comparativa"*; Corso di Laurea in Ingegneria Elettronica e delle Telecomunicazioni, Alma Master Studiorum-Università di Bologna, sede di Cesena.

[8] Bingting Wang, Ziping Cao; *"A Review of Impedance Matching Techniques in Power Line Communications"*; College of Telecommunications & Information Engineering, Nanjing University of Posts and Telecommunications, Nanjing 210003, China; College of Mechanical and Electrical Engineering, Chuzhou University, Chuzhou 239000, China.

[9] Prof. Luca Perregrini; *"Campi Elettromagnetici e Circuiti I, Linee di trasmissione"*; Facoltà di Ingegneria Università degli studi di Pavia, Corso di Laurea Triennale in Ingegneria Elettronica e Informatica.

Sitography

[S1] augier.com

[S2] HD-PLC.com

[S3] Electrical Academia.com

[S4] allaboutcircuits.com

[S5] ResearchSpace.com

[S6] prysmiangroup.com

[S7] elandcables.com

[S8] BCCampus.com

[S9] Sudonull.com

[S10] tutorialspoint.com

[S11] csie.com

[S12] wikipedia.org

[S13] Imeko.org

[S14] physics.com

[S15] researchgate.net

[S16] quora.com

[S17] campielettromagnetici.com

[S18] agilent.com

[S19] electricaltechnology.org

[S20] dipslab.com

[S21] megger.com

[S22] electronics-tutorial.com